The Journal of American Science

ISSN 1545-1003
Volume 5 - Number 2, March 20, 2009

Journal of American Science

The ***Journal of American Science*** is an international journal with a purpose to enhance our natural and scientific knowledge dissemination in the world under the free publication principle. Any valuable paper that describes natural phenomena and existence or any report that conveys scientific research and pursuit are welcome, including both natural and social sciences. Papers submitted could be reviews, objective descriptions, research reports, opinions/debates, news, letters, and other types of writings that are nature and science related. The journal is calling for papers and seeking co-operators and editors as well.

Introductions to Authors

1. General Information

(1) Goals: As an international journal published both in print and on internet, the *Journal of American Science* is dedicated to the dissemination of fundamental knowledge in all areas of nature and science. The main purpose of the *Journal of American Science* is to enhance our knowledge spreading in the world under the free publication principle. It publishes full-length papers (original contributions), reviews, rapid communications, and any debates and opinions in all the fields of nature and science.

(2) What to Do: The *Journal of American Science* provides a place for discussion of scientific news, research, theory, philosophy, profession and technology - that will drive scientific progress. Research reports and regular manuscripts that contain new and significant information of general interest are welcome.

(3) Who: All people are welcome to submit manuscripts in any fields of nature and science.

(4) Distributions: Web version of the journal is freely opened to the world, without any payment or registration. The journal will be distributed to the selected libraries and institutions for free. For the subscription of other readers please contact with: editor@americanscience.org or americansciencej@gmail.com or editor@sciencepub.net

.

(5) Advertisements: The price will be calculated as US$400/page, i.e. US$200/a half page, US$100/a quarter page, etc. Any size of the advertisement is welcome.

2. Manuscripts Submission

(1) Submission Methods: Electronic submission through email is encouraged and hard copies plus an IBM formatted computer diskette would also be accepted.

(2) Software: The Microsoft Word file will be preferred.

(3) Font: Normal, Times New Roman, 10 pt, single space.

(4) Indent: Type 4 spaces in the beginning of each new paragraph.

(5) Manuscript: Don't use "Footnote" or "Header and Footer".

(6) Cover Page: Put detail information of authors and a short title in the cover page.

(7) Title: Use Title Case in the title and subtitles, e.g. "**Debt and Agency Costs".**

(8) Figures and Tables: Use full word of figure and table, e.g. "Figure 1. Annul Income of Different Groups", Table 1. Annual Increase of Investment".

(9) References: Cite references by "last name, year", e.g. "(Smith, 2003)". References should include all the authors' last names and initials, title, journal, year, volume, issue, and pages etc.

Reference Examples:

Journal Article: Hacker J, Hentschel U, Dobrindt U. Prokaryotic chromosomes and disease. Science 2003;301(34):790-3.

Book: Berkowitz BA, Katzung BG. Basic and clinical evaluation of new drugs. In: Katzung BG, ed. Basic and clinical pharmacology. Appleton & Lance Publisher. Norwalk, Connecticut, USA. 1995:60-9.

(10) Submission Address: editor@sciencepub.net, Marsland Press, P.O. Box 21126, Lansing, Michigan 48909, The United States, 517-349-2362.

(11) Reviewers: Authors are encouraged to suggest 2-8 competent reviewers with their name and email.

2. Manuscript Preparation

Each manuscript is suggested to include the following components but authors can do their own ways:

(1) Title page: including the complete article title; each author's full name; institution(s) with which each author is affiliated, with city, state/province, zip code, and country; and the name, complete mailing address, telephone number, facsimile number (if available), and e-mail address for all correspondence.

(2) Abstract: including Background, Materials and Methods, Results, and Discussions.

(3) Key Words.

(4) Introduction.

(**5) Materials and Methods**.

(**6) Results**.

(**7) Discussions**.

(**8) Acknowledgments**.

(9) Correspondence to.

(10) Submission date

(**11) References**.

Journal Address:

Marsland Press
2158 Butternut Drive
Okemos, MI 48864
The United States
Telephone: (517) 349-2362
E-mail: editor@americanscience.org;
editor@sciencepub.net;
americansciencej@gmail.com
Websites: http://www.americanscience.org;
http://www.sciencepub.org

Journal of American Science
Volume 5 - Number 2, March 20, 2009, ISSN 1545-1003

Contents

Marsland Press
Journal of American Science 2009:5(2) 1-12

Using the Sound Recognition Techniques to Reduce the Electricity Consumption in Highways

[1] Khalid T. Al-Sarayreh, [2] Rafa E. Al-Qutaish, [3] Basil M. Al-Kasasbeh

[1] School of Higher Technology (ÉTS), University of Québec, Montréal, Québec H3C 1K3, Canada

[2] Faculty of IT, Alzaytoonah University of Jordan, Airport Street, PO Box: 130, Amman 11733, Jordan

[3] Faculty of IT, Applied Science University, PO Box: 926296, Amman 11931, Jordan

Abstract:

The lighting is available for the highways to avoid accidents and to make the driving safe and easy, but turning the lights on all the nights will consume a lot of energy which it might be used in another important issues. This paper aims at using the sound recognition techniques in order to turn the lights on only when there are cars on the highway and only for some period of time. In more details, Linear Predictive Coding (LPC) method and feature extraction will be used to apply the sound recognition. Furthermore, the Vector Quantization (VQ) will be used to map the sounds into groups in order to compare the tested sounds. [Journal of American Science 2009:5(2) 1-12] (ISSN: 1545-1003)

Key word: Linear Predictive Analysis; Sound Recognition; Speaker Verification; Electricity Consumption

1. Introduction

Conserving Energy is one of the most important issues in many countries since they have limited resources of fuel to depend on, and they may be import all their need of energy from other countries. Therefore many conferences have been held urge the people to conduct the consumption of energy. This paper will introduce a system to control the lighting of lamps in highways. The system will turn the lights on only if there is a car in the highway for a pre-defined period of time, and will keep the lights off for any other sound.

Conserving energy of highways lights system could be used to reduce the power invoice by controlling the lights of lamps in the highways and will save a lot of energy. The algorithms that define the Conserving Energy of Street Lights system use the Database which consists of 250 sounds of cars and a lot of sounds from other domains.

2. An Overview of the Related Techniques

2.1 Voice Recognition

Voice recognition consists of two major tasks, that is, Feature Extraction and Pattern Recognition. Feature extraction attempts to discover characteristics of the sound signal, while pattern recognition refers to the matching of features in such a way as to determine, within probabilistic limits, whether two sets of features are from the same or different domain [Rabiner and Juang, 1993]. In general, speaker recognition can be subdivided into speaker identification, and speaker verification. Speaker verification will be used in this paper to recognize the sound of cars.

2.2 Linear Predictive Coding (LPC)

Linear predictive coding (LPC) is defined as a digital method for encoding an analogue signal in which a particular value is predicted by a linear

function of the past values of the signal. It was first proposed as a method for encoding human speech by the United States Department of Defence (DoD) in federal standard, published in 1984. The LPC model is based on a mathematical approximation of the vocal tract. The most important aspect of LPC is the linear predictive filter which allows determining the current sample by a linear combination of P previous samples. Where, the linear combination weights are the linear prediction coefficient.

The LPC based feature extraction is the most widely used method by developers of speech recognition. The main reason is that speech production can be modelled completely by using linear predictive analysis, beside, LPC based feature extraction can also be used in speaker recognition system where the main purpose is to extract the vocal tract [Nelson and Gailly, 1995].

2.3 Vector Quantization (VQ)

The quantization is the process of representing a large set of values with a much smaller set [Sayood, 2005]. Whereas, the Vector Quantization (VQ) is the process of taking a large set of feature vectors, and producing a smaller set of feature vectors, that represent the centroids of the distribution, i.e. points spaced so as to minimize the average distance to every other point.

However, optimization of the system is achieved by using vector quantization in order to compress and subsequently reduce the variability among the feature vectors derived from the frames. In vector quantization, a reproduction vector in a pre-designed set of K vectors approximates each feature vector of the input signal. The feature vector space is divided into K regions, and all subsequent feature vectors are classified into one of the corresponding codebook-elements (i.e. the centroids of the K regions), according to the least distance criterion (Euclidian distance) [Kinnunen and Frunti, 2001].

2.4 Digital Signal Processing (DSP)

The Digital Signal Processing (DSP) is the study of signals in a digital representation and the processing methods of these signals [Huo and Gan, 2004]. The DSP and analogue signal processing are subfields of signal processing. Furthermore, the DSP includes subfields such as audio signal processing, control engineering, digital image processing, and speech processing. RADAR Signal processing, and communications signal processing are two other important subfields of DSP [Lyons, 1996].

2.5 Frequency Domain

The signals are converted from time or space domain to the frequency domain usually through the Fourier transform. The Fourier transform converts the signal information to a magnitude and phase component of each frequency. Often the Fourier transform is converted to the power spectrum, which is the magnitude of each frequency component squared. This is one of the features that we have depended on in our analysis [Fukunaga, 1990].

2.6 Time Domain

The most common processing approach in the time or space domain is enhancement of the input signal through a method called filtering. Filtering generally consists of some transformation of a number of surrounding samples around the current sample of the input or output signal. There are various ways to characterize filters [Smith, 2001].

Most filters can be described in Z-domain (a superset of the frequency domain) by their transfer

functions. A filter may also be described as a difference equation, a collection of zeroes and poles or, if it is an FIR filter, an impulse response or step response. The output of an FIR filter to any given input may be calculated by convolving the input signal with the impulse response. Filters can also be represented by block diagrams which can then be used to derive a sample processing algorithm to implement the filter using hardware instructions [Garg, 1998].

3. The Methodology

In this paper, first we have collect many samples for cars sound from many areas. Then the feature extraction was applied on the sound. The sound was passed through a high-pass filter to eliminate the noise. The extraction of the LPC coefficient, the magnitude of the signal, and the pitch of the signal were made. These features were normalized and clustered into codebooks using vector quantization and the Linde-Buzo-Gray (LBG) algorithm for clustering which based on the k-mean algorithm. Finally a comparison with the template database that we have built before was made.

3.1 Database

The database which was used in this system was built from the recorded sounds which we record from different places, also from sounds for rain, thunder, and plane which we have brought them from internet, also from different human sounds. For the cars, rain, and plane groups, vector quantization method is used for clustering based on LBG algorithm and k-mean algorithm, and the Euclidian distance for matching. Statistical analyses were used for the human group, since the sounds of the human are very different and can't be bounded. Statistical analyses were based on the power spectrum of the sound then the mean and slandered deviation was taken to make the comparison.

3.2 Collecting Samples

We have collected about 250 sample of car's sound from different places beside the highways. These samples were taken after the mid night to assure that we have taken the pure sound of the car with the least possible noise. A microphone connected to a laptop was used; it was at a high place to assure to collect all the sound, since the proposed hardware should be beside the light of the highway, which is about 5 to 50 meters above the cars. We have used a program called Sound Forge for recording the sounds. Most of the sounds were recorded at a sample frequency of 44Khz to make sure that the sound has a high quality, and all the component of the sound will be shown when converting the sound to the frequency domain.

3.3 Feature Extraction

In order to recognize the sound of the car among other sounds we need to extract the parameters from the sound signal, these parameters help us to distinguish the sounds domain from others (car, plane, weather, and human sounds). Feature extraction consists of choosing those features which are most effective for preserving class separately [Fukunaga, 1990]. The main features that we have chosen which most effectively describe the sounds are LPC analysis, magnitude of the signal, and pitch of the signal.

3.4 Pitch Extraction

The harmonic-peak-based method has been used to extract pitch from the wave sound. Since harmonic peaks occur at integer multiples of the pitch frequency, then we compared peak

frequencies at each time (t) to locate the fundamental frequency in order to find the highest three magnitude peaks for each frame. Therefore, the differences between them computed. Since the peaks should be found at multiples of the fundamental, we know that their differences should represent multiples as well. Thus, the differences should be integer multiples of one another. Using the differences, we can derive our estimate for the fundamental frequency.

The peak vector consists of the largest three peaks in each frame. This forms a track of the pitch for the signal [Ayuso-Rubio and Lopez-Soler, 1995]. First we have found the spectrogram of the signal; spectrogram computes the windowed discrete-time Fourier transform of a signal using a sliding window.

The spectrogram is the magnitude of this function which shows the areas where the energy is mostly appear, after that we have take the largest three peaks in each frame. A major advantage to this method is its very noise-resistive. Even as noise increases, the peak frequencies should still be detectable above the noise.

3.5 Feature Comparison

After the feature extraction, the similarity between the parameters derived from the collected sound and the reference parameters need to be computed. The three most commonly encountered algorithms in the literature are Dynamic Time Warping (DTW), Hidden Markov Modelling (HMM) and Vector Quantization (VQ). In this paper, we use the VQ to compare the parameter matrices.

3.6 Decision Function

There are usually three approaches to construct the decision rules [Gonzales and Woods, 2002], that is; Geometric, Topological, or Probabilistic rules.

If the probabilities are perfectly estimated, then the Bayes Decision theory is the optimal decision. Unfortunately, this is usually not the case. In that case, the Bayes Decision might not be the optimal solution, and we should thus explore other forms of decision rules. In this paper, we will discuss two types of decision rules, which are based either on linear functions or on more complex functions such as Support Vector Machines (SVM).

4. Theoretical Implementation

4.1 LPC Analysis

LPC based feature extraction is the most widely used method by developers of speech recognition. The main reason is that speech production can be modelled completely by using linear predictive analysis, beside, LPC based feature extraction can also be used in speaker recognition system where the main purpose is to extract the vocal tract parameters from a given sound, in speech synthesis, linear prediction coefficient are the coefficient of the FIR filter representing a vocal tract transfer function, therefore linear prediction coefficient are suitable to use as a feature set in speaker verification system. The general idea of LPC is to determine the current sample by a linear combination of P previous samples where the linear combination weights are the linear prediction coefficient. Since LPC is one of the most powerful speech analysis techniques for extracting good quality features and hence encoding the speech. The LPC coefficients (ai) is the coefficients of the all pass transfer function H(z) modelling the vocal tract, and the order of the LPC (P) is also the order of H(z), which has been defined to be 10 in this paper.

Linear predictive coding (LPC) offers a powerful and simple method to exactly provide this type of information. Basically, the LPC algorithm produces a vector of coefficients that represent a smooth spectral envelope of the DFT magnitude of a temporal input signal. These coefficients are found by modelling each temporal sample as a linear combination of the previous P samples.

To be noted that the order of the LPC which used in this paper is 10. The LPC filter is given by:

$$H(Z) = \frac{1}{1 + a_1 Z^{-1} + a_2 Z^{-2} + ... + a_a 10 Z^{-10}}$$

This is equivalent to saying that the input-output relationship of the filter is given by the linear difference equation:

$$u(n) = s(n) + \sum_{i=1}^{10} a_i s(n-i)$$

Where u(n) is the innovation of the signal, s(n) is the original signal, H(Z) is LPC filter, and ai are the coefficient of the filter.

Another important equation that is used to predicate the next output from previous samples is:

$$\hat{s}[n] = G \cdot u[n] - \sum_{k=1}^{10} a_k s[n-k] \cong -\sum_{k=1}^{10} a_k s[n-k]$$

Where ŝ[n] (the prediction for the next output value) is a function of the current input and previous outputs, G is the gain.

The optimal values of the filter coefficients are gotten by minimizing the Mean Square Error (MSE) of the estimate, that is:

$$e[n] = s[n] - \hat{s}[n] \to \min\left(E\left(e^2[n]\right)\right)$$

Where E[n] is the mean square error.

A popular method to get a Minimum Mean Square Error (MMSE) is called the autocorrelation method, where the minimum is found by applying the principle of orthogonality. To find the LPC parameters, the Toeplitz autocorrelation matrix is used:

$$\begin{bmatrix} R(0) & R(1) & R(2) & R(3) & R(4) & R(5) & R(6) & R(7) & R(8) & R(9) \\ R(1) & R(0) & R(1) & R(2) & R(3) & R(4) & R(5) & R(6) & R(7) & R(8) \\ R(2) & R(1) & R(0) & R(1) & R(2) & R(3) & R(4) & R(5) & R(6) & R(7) \\ R(3) & R(2) & R(1) & R(0) & R(1) & R(2) & R(3) & R(4) & R(5) & R(6) \\ R(4) & R(3) & R(2) & R(1) & R(0) & R(1) & R(2) & R(3) & R(4) & R(5) \\ R(5) & R(4) & R(3) & R(2) & R(1) & R(0) & R(1) & R(2) & R(3) & R(4) \\ R(6) & R(5) & R(4) & R(3) & R(2) & R(1) & R(0) & R(1) & R(2) & R(3) \\ R(7) & R(6) & R(5) & R(4) & R(3) & R(2) & R(1) & R(0) & R(1) & R(2) \\ R(8) & R(7) & R(6) & R(5) & R(4) & R(3) & R(2) & R(1) & R(0) & R(1) \\ R(9) & R(8) & R(7) & R(6) & R(5) & R(4) & R(3) & R(2) & R(1) & R(0) \end{bmatrix} \begin{bmatrix} a_1 \\ a_2 \\ a_3 \\ a_4 \\ a_5 \\ a_6 \\ a_7 \\ a_8 \\ a_9 \\ a_{10} \end{bmatrix} = \begin{bmatrix} -R(1) \\ -R(2) \\ -R(3) \\ -R(4) \\ -R(5) \\ -R(6) \\ -R(7) \\ -R(8) \\ -R(9) \\ -R(10) \end{bmatrix}$$

Where:

$$R(k) = \sum_{n=0}^{159-k} s(n)s(n+k)$$

and R(k) is the autocorrelation of the signal.

The above matrix equation could be solved using the Gaussian elimination method. Any matrix inversion method or The Levinson-Durbin recursion (described below). To compute this vector, the recursive Levinson-Durbin Algorithm (LDR) was used.

4.2 Pre-emphasis

In general, the digitized speech waveform has a high dynamic range and suffers from additive noise. In order to reduce this range pre-emphasis is applied. By pre-emphasis [Robiner and Juang, 1993], we imply the application of a high pass filter, which is usually a first-order FIR of the form:

$$H(z) = 1 - az^{-1}, \ 9 \le a \le 1.0$$

The pre-emphasis is implemented as a fixed-coefficient filter or as an adaptive one, where the coefficient ai is adjusted with time according to the autocorrelation values of the speech. The pre-emphasize has the effect of spectral flattening which renders the signal less susceptible to finite precision effects (such as overflow and underflow) in any subsequent processing of the signal. The selected value for a in our work was 0.9375. Fig.1 and Fig.2 below represent the process of LPC analysis.

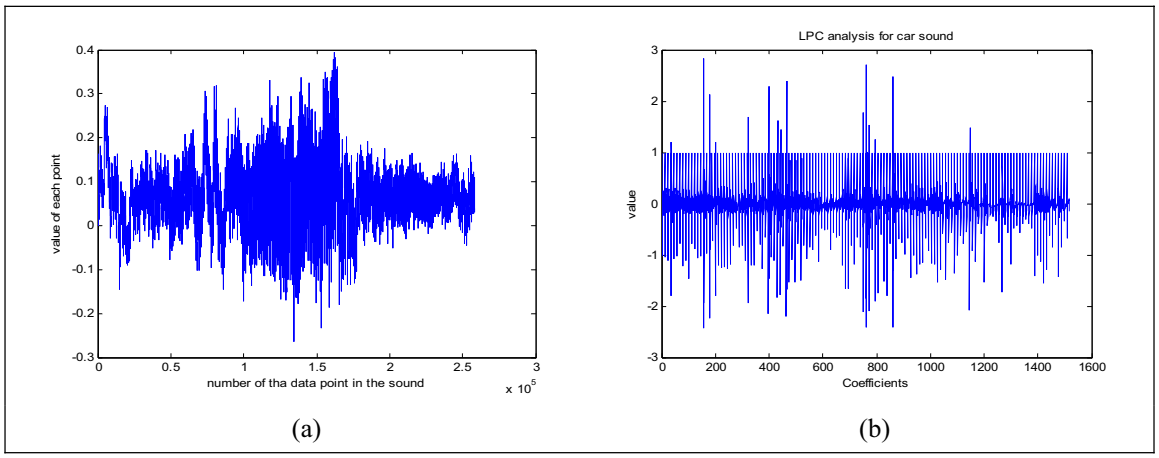

Fig.1 Presents (a) the Car Sound Wave, (b) the Coefficient of LPC Analysis for Same Sound

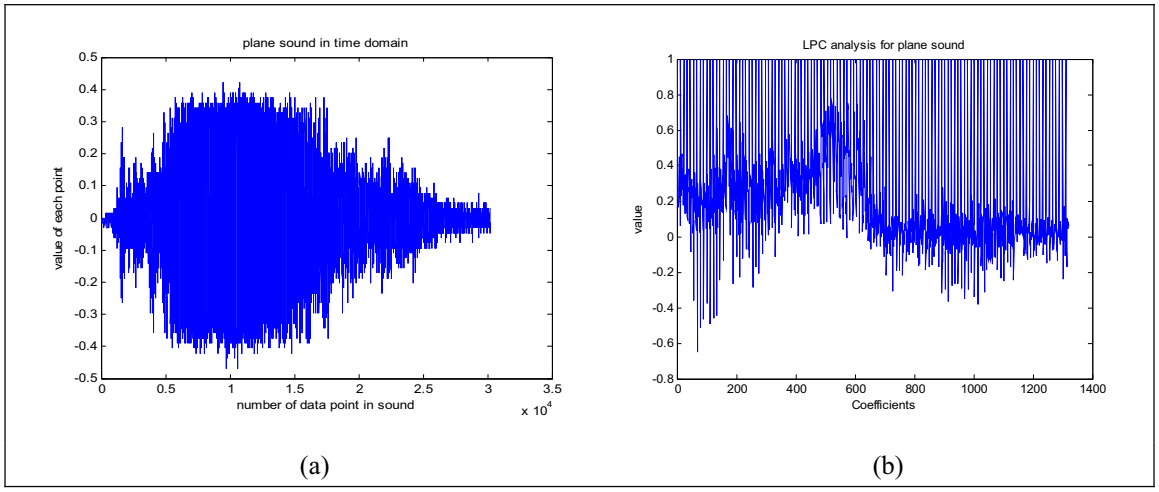

Fig.2 Presents (a) the Plane Sound Wave, (b) the Coefficient of LPC Analysis for Same Sound

4.3 Factors Affecting Linear Predictive Analysis

The main factors which the LPC equations depend on are the number of predictor parameters [Goldberg and Riek, 2000]. Depends upon the order, in this paper P is chosen to be 10, and the frame length N the choice of P depends primarily on the sampling rate and is essentially independent of the LPC method and we can summarize the dependency as the following:

1. The prediction error decrease steadily as P increase.
2. For P in the order of 13-14, the error has essentially flattened off showing only small decrease as P increases further [Klevans and Rodman, 1997].

There are a number of clustering algorithms available for use; however it has been shown that the one chosen does not matter as long as it is computationally efficient and works properly. A clustering algorithm is typically used for vector quantization, Therefore, One popular approach to designing vector quantization is a clustering procedure known as the k-means algorithm, which was developed for pattern recognition applications and LBG algorithm proposed by Linde, Buzo, and Gray.

4.4 The k-means algorithm

The K-means is one of the simplest unsupervised learning algorithms that solve the well known clustering problem. The procedure follows a simple and easy way to classify a given data set through a certain number of clusters (assume k clusters) fixed a priori. The main idea is to define k centroids, one for each cluster. These centroids should be placed in a cunning way because of different location causes different result. So, the better choice is to place them as much as possible far away from each other.

The next step is to take each point belonging to a given data set and associate it to the nearest centroid. When no point is pending, the first step is completed and an early group is done. At this point we need to re-calculate k new centroids as bar centers of the clusters resulting from the previous step. After we have these k new centroids, a new binding has to be done between the same data set points and the nearest new centroid. A loop has been generated. As a result of this loop we may notice that the k centroids change their location step by step until no more changes are done. In other words centroids do not move any more [MacQueen, 1997].

Finally, this algorithm aims at minimizing an objective function, in this case a squared error function. The objective function:

$$j = \sum_{j=1}^{k} \sum_{i=1}^{n} \left\| x_i(j) - C_j \right\|^{(2)}$$

Where $\left\| x_i(j) - C_j \right\|^{(2)}$ is a chosen distance measure between a data point $x_i^{(j)}$ and the cluster centre is an indicator of the distance of the n data points from their respective cluster canters [Zha et al, 2001]. The algorithm is composed of the following steps:

1. Place K points into the space represented by the objects that are being clustered. These points represent initial group centroids.
2. Assign each object to the group that has the closest centroid.
3. When all objects have been assigned, recalculate the positions of the K centroids.

Repeat Steps 2 and 3 until the centroids no longer move. This produces a separation of the objects into groups from which the metric to be minimized can be calculated [Moore, 2007].

4.5 Distance Measure

After quantizing a sound into its codebook, we need a way to measure the similarity/dissimilarity between and two sound domains. It is common in the field to use a simple Euclidean distance measure, and so this is what we have used.

4.5.1 Euclidian distance

Euclidean metric is the distance between two points that one would measure with a ruler, The Euclidean distance between two points $P=[p_1\ p_2\ p_3\ p_n]^T$ and $Q=[q_1\ q_2\ \ q_3\ \ q_n]^T$ and, in Euclidean n-space, is defined as:

$$\sqrt{\sum_{i=1}^{n} (p_i - q_i)^2}$$

4.5.2 Distance Weighting Coefficients

We follow the algorithm proposed above to weight distances so as to increase the likelihood of choosing the true sound domain. This algorithm, basically, reflects the greater importance of unique codewords as opposed to similar ones. This is a very important portion of our system. The training system architecture we created consists of two main parts. The first part consists of processing

each sound input voice sample to condense and summaries the characteristics of the sound features. The second part involves pulling each sound's data together into a single, easily manipulated, three dimensional matrix.

5. Practical Implementation

First we have high-pass filtered the signal because the more important information for speech processing lies in the higher frequencies according to Kinnunen and Franti [2004]. Then we split the signal into frames, each about 30ms long. By breaking the signal into frames, we approximate these distinct sounds in our analysis. For each frame we calculate the LPC coefficient. We also calculated the Magnitude and the pitch of the sound. These coefficients characterize each sound domain. The next step is to map these data. This is called vector quantization (VQ) and is accomplished by a clustering algorithm.

However, the clustering algorithm takes a number of random vectors and condenses the vectors that are nearest to it, iterating until the least mean error between the vectors is reached. We clustered the data into vectors, and each of these vectors is called a codeword. This set of vectors, or codewords is created for each sound. The codewords for a given sound are then stored together in a codebook for that sound domain. Each speaker's codebook (sound group) is then stored together in a master codebook which is compared to the test sample during the testing phase to determine the sound domain.

Suppose there is a region of space where codeword vectors from several different sounds were laid. If a test vector also falls in this region, the codewords do not help determine the identity of the sound domain because the errors between the test vector and the various codewords will be roughly equal.

Kinnunen and Franti [2004] present an algorithm for discriminating between code vectors during the testing phase to help solve this problem. Their idea is to give a higher precedence to code vectors which give a more definite idea of a domain's identity by weighting them. We used the algorithm they presented and computed weighting coefficients for my codebook data during the training phase. In parts (a) and (b) of Fig.3, we present the features of the sounds for the different domains before and after clustering [MacQueen, 1997].

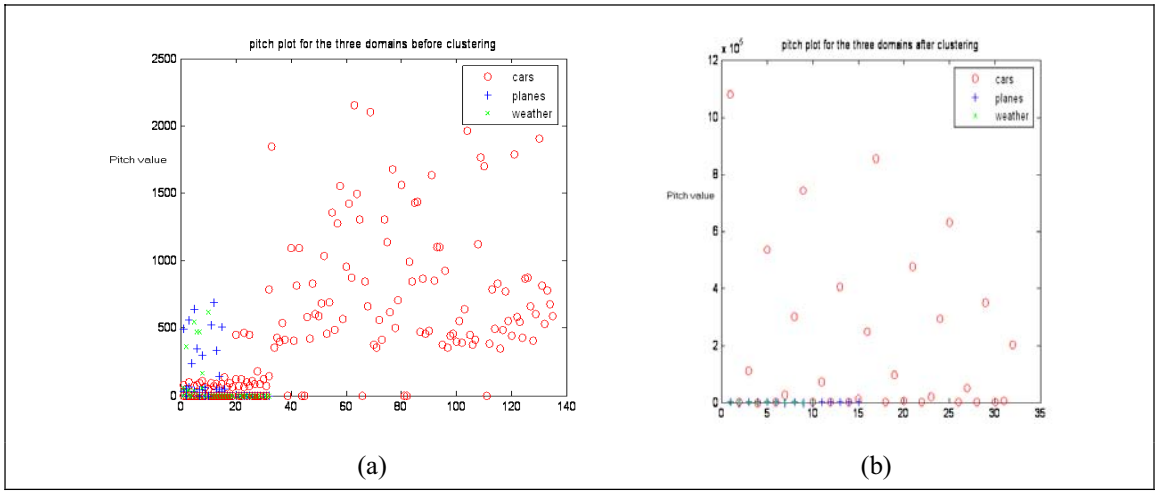

Fig.3 (a) the pitch feature for all sounds in all domains before clustering, (b) the pitch feature for all sounds in all domains after clustering

The figures above depict code vectors before and after clustering, and each shape represents a different group (car, plane, weather). You can see that the distribution of the vectors before and after clustering is different. Weighting the vectors does make a difference.

6. Testing, Results, and Discussion

6.1 Testing

For all of the following tables, denote "recognizing the sound as a car" to be T, "not recognizing the sound as a car" to be F, and we assume that the acceptable interval is between 0.607 and 1.0622. However, we have conducted two types of testing as the following:

1. Using the first method in testing (Feature Extraction based on Statistical analysis), the percentage of recognizing the cars sounds as a car is 92.5% and the percentage of recognizing the plane and rain sounds as a car is 6%; see Tables 1 and 2 below for more details.

Table 1: The performance of the first method in recognition for cars samples

Number of Sample Cars	Recognized	Value of the mean calculation for the sound
1	T	0.70
5	F	0.45
9	F	0.59
10	T	0.77
13	T	0.70
20	T	0.69
35	T	0.80
49	T	0.88
57	T	0.90
62	T	0.96
77	T	0.92
99	T	0.85

Table 2: The performance of the first method in recognition for planes samples

Number of sample Planes and rains	Recognized	Value of the mean calculation for the sound
1	T	0.650
5	F	0.005
9	F	0.020
10	F	0.100
13	F	0.217
15	F	0.168
19	F	0.020
22	F	0.180
25	F	0.054
29	T	0.600
33	F	0.322

2. Second Method in Testing (Vector Quantization); see Tables 3 and 4.

Table 3: The performance of the second method in recognition for cars samples

Number of Sample Cars	Recognized
1	T
5	T
9	T
10	T
13	T
20	T
35	T
49	T
57	T
62	T
77	T
99	T

Table 4: The performance of the second method in recognition for planes and rains samples

Number of sample Planes and rains	Recognized
1	F
5	F
9	F
10	F
13	F
15	F
19	F
22	F
25	F
29	F
33	F

6.2 Results

The voice recognition system that we have built identifies the three main sound domains which are planes, cars, and weather. The recognition for these domains was 100% according to the vector quantization method but the vector quantization method divided all the sound into three mainly regions so any new sound will be approximated into one of these region so to get more accuracy and to avoid any similar sound to the car sound we have developed a new code called feature extraction based on statistical analysis to discard any sound that is similar to the car sound but really not car sound this method with the vector quantization method get accuracy 100% and we assure to make energy conserving with probability reached 100% since the lights will turn only for cars .the feature extraction based on statistical analysis method gain accuracy of 92.5% when work alone.

6.3 Discussion

The idea of the feature selection based on statistical hypothesis testing is to set two classes let's say x1 and x2 and each class has its own shape, distribution, mean, and standard deviation then for a specific sample we will try to investigate whether the values which it takes differ significantly or belongs to these sets. For the feature extraction, we have take the power spectral density for each sound and the mean of all the samples and their standard deviation, then we have make dot multiplication between the mean (power spectral density), of all the samples and the new test sound and upon this number(the result of multiplication) we have decide if this test sound lie in the pre-determined classes or not and the range of comparison was ($\mu - 2*\sigma$, $\mu + 2*\sigma$) so the probability that the data will lie within this range is 95% according to statistical analysis and rules. However, the results of this method were as the following three choices:

1. When executing the code as it is (with

acceptable interval [av-2*std, av+2*std]), the results were as the following:

- Average = 0.8346,
- STD = 0.1138
- The probability of data that will lie here = 95%.
- The correct recognition of car sound = 92.5%.
- Recognizing sound of planes as car= 4%
- Recognizing sound of rain as car= 2%
- Recognizing sound of animals as car= 0%

2. When executing the code and taking the acceptable interval to be [av-sd , av+sd], the results were as the following:
   - Average = 0.8346
   - Std = 0.1138
   - The probability of data that will lie here = 67%.
   - The correct recognition of car sound= 87%
   - Recognizing sound of planes as car= 0%
   - Recognizing sound of rain as car= 0%
   - Recognizing sound of animals as car =0%
3. When executing the code and taking the FFT(sound, 11000) and summing the area under the curve from 0-5500 and interval to be [av-2*sd, av+2*sd] the results were as the following:
   - Average = 0.8324
   - Std = 0.1155
   - Acceptable interval [av-2*std, av+2*std].
   - The correct recognition of car sound =91%
   - Recognizing sound of planes as car= 0%
   - Recognizing sound of rain as car= 8%
   - Recognizing sound of animals as car= 0%.

Based on the results of this paper, we can note that the choice number one is the best

7. Conclusion

The lighting is available for the highways to avoid accidents and to make the driving more safety and more easy, but turning the lights on all the nights will consume a lot of energy which it might be used in another important issues. This paper presented a methodology of using the sound recognition techniques in order to turn the lights on only when there are cars on the highway and only for some period of time. In more details, Linear Predictive Coding (LPC) method and feature extraction have been used to apply the sound recognition. Furthermore, the Vector Quantization (VQ) has been used to map the sounds into groups in order to compare the tested sounds.

However, this paper made the following contributions:

1. Designing a new system for conserving energy based on the voice recognition of the car sound.
2. This system is the first application of this type that concern the street lights.
3. This paper also demonstrates that the weighted Euclidian distance with the LBG algorithm was very helpful and achieved high accuracy.

This paper shows that the feature of the sound that we have extracted is very valuable and really can distinguish between different sounds, so it is differentiate sounds from other or which we can call that it makes speaker identification with high accuracy.

References

Ayuso-Rubio, A. J., Lopez-Soler, J. M., 1995, Speech Recognition and Coding: New Advances and Trends, Springer, Berlin, Germany.

Fukunaga, K., 1990, Introduction to Statistical Pattern Recognition, 2nd edition, Academic Press, London, UK.

Goldberg, R., Riek, L., 2000, A Practical Handbook

of Speech Coders, CRC Press, Boca Raton, FL, USA.

Gonzales, R., Woods, R., 2002, Digital image processing, 2nd edition, Prentice-Hall.

Garg, H. K., 1998, Digital Signal Processing Algorithms: Number Theory, Convolution, Fast Fourier Transforms, and Applications, CRC Press, Boca Raton, FL, USA.

Kinnunen, T., Frunti, P., 2001, Speaker Discriminative Weighting Method for VQ-Based Speaker Identification, In proceedings of the. 3rd International Conference on Audio-and Video-Based Biometric Person Authentication (AVBPA'01), Halmstad, Sweden, pp. 150-156.

Klevans, R., Rodman, R., 1997, Voice Recognition, Artech House Inc., Northfield, MN, USA.

Kuo, S. M., Gan, W.-S., 2004, Digital Signal Processors: Architectures, Implementations, and Applications, Prentice Hall, Englewood Cliffs, New Jersey, USA.

Lyons, R. G., 1996, Understanding Digital Signal Processing, Pearson Education, London, UK.

MacQueen, J., 1967, Some Methods for Classification and Analysis of Multivariate Observations, In proceedings of the 5th Berkeley Symposium on Mathematical statistics and probability, Berkeley, California, University of California Press, pp. 281-297.

Moore, A., 2007, K-means and Hierarchical Clustering, Tutorial Slides, School of Computer Science, Carnegie Mellon University, Online: http://web.cecs.pdx.edu/~york/cs510w04/kmeans09.pdf, Accessed on Dec. 3, 2007.

Nelson, M., Gailly, J.-L., 1995, The Data Compression Book, M&T Books.

Rabiner, L. R. and Juang, H., 1993, Fundamentals of Speech Recognition, Prentice Hall, Englewood Cliffs, New Jersey, USA.

Sayood, K., 2005, Introduction to Data Compression, Morgan Kaufmann, San Francisco, CA, USA.

Smith, D., 2001, Digital Signal Processing Technology: Essentials of the Communications Revolution, American Radio Relay League, Newington, CT, USA.

Zha, H., Ding, C., Gu, M., He, X., Simon, H. D., 2001, Spectral Relaxation for K-means Clustering, Advances in Neural Information Processing Systems, Vol. 14, pp. 1057-1064.

Marsland Press
Journal of American Science 2009:5(2) 13-17

Measurement of refractive index of liquids using fiber optic displacement sensors

Gobi Govindan, Srinivasan Gokul Raj, Dillibabu Sastikumar
Department of Physics, National Institute of Technology, Tiruchirappalli – 620015, INDIA
Tel: +91-431-2503601, Fax: +91-431-2500133, e-mail: sasti@nitt.edu

Abstract:
The paper describes a technique to determine the refractive index of liquids using reflective type fiber optic displacement sensor. The sensor consists of two multimode step index fibers and a mirror. The output light intensity from the receiving fiber is measured as a function of displacement of the fiber with respect to mirror in various solvents. The study shows that the light peak intensity position depends upon the refractive index of the medium. Different liquids such as water, carbon tetrachloride and chlorobenzene were used as a medium. [Journal of American Science 2009:5(2) 13-17] (ISSN: 1545-1003)

Key word: Refractive index measurement; fiber optic sensor; Liquids.

1. Introduction

The refractive index measurement sensors find numerous applications in industries for finding the physical parameters such as concentration, temperature, pressure, etc. Many people have proposed different optical fiber sensors for measuring the refractive index of liquids [M.Laguesse, 1988; Jan Turan et al., 2001; S. Kang et al., 1997; T.Suga et al., 1986; Brant C.Gibson et al., 2003]. Fiber optic sensors are more advantageous than conventional sensors. They exhibit high sensitivity and wide frequency response. They are non-contact and could be used in hostile environments.

Yu-Lung Lo et al., have proposed a fiber optic sensor based on Path-Matching Differential Interferometries (PMDI). It measures change of refractive index in the resolution of about 10^{-5}. Meriaudeau et al., presented a fiber optic chemical sensor based on surface plasmon excitation for refractive index sensing. It can be used to measure the refractive index in the range of 1 to 1.7. A.Suhadolnik et al., proposed an optical fiber reflection refractometer using three optical fibers in which one acts as an emitting fiber and others two as receiving fibers. The intensity ratio of two receiving fibers was found to be function of the refractive index of the medium. The study was carried out in the aqueous solutions of NaCl and LiBr. A.L.Chaudhari and A.D. Shaligram proposed two fiber model sensor (emitting and receiving fibers) based on reflective type fiber optic displacement sensor. The receiving fiber output intensity was measured as a function of a separation between the mirror and fiber for various liquids. It was found that the sensor distinguished the liquids of different refractive index for the separation greater than 6 mm. In these two techniques, the refractive index of liquids was measured in terms of the output intensity of the receiving fiber.

In this paper, we propose a simple and high sensitivity fiber optic sensor. In this technique, the sensor probe under goes linear displacement and

the output corresponding to each displacement is measured. The intensity profile peak is related to the refractive index of the medium.

2. Sensor structure

The sensor was fabricated using two multimode step index optical fibers, which were cemented together with the small spacing between them. Among these, one act as an emitting fiber and other act as receiving fiber which are arranged side by side as shown in fig.1.

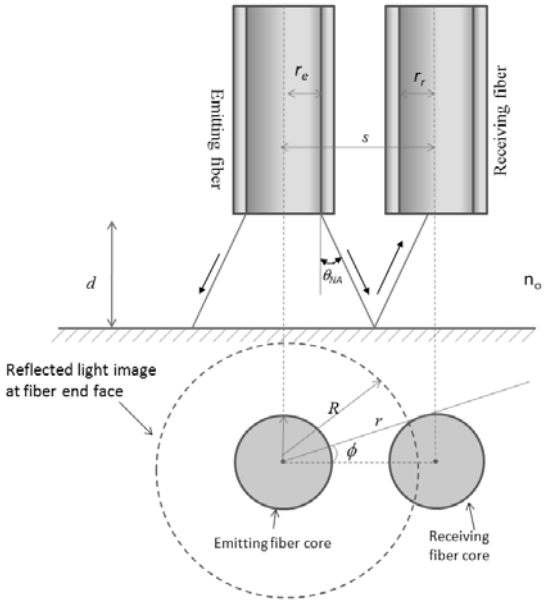

Fig. 1. Schematic structure of the proposed fiber optic sensor

The output of the emitting light spot overlaps the core of the receiving fiber and the output goes through a maximum, when distance between the mirror and optical fibers is changed. At particular position, the intensity peak gets maximum for a given liquid. The characteristics of the sensor depend on the fiber core diameter, numerical aperture, the spacing between the two fibers and refractive index of medium. In this study, fiber core diameter, numerical aperture and spacing between the two fibers are kept fixed.

3. Working model

The working model of the sensor is based on two-fiber model, one act as an emitting fiber and other as receiving fiber. The emitting light angle and receiving fiber capturing light angle are depended on the refractive index of medium (n_0) and numerical aperture (NA) of the fiber. When the fibers have same numerical aperture, the maximum emitting angle θ_{NA} is given by,

$$\theta_{NA} = \sin^{-1}\left(\frac{NA}{n_0}\right)$$

The efficiency factor $\eta(2d,n_0)$ is given as the ratio between the light power captured in the receiving fiber $P_0(2d,n_0)$and the total power P_t launched into the incoming fiber [A.Suhadolnik et al., 1995].

$$\eta(2d,n_0) = \frac{P_0(2d,n_0)}{P_t} = 2\int_{R_1}^{R_2}\int_{0}^{\phi_c} R_m T_i(n_0) T_0(r,2d,n_0) \frac{2}{\pi R^2(d)}\left(1-\frac{r^2}{R^2(d)}\right) r\,d\phi\,dr$$

Where, P_t is the total optical power transmitted through the input fiber, $P_0(2d,n_0)$ the light power captured by the receiving fiber and 'R_m' is the mirror reflectivity. The $Ti(n_0)$ and $T_0(r,2d,n_0)$ are Fresnel transmittance coefficients of the emitting fiber and receiving fiber, respectively. The 'r' is the distance from the emitting fiber axis, ϕ is the azimuth angle, 'r_e' and 'r_r' are input and receiving fiber radius respectively. The 's' is spacing between the fiber cores, 'd' is distance between the mirror and fiber tip and 'R' is the radius of the light cone at the distance 2d, and R is given by

$R = r_e + 2d \tan(\theta_{NA})$.

The fig. 2. gives the theoretical curve for s = 1.2mm, NA =0.47 and nc = 1.495 (refractive index of fiber core) for a air medium [A.Suhadolnik et al., 1995].

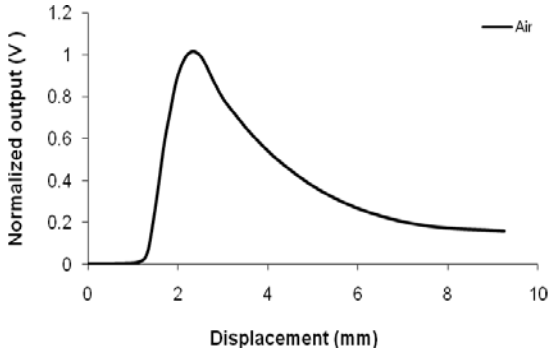

Fig. 2. Theoretical curve for air medium

4. Experiment

The optical fibers were attached to a movable micrometer stage, as shown in fig.3. The core and cladding diameters of input fiber and output fibers were 200 & 225 μm and 400 & 425μm, respectively. The core separation of input fiber and receiving fiber was 500 μm. Displacement measurements were carried out by mounting the sensor in front of aluminium coated mirror. The LED (λ=625nm) was used as a light source.

The output intensity of the receiving fiber is measured by the photodectector. Various solvents such as water, carbon tetrachloride and chlorobenzene were used.

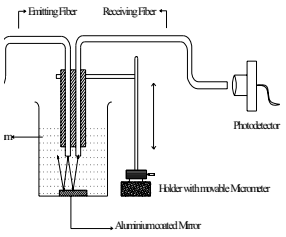

Fig. 3. Block diagram of the experimental set-up.

5. Results & Discussion

Fig. 4. shows the variation of the output of the receiving fiber for various displacements. It is seen initially that the output is almost zero for small displacements (about 1.2mm). When the displacement is increased, the output starts increasing rapidly and reaches a maximum. Further increase in the displacement leads to decrease in the output as shown in figure. These behaviors are similar to that observed by theoretical model (eg. air medium) [A.Suhadolnik et al., 1995] (Fig.2).

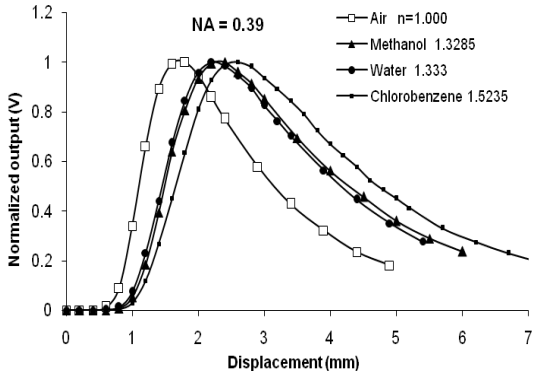

Fig. 4. Normalized output Vs Displacement (NA:0.39)

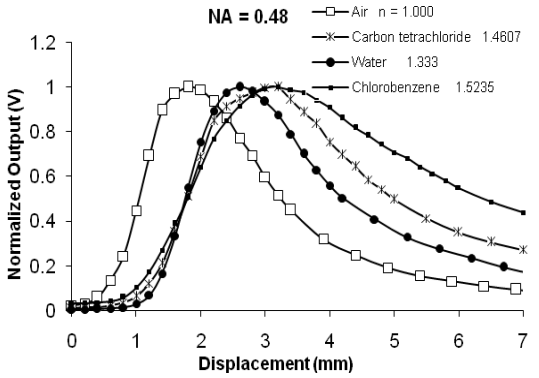

Fig. 5. Normalized output Vs Displacement (NA:0.48)

The variation of output intensity with displacement may be understood as follows. For smaller displacements, the size of the cone of light from the emitting fiber is very small and doesn't reach the receiving fiber after reflection.

This results in almost zero output. When the displacement is increased, the size of reflected cone of light increases and starts overlapping with the core of the receiving fiber leading to presence of small output. Further increase in the displacement leads to large overlapping resulting in rapid increase in the output and reaches a maximum. The output after reaching the maximum starts decreasing for larger displacements due to increase in the size of the light cone as the power density decreases.

It is seen in the fig. 4. that the maximum intensity varies for different solvents. It may be related to the change in the size of the cone of the emitting light due to change in the refractive index of the medium. Fig.5. shows the plot observed for the optical fibers with numerical aperture of 0.48.

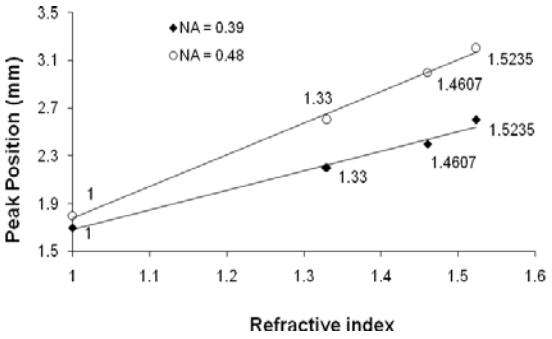

Fig. 6. Variation of peak position for different refractive index of medium

Fig.6. shows a plot between the refractive index of the medium and peak position. It is seen that when the refractive index increases, the peak position occurs at larger displacements. There is a linear relation ship between the peak position and the refractive index of the medium. The results suggest that the sensitivity increases when the numerical aperture is large.

Different light powers were used (1.5 to 3.5 μW) to understand the effect of light power on the output characteristics of the sensor. Fig.7. shows the output characteristics of the sensor for various powers for a water medium.

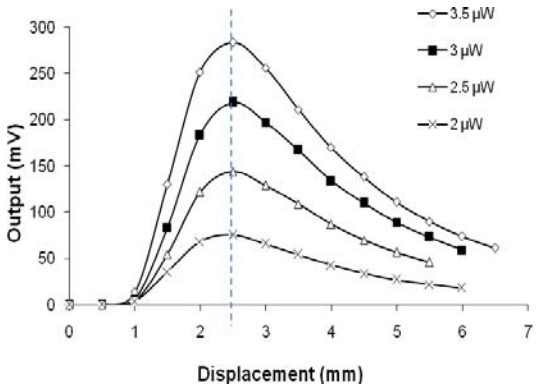

Fig. 7. The output characteristics of the sensor

It is seen that the intensity peak remains constant though the intensity profile varies for various powers. It shows that the output intensity peak position in a given liquid is independent of the power change or absorption of light by the medium.

6. Conclusions

A simple fiber optic sensor is presented to determine the refractive index of liquids. The study shows that the output light intensity peak observed in various liquids is function of the refractive index of the medium and there is a linear relationship between them. The paper presents the results obtained for the liquids over the refractive index range of 1 to 1.52. The light intensity peak in a given medium is independent of the change in the light power or any light absorption by the medium.

References

M.Laguesse, 1988. An optical fiber refractometer for liquids using two measurement channels to reject optical attenuation. J.Phys.E: Sci.Instrum.,

21: 64-67.

Jan Turan, Edward F.Carome and Lubos Ovsenik, 2001. Fiber Optic Refractometer for Liquid Index of Refraction Measurements. TELSIKS 2001, 19-21: 489- 492.

Yu-Lung Lo, Hsin-Yi Lai and Wern-Cheng Wang, 2000. Developing stable optical fiber refractometers using PMDI with two-parallel Fabry-Perots, Sensors and Actuators B, 62: 49-54.

F.Meriaudeau, A.Wig, A.Passian, T.Downey, M.Buncick and T.L.Ferrell, 2000. Gold island fiber optic sensor for refractive index sensing, Sensors and Actuators B, 69: 51-57.

A.Suhadolnik, A. Babnik and J.Mozina, 1995 Optical fiber reflection refractometer, Sensors and Actuators B 29: 428-432.

A.L. Chaudhari and A.D. Shaligram, 2002. Multi-wavelength optical fiber liquid refractometry based on intensity modulation, Sensors and Actuators A, 100: 160-164 ().

S. Kang, Delbert E.Day and James O.Stoffer, 1997. Measurement of the refractive index of glass fibers by the Christiansen-Shelyubskii method, Journal of Non-Crystalline Solids, 220: 299-308.

T.Suga, N.Saiga and Y.Ichioka, 1986. Measurement of the refractive-index profile a graded-index optical fiber by the interference microscope employing fringe scanning, Optica Acta, 33(2): 97-101.

Brant C.Gibson, Shane T.Huntington, John D.Love, Tom G.Ryan, Laurence W.Cahill and Darrell M.Elton, 2003 . Controlled modification and direct characterization of multimode-fiber refractive–index profiles, Applied optics 42(4): 627-633.

Roger H.Stolen, William A.Reed, Kwang S.Kim and G.T.Harvey, 1998. Measurement of the nonlinear refractive index of long dispersion-shifted fibers by self-phase modulation at 1.55μm Journal of Lightwave Technology, 16 (6): 1006-1012.

Marsland Press
Journal of American Science 2009:5(2) 18-28

Temporal Object-Oriented System (TOS) for Modeling Biological Data

Abad Shah, Syed Ahsan, Ali Jaffer
Department of Computer Science and Engineering, University of Engineering and Technology, Lahore, Pakistan

Abstract:

In the last two decades, exponential growth of biological data has posed enormous challenges for the computing and database communities. This wealth of complex and diverse data demands new modeling techniques for seamless and efficient data management. The object-oriented data modeling technique emerged as an optimum choice for modeling scientific data types due to its flexibility and ability to cope with complexity and diversity of the data. In this paper, we investigate the possible applicability of the Temporal Object-Oriented System (TOS) in Bioinformatics domain. We have extended TOS by developing a methodology for dynamic evolution of ROF (Root of Family). Temporal Object Query Language (TOQL) has also been extended by including new operators. In our opinion, our proposed model due to its inherent temporal nature, offers better support to deal with peculiarities of biological data such as data and schema evolution, data provenance and temporal instability. [Journal of American Science 2009:5(2) 18-28] (ISSN: 1545-1003)

Keywords: Bioinformatics, temporal object-oriented system, schema evolution, data provenance, temporal instability

1. Introduction

Current research in biology has produced a huge amount of data owning to advances in hardware and wet lab experimental techniques. Further success in the life sciences hinges critically on the availability of better computational and data management tools and techniques to analyze, interpret, compare, and manage this huge volume of data[Ahsan and Shah, 2008; Ferrandina et al., 1995]. The existing data management techniques are often challenged by the inability to handle instability, evolving nature and implicit scientific knowledge that is characterized by biological data [Ahsan and Shah, 2005]. These problems stem from various inherent peculiar characteristics of biological data [Ahsan and Shah, 2008; Jagadish and Olken, 2003].

We identify these characteristics of the biological data and information which makes it different and difficult to handle from the conventional (or non-biological) data. Consequently, these characteristics also makes different and difficult to develop a database management system for the handling and maintaining of this type of data [Achard et al., 2001]. In biology, the data and its inter-relationships have a profound effect on the system of which they are part of therefore it is important and useful to identify the characteristics of both data and the information of their relationships in a biological system [Ahsan and Shah, 2008; Bornberg and Paton, 2002]. The characteristics are listed and described as follows.

(i) Biological data and its information are highly evolutionary, uncertain and incomplete. The latest research invalidates the established facts as they are completely changed or modified [Ostell et al., 2001].

(ii) This is unprecedented type of data [Marijke Keet, 2003]. For example, a molecule, such as a bacteriocin, can be coded ‘mostly’ on plasmids and transposons, though ‘rarely’ on chromosomal DNA, plus a transposon can insert itself into a plasmid: should one classify the gene location as transposon or plasmid, or both.

(iii) Depending on the environment, the behavior of an object/entity of a biological system can vary [Albert, 2002].

(iv) Same data item (biological object) can have different structure in the different environments [Baldi and Brunak, 2004].

(v) Data in bioinformatics is semi-structured [Albert, 2002].

(vi) Even accurately studied and analyzed a biological system can become erroneous and liable to be discarded due to data curation, interpretations, tinkering and

experimentation at some later stage [Baldi and Brunak, 2004].

(vii) A biological data object can increase its size in the incremental fashion with the availability of new information about the object [Marijke Keet, 2003].

(viii) Biological data is explorative and iterative in nature as it depends upon scientific inquiry.

In our opinion, the conventional data management approaches such as hierarchical, network, structured and relational, although used in certain application areas of biology, are unsuitable and constrained to handle biological data due to the above mentioned characteristics.

In this paper we propose Temporal Object-Oriented System (TOS) for modeling biological data. In our opinion, due to its inherent temporal nature, it offers better support to deal with peculiarities of biological data such as data and schema evolution, data provenance and temporal instability.

Section 2 presents an introduction to TOS and summary of similar significant efforts available in literature. Suitability of TOS for Bioinformatics is explored in Section 3.In section 4 we have presented a methodology for dynamic evolution of ROF as well an algorithm is provided to serve as basis for the implementation of proposed methodology. In Section 5 we provide new operators for TOQL [Fotouhi, 2001] to manipulate semi-structured biological data; use of proposed operators is illustrated with the help of sample queries. Last section identifies some future directions which be perused for more research in Bioinformatics using TOS as basic platform.

2. Related Work

Object-oriented databases and data models have been favored by researchers to store and manipulate complex data in engineering and science. In the last fifteen years, Temporal data modeling for object oriented databases have been an active area of research [Bertino et al., 1997; Rose and Segev, 1991; Su and Chen, 1991] and significant work regarding schema evolution for Object-oriented databases is available in the literature [Goralwalla and Szafron, 1997; Ferrandina et al., 1995]. Temporal and evolutionary Object-oriented data modeling practices have been used in the areas of clinical and medical informatics successfully [Aberer, 1995; Chu et al., 1992; Combi et al., 1995; Goralwalla et al., 1997].

A new domain of applications is identified in [Ahsan and Shah, 2008; Shah, 2001] by specifying characteristics of the domain for which Temporal Object-Oriented System (TOS) is more suitable. The applications such as Computer-Aided Construction (CAC) and the Web-based applications belong to this class of applications or domain. One typical characteristic of the objects of this class of applications is that they frequently change their structure (instance-variables and methods), state (or data values), or both. Here, we list the main characteristics of the application domain as identified by Shah in [Shah, 2001]. More details can be seen in [Ahsan and Shah, 2008; Shah, 2001]. We also add a few more characteristics which are endemic to Bioinformatics, thus broadening the scope of the applications conforming to these characteristics. .

i) Applications without hierarchical structure
ii) Rapid prototype development
iii) Incremental growth of objects
iv) Desirability to trace back changes to a specific object
v) Where the grouping of objects is not important
vi) Simultaneous capturing of changes to both parameters (i.e., structure and state) of objects
vii) Polymorphic behavior of objects.
viii) Evolutionary Behavior of the Objects.
ix) Vague Functional Characteristics(This results from imprecise and incomplete data and information about the application domain)
x) The requirements are emergent i.e., the activity of developing, delivering and using the software itself yields more requirements thorough better understanding of the problem.

These characteristics can form the basis of identifying the situations where Temporal Object-Oriented System (TOS) approach is more suited as compared to traditional approaches [Ahsan and Shah, 2008]. Most of the characteristics of bioinformatics domain listed in Section 1 and those listed above are common. These common characteristics suggest that bioinformatics also belong to same class of applications for which Temporal Object-

Oriented System (TOS) approach is more suitable.

2.1 The Temporal Object System (TOS)

An object is represented by its structure and state. With the passage of time an object may change its structure and/or its state. By associating time to both the structure and the state of an object, we can keep the history of changes to that object. The Temporal Object System (TOS) data model was introduced in 1992 to capture all types of changes (structural, stature or combination of both) to an object in a uniform fashion [Fottouhi and Shah, 1994; Shah, 1992; Fotouhi et al., 1992].

[Fottouhi and Shah, 1994; Shah, 1992; Fotouhi et al., 1992] also defines a temporal object (TO) to be an ordered set of objects which is constructed at different time instances. A temporal object is represented as *TO = {(SR t1, STt1), (SRt2, STt2),..., (SRtn STtn)}* where $ti \leq ti+1$ for all $1 \leq i < n$, and where the ordered pair *(SRti, STti)* is the *i*-th object of the temporal object which is constructed at the time instance *ti*, with structure *SRti* and state *STti*. An *i*-th object of the temporal object is referred to as its *i*-th stage [Fottouhi and Shah, 1994; Shah, 1992; Fotouhi et al., 1992]. A new stage (or *current stage*) of a temporal object shares the structure and/or state from the previous stage, which is not defined in the new stage. A temporal object may also be referred to as *an ordered set of stages*. For example, in Figure 1 the temporal object *TOa* of the family

Fi has *n* number of stages. The first and last stages of a temporal object are significant because they hold the initial and current knowledge of the temporal object. We refer to these stages as the *birth stage* (stage *Si.a* in Figure 1) and the *current stage* (stage *Sn.a* in Figure 1) of the temporal object *TOa*. The current stage (or the *n*-th stage) is the latest stage that is appended to the temporal object. A new stage is appended to a temporal object when a change occurs to the structure and/or state of the temporal object.

In Fig1, a Temporal Object TO_a is represented by large oval, circles represent the stages, double oval represents root-of-family (ROF), down arrows show transition from one stage to another, where $S_{1,a}$ is birth stage and $S_{n,a}$ is current stage of TO_a, up arrow from TO_a to ROF shows Temporal Inheritance

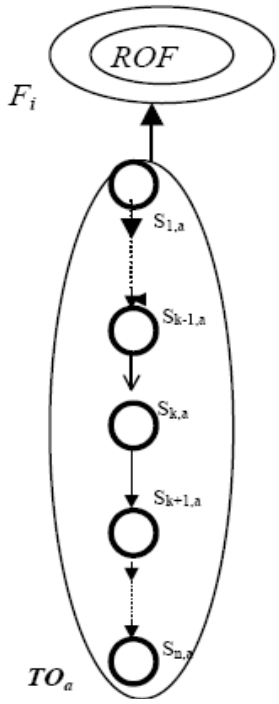

Figure 1: A Temporal Object TO_a

TOS [Fottouhi and Shah, 1994; Shah, 1992; Fotouhi et al., 1992] introduces notion of family to group temporal objects sharing a common context. All temporal objects within a family can be treated in similar way by responding uniformly to a set of messages. A set of similar structures and/or states defines a common context of a family. The common context of family is refereed to as the *root-of-family* (ROF) where common knowledge about all its temporal objects is maintained [Fottouhi and Shah, 1994; Shah, 1992; Fotouhi et al., 1992]. Formation of ROF must be preceding the creation of any of the temporal object of a family. Apparently the concept of family sounds similar to concept of Class which serves as a specification of objects in Class-based object oriented systems. But family in TOS encapsulates more features than a Class. For example, in a Class, the structure of Class is always shared by all of its instances (objects) and change in structure affects all of the created objects. Where as in a family, the structure or state of each temporal object share the ROF only at the time instance of its birth. After that each temporal object is independent and a change in a particular TO doesn't affect the ROF or any other object of the family. In other words, the ROF of family is read only, it doesn't change with the passage of time.

Frequent and rapid changes in biological data demand evolution of schemas. Concept of ROF is not exactly same but analogous to schemas in databases; current architecture of TOS does not provide support for the evolution of ROF when temporal objects of a family change their stages during their life span. Since creation of new temporal objects in TOS is dependent on ROF, that is why we believe that ROF for TOS should have provision for evolution to make a consistent schema available for new temporal objects.

3. TOS for Bioinformatics

Historically object-oriented paradigm is favorable for the problem solving in complex domains. It is a well acknowledged theory that the object-oriented databases and data models are an appropriate approach for biological data modeling, because they allows to represent strongly interconnected data more directly for simpler usage and maintenance. Biological data is available in so many different types ranging from semi-structured text, unstructured text, images, 3D structures, tables, trees and graph structures. In object oriented models, scientific data types can be efficiently implemented through abstract data type definitions. By means of encapsulation, object-oriented database systems allow to support complex operations within the database schema. Encapsulation is important to maintain complex consistency constraints and to maintain consistency of derived data, but also to integrate complex external operations. In [Aberer, 1995], a comprehensive discussion is presented on the use of object-oriented data model for biomolecular databases. It is also considered that object-oriented data models are a suitable basis for the integration of heterogeneous databases which is among the important challenges faced by Bioinformatics community.

In the past, research [Marijke Keet, 2003] has shown good results on integration of object-oriented and temporal databases.

Keeping all above facts in mind we have investigated the suitability of TOS [Fottouhi and Shah, 1994; Shah, 1992; Fotouhi et al., 1992] for Bioinformatics. It is unjust to claim that any single data model can serve as solution to all issues, challenges and problems of Bioinformatics; similarly we hereby don't declare that TOS is capable of addressing all the issues of biological data modeling. But important is to note that, TOS provides good support to tackle with the issues of data evolution, data provenance, and temporal instability in particular and data size, distribution in general.

TOS presents an elegant mechanism for evolution of data objects, a temporal object evolves throughout its life as change occurs to its state and\or structure, but TOS does not allow *root-of-family* (ROF)to evolve and imposes a read-only restriction on it, to make TOS model completely evolutionary we have extended this particular aspect of TOS, detail of which is presented in section 3.2. TOS is also capable for addressing the data provenance issue of biological data. Data provenance is knowledge about the origin of some piece of data and the process by which a particular data object reached at its current status and form. Data provenance replies two important queries i.e. about the originating source and derivation history of data items.

With the help of temporal parameters (life sequence, life span and time span) described by TOS, lineage or provenance of data objects can be traced easily. An ordered sequence of stages

of a temporal object is referred to as its life sequence. Suppose temporal object TO_a has its life sequence given as:

$L_{TOa} = \{ S_{1,a}, S_{2,a}, \ldots, S_{j,a} \}$

Where $S_{1,a}$ is the birth stage and $S_{j,a}$ is the j-th stage of the TO_a , if we consider the j-th stage as current stage of a temporal object then L is referred to as a complete life sequence of temporal object.

Our proposed extension in TOS described in section 4 particularly deals with the issue of temporal instability of biological data.

3.1 The Cell Structure Example:

It is perceived that Bioinformatics domain may face a crisis due to hesitation of computing and database professionals towards Bioinformatics, as normally computer science professionals are not well equipped with the knowledge of microbiology, exceptions apart [Ahsan and Shah, 2005]. To avoid the crisis it is suggested to choose examples from the domains more familiar to computer science specialists and issues addressed by those scenarios can be mapped to Bioinformatics problems as well [Ahsan and Shah, 2005].

Keeping the above fact in mind, we present a simple hypothetical example to explain the TOS [Fottouhi and Shah, 1994; Shah, 1992; Fotouhi et al., 1992] concepts in detail. The following example will be of equal interest to computing experts due to its simplicity and to microbiologist due to its relevancy.

Cell, in biology, the unit of structure and function of which; all plants and animals are composed. The cell is the smallest unit in the living organism that is capable of integrating the essential life processes. Cells can be separated into two major groups—prokaryotes, cells whose DNA is not segregated within a well-defined nucleus surrounded by a membranous nuclear envelope, and eukaryotes, those with a membrane-enveloped nucleus. Though the structures of prokaryotic and eukaryotic cells differ, their molecular compositions and activities are very similar. Fig 2 shows the structure of a TOS for two basic categories of a cell, where RTOS denotes the root node of the system and there are two simple families (rectangles): Prokaryote family and Eukaryote family.

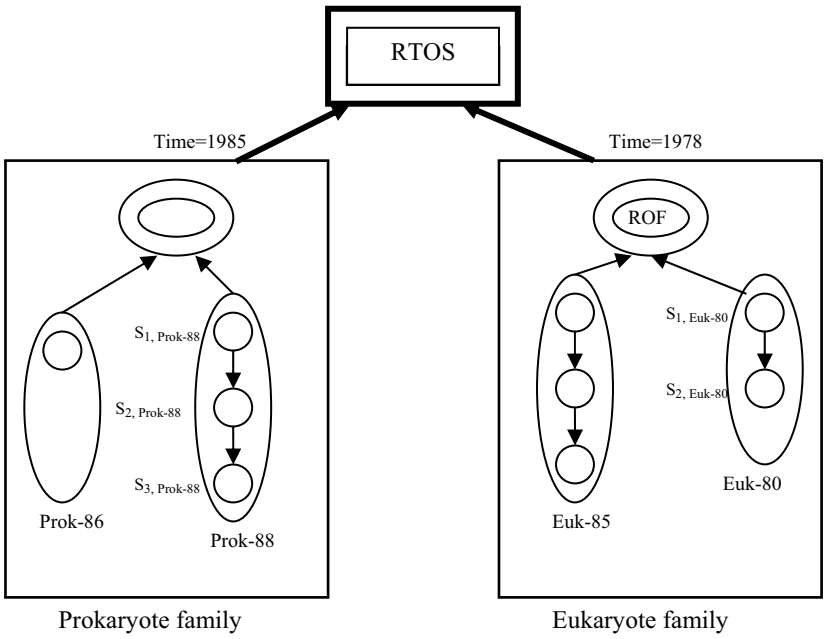

Figure 2: Simple families of two basic cell groups

TOS supports representation of time with different granularities depending upon application domain, but to keep our example simple, in this paper we use an abstract time "year" in each stage, temporal object and family. There are two temporal objects representing information of two prokaryotic cells Prok-86 and Prok-88 (say Bacteria and Archaea) in prokaryote family, Prok-86 comprised of only one stage which is the birth and current stage created at time instance, time=1986. Prok-88 cell is at its current stage S_3 due to evolution in structure or state, maybe due to metabolic reactions etc. , A new sage is appended to a TO only if the structure and/or state associated with its existing current state changes. Two eukaryotic cells Euk-80 and Euk-85 are also modeled in the similar fashion showing transition from their birth stage to current stage.

Table 1: ROF's of simple families: Prokaryote and Eukaryote

ROF (Prokaryote)	ROF (Eukaryote)

Instance-variables
{
Time: 1985
Diameter: ,
Surface-to-volume ratio: ,
Num-of-basic-chemicals:
}
Methods {growth_rate: }
	Instance-variables
	{
	Time: 1978
	Diameter: ,
	Surface-to-volume ratio: ,
	Num-of-basic-chemicals: ,
	Metabolism type: ,
	Cell division type:
	}
	Methods {metabolic_rate: }

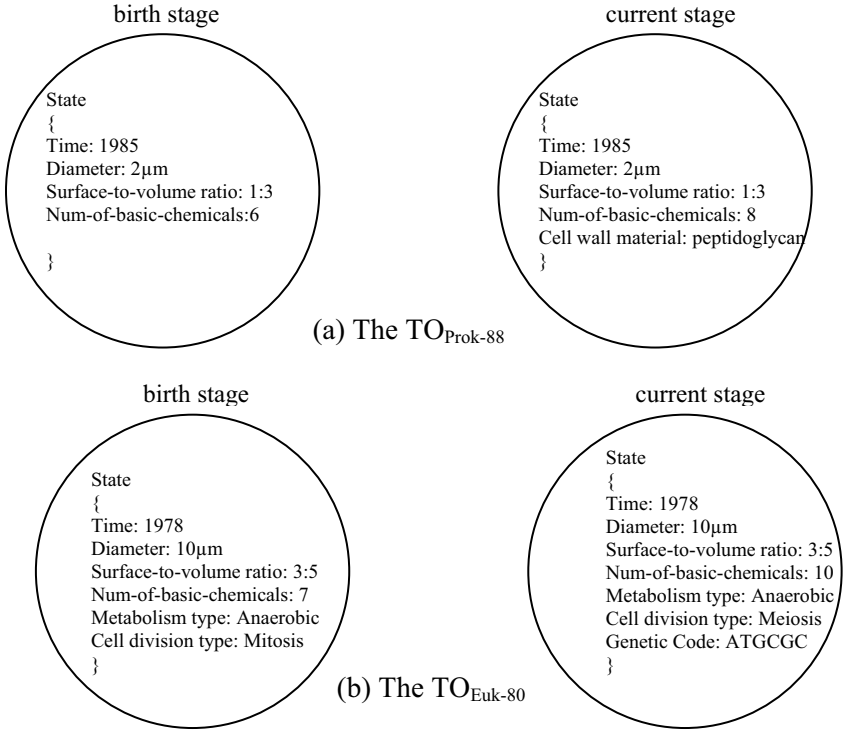

Figure 3: The birth and current stages of temporal objects Prok-88 and Euk-80

Fig 3(a) shows the birth stage of temporal object Prok-88 and its current stage which resulted due to change in value of one instance variable i.e. Num-of basic-chemicals and addition of one more instance variable i.e Cell wall material, where as Fig 3(b) represents birth stage of temporal object Euk-80 and its current stage which resulted due to change in value of two instance variables i.e. Num-of basic-chemicals and Cell division type and due to addition of one more instance variable i.e Genetic Code.

3.2 ROF Evolution Methodology

Schemas for biological (or medical) databases have a marked tendency to grow to large sizes to model the diverse sorts of data, and to evolve rapidly as laboratory protocols, instrumentation, and knowledge of molecular biology evolves. Robustness over the long term is a challenge because of evolution to the schema as our understanding of biological systems grows and as new experimental techniques are developed [Baldi and Brunak, 2004]. For this to achieve, biological databanks need a dynamic evolving schema [Ahsan and Shah, 2005].

Schema or class evolution normally takes place due to change in requirements or computational environment or due to discovery of new facts and all of these factors are very common in Bioinformatics. Requirements of biological scientists cannot be precisely determined and generalized. What at present is considered as an attribute may become of such importance over time, that it has to be upgraded to an entity type [Ahsan and Shah, 2005]. Keeping in mind the temporal instability of biological data, ROF must evolve to capture the homogeneous changes available in all the temporal objects of a family. There are there possible situations for a class to change its structure [Fottouhi and Shah, 1994; Shah, 1992; Fotouhi et al., 1992]. These are:

Type I: Adding new instance variables, methods, and/or rules

Type II: Deleting instance variables, methods, and/or rules

Type III: Changes to an instance variable, a method, and/or a rule

We propose a methodology for evolution of ROF when any of above type of change causes a temporal object to promote from a previous stage to its current stage, so whenever some structural change is observed in temporal object of a family, it will become a candidate for ROF update process. If with the passage of time a new attribute become member of all TOs of a family then ROF of this family must be updated by including this new attribute as a member of ROF. We propose that, structure of a TO should be divided in two logical portions i.e. primary portion and secondary portion. Primary portion will contain information about those members which a temporal object inherits from ROF at its birth time where as secondary portion of temporal object will retain information of members which specifically belong to this temporal object and are not part of ROF. This approach will make comparison process very fast which is required to analyze the consistency and uniformity in the structure of TOs as a result of any change.

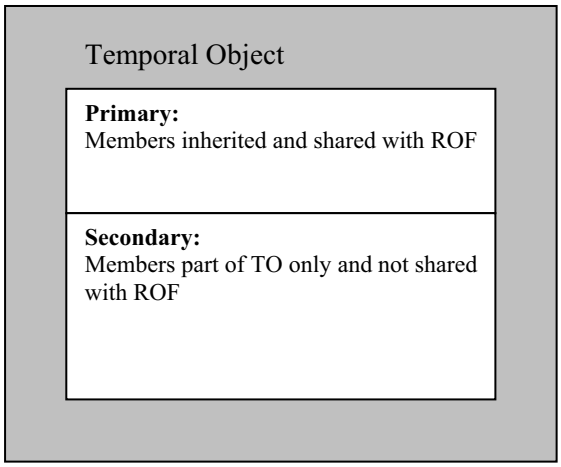

Figure 4: Proposed Structure of Temporal Object

Our proposed methodology presents an efficient solution of the problem, whenever a TO moves to a new stage as a result of any change, first of all that change will be analyzed to find out the nature of the change, if new stage resulted due to change in state, then this change will be ignored simply because only change in structure demands schema (ROF) to be evolved. But if structural change is observed then further analysis will be done to find out the type of change i.e. either type I, type II or type III change in a TO. Further analysis will identify that whether the change occurred to the primary or secondary portion of a temporal object.

Type I change is possible only in secondary portion of the temporal object; ROF of a family can be updated only in case of Type I change. Type II and Type III changes are applicable to

both primary and secondary portions of a TO, but ROF will not be updated in case of Type II and Type III changes, to keep the history of database consistent we do not allow deletion and modification in ROF.

If some change occurred to the primary portion of a TO, then only the primary portions of the BTOs (Brother Temporal Objects: a term used to denote the temporal objects belonging to a single family of TOS) will be searched to check that whether the change is available in all BTOs. ROF of this family will be updated only if the change is consistent with all the BTOs. By this methodology we do not have to compare the change against each member of a temporal object, simply the relevant portions of TOs will be searched to check the consistency and uniformity of the change.

In case of Type I change to a temporal object, if that change is available in all BTOs, the newly added member(s) will be included in ROF as well as moved from secondary portion to primary portion. For Type II and Type III change, ROF update process will not be initiated.

Suppose, with the passage of time, a new instance variable "Cell wall material" got inducted in each temporal object of Prokaryote family, now further creation of temporal objects of this family requires inclusion of instance variable "Cell wall material" in each newly created temporal object. Using our ROF evolution methodology, ROF of Prokaryote family will be updated against this homogeneous change.

Table 2: ROF of simple family Prokaryote after ROF evolution

ROF (Prokaryote)
Instance-variables
{
Time: 1985
Diameter: ,
Surface-to-volume ratio: ,
Num-of-basic-chemicals: ,
Cell wall material:
}
Methods {growth_rate: }

3.2.1 Algorithm

We provide a pseudo code implementation of above described Methodology to make TOS an evolutionary model by giving provision to update ROF.

```
START
Monitor TOs, when new stage is appended to a temporal object
        Analyze the nature of change
                If new stage is appended to a TO due to change in state only
                        Transfer control to END
                Else
                        Determine the type of change
                        type I change:
                                Search the secondary portion of all BTOs to verify the presence of
                                definition of newly added member
                                        If definition available in all BTOs
                                                Move the definition of newly added member(s) to
                                                primary portion of all BTOs
```

```
                                        Update the ROF by including definition of new
                                        member(s)
                                ELSE
                                        Transfer control to END
                        type II change:
                                Transfer control to END
                        type III change:
                                Transfer control to END
END
```

4. Conclusion

Biological data poses unprecedented challenges to data management community due to its peculiar characteristics. These characteristics make biological data volatile and temporally unstable, characterized by an evolving schema. Object oriented and Temporal Object System has been used to model complex data such as in CAD, CAM and clinical data. In this paper we identified those characteristics of biological data which suggest that it belongs to the class of applications for which TOS has been suggested as a suitable model. In this paper we proposed modifications to TOS to make it suitable for modeling biological data. The modifications were primarily in Root Of Family (ROF), which was made evolutionary to accommodate and handle the three types of changes which a biological object may go through. In out opinion, TOS is inherently equipped to model biological data and the case study provided in our paper supports this. In our future work we are looking in to the possibility of using TOS to model data provenance, versioning and other related issues. We are also extending Temporal Object Query Language (TOQL) to include new operators for providing natural support to temporal biological queries.

References:

Alberts, B..Molecular Biology of the Cell. Garland Science Publishers , New York (2002)

A. Shah, "TOS: A Temporal Object System," Ph.D Dissertation, Wayne state University, Detroit, Michigan, 1992

Ahsan S. and Shah, A. 'An Agile Development Methodology for the Development of Bioinformatics'. The journal of American Science" Volume 4 (1), 2008, USA. ISSN 1545-1003.

Bornberg-Bauer, E. and Paton, N.W.,,'Conceptual Data Modeling for Bioinformatics, *Briefings in Bioinformatic s, 2*002

C. Combi, F. Pinciroli, and G. Pozzi. Managing Different Time Granularities of Clinical Information by an Interval-Based Temporal Data Model. *Methods of Information in Medicine*, 34(5):458–474, 1995.

E. Bertino, E. Ferrari, and G. Guerrini. T Chimera - A Temporal Object-Oriented Data Model.*Theory and Practice of Object Systems*, 3(2):103–125, 1997.

F. Fotouhi, A. Shah, I. Ahmed and W. Grosky, "TOS: A Temporal Object-Oriented System," *Journal of Database Management*, *5(4),* pp. 3-14. 1994.

F. Fotouhi, A. Shah and W. Grosky, "TOS: A Temporal Object System," The 4th International Conference on Computing & Information, Toronto, Canda, 353-356, 1992.

F. Achard, G. Vaysseix, and E. Barillot, "XML, bioinformatics and data integration". Bioinformatics Review, vol. 17 no. 2, 2001 pages 115-125, Oxford University Press. 2001.

F. Ferrandina, T. Meyer, R. Zicari, G. Ferran, and J. Madec. Schema and Database Evolution in the O2 Object Database System. In *Proc. 21st Int'l Conf. on Very Large Data Bases*, pages 170–181, September 1995

H.V. Jagadish, and F. Olken, "Database Management for Life Science Research," *OMICS: A Journal of Integrative Biology* 7(1):131-137, 2003.

I.A. Goralwalla, D. Szafron, M.T. O¨ zsu, and R.J. Peters. Managing Schema Evolution using a Temporal Object Model. In *Proc. 16th International Conference on Conceptual Modeling (ER'97)*, pages 71–84, November 1997.

I.A. Goralwalla, M.T. O¨ zsu, and D. Szafron. Modeling Medical Trials in Pharmacoeconomics using a Temporal Object Model. *Computers in Biology and Medicine - Special Issue on Time-Oriented Systems in Medicine*, 27(5):369 – 387, 1997.

K. Aberer, "The Use of Object–Oriented Data Models for Biomolecular Databases," Proceedings of the Conference on Object–Oriented Computing in the Natural Sciences (OOCNS) '94 , Heidelberg, 1995.

Marijke Keet. (2003). Biological Data and Conceptual Modeling Methods. *the Journal of Conceptual Modeling, Issue: 29*

Ostell, JM., S.J. Wheelan, J.A. Kans "The NCBI Data Model in Bioinformatics: A Practical Guide to the Analysis of Genes and Proteins 2ne Edition. John Wiley & Sons Publishing. . 2001. ISBN: 0471383910 pp. 19-44.

P. Baldi and S. Brunak, (2004). Bioinformatics: The Machine Learning Approach " 2nd edn, MIT Press**,** Volume 19 , Issue 1.

Rose and A. Segev. TOODM - A Temporal Object-Oriented Data Model with Temporal Constraints. In *Proc. 10th Int'l Conf. on the Entity Relationship Approach*, pages 205–229, October 1991.

S. Ahsan and A. Shah, "Identification of Biological Data Issues and Challenges through Real World Examples", *ACIT'2005 conference*, Jordan. December 2005.

S.Y.W. Su and H.M. Chen. A Temporal Knowledge Representation Model OSAM*/T and its Query Language OQL/T. In *Proc. 17th Int'l Conf. on Very Large Data bases*, pages 431–442, 1991.

http://www.dagstuhl.de/Reports/98471.pdf Seminar Report for Dagstuhl Seminar on Integrating Spatial and Temporal Databases, Schloss Dagstuhl-Wadern, Germany, 1998. [Accessed: May 7, 2007].

http://hpcrd.lbl.gov/staff/olken/wdmbio/wsproposal1.htm Web page of Workshop on Data Management for Molecular and Cell Biology, 2003. [Accessed: April 25, 2007].

Shah, A., (2001) .A Framework for Life-Cycle of the Prototype-Based Software Development Methodologies. *the Journal of King Saud University*, *Vol. 13*, Pp. 105-125.

W.W. Chu, I.T. Ieong, R.K. Taira, and C.M. Breant. A Temporal Evolutionary Object-Oriented Data Model and Its Query Language for Medical Image Management. In *Proc. 18th Int'l Conf. on Very Large Data Bases*, pages 53–64, August 1992.

Marsland Press
Journal of American Science 2009:5(2) 29-35

Experimental Study on the Dynamic Behaviors of the Material for Clay core wall sand dams

[1, 2] Shangjie Xu,[1] Faning Dang, [1]Wei Tian, [2]Mo Cheng

[1]Institute of Geotechnical Engineering,Xi'an University of Technology,Xi'an,China,710048

[2]Detecting Institute for Engineering, Shandong Provincial Institute of Water Resources,Jinan,China, 250013

Abstract:

The Clay core wall sand dams are mostly constructed on the tremendously thick covering layers with the base built with gravelly coarse sand and the upstream and downstream built with sanded shell into which gravelly coarse sand by manpower. The structures of these dams are generally loose and are presumably thereby considered not to meet the requirements against earthquake. In order to perform further safety analysis and liquefaction judgment with these dams in relation to their anti-seismic capacity, a typical dam with clay core and sanded shell was chosen and experiments were carried out to observe the dynamic behaviors of the dam, including the dynamic strength, the dynamic deformation and the dynamic pore pressure of the dam base and its upstream sanded shell. The results showed that the vibration stress ratio of gravelly coarse sand decreased with the increment in vibration frequency and increased with the increment in consolidation ratio, that the elastic modulus of gravelly coarse sand decreased with the increment in strain, and that the damping ratio of gravelly coarse sand increased with the increment in strain. In conclusion, the denser the dam material is, the better the anti- seismic behavior is, the sand used in the dam is non-linear in nature, The model of vibration pore water pressure growth is characterized by simplicity in expression, convenience in application, and being able to used in widespread way, etc. It reveals what inherent in the relationship of the increment of residual pore pressure with multiple factors, and hence can be used in the dynamic analysis of effective stress. [Journal of American Science 2009:5(2) 29-35] (ISSN: 1545-1003)

Key word: gravelly coarse sand; earthquake liquefaction; dynamic behaviors; upstream sanded shell

1. Introduction

More than 90% of reservoirs were constructed during the period of the so-called "Great leap forward" around the year of 1958 as some kind of special products with most of the dams being of clay-core- sand-shell type. And the filling of these dams were accomplished using the so-called "tactics of human sea" with their internal structures comparatively loosely built with no consideration into their capacity against seism at all. Consequently, these dams have been presumed not to be able to reach anti-seismic requirements from the beginning. Even worse, these dams have undergone operation of 50 years with severe problems associated with aging. Therefore, it has been extremely critical to evaluate the real property of anti-seism of these dams so as to perform reasonable measures for improving their

anti-seismic capacity, and thus reducing probability of their leading to catastrophic outcomes brought by possibly occurring seism in the future while leaving them there for multiple usages. In this study, the materials from the dam for Houlonghe reservoir were chosen to observe experimentally their dynamic properties with respect to the anti-seismic capacity of the present dam made from them. The dam for Houlonghe reservoir is located on the middle stream of the east branch of Gu River at Yatou town, Rongcheng city, Shandong province, China, which is a typical clay-core-sand-sand-shell dam. This dam controls water flow of about 61km^2. And the reservoir with a total capacity of about 5.3 million m^3, is an important medium sized one of its kinds and comprehensively applied for flood prevention and water supply. The dam was constructed in 1959 and has affiliated with aging diseases seriously after undergoing operation of 50 years. In 2004, it was listed as dangerous one after safety assessment by the national security department for reservoir and dam, and thus needs danger control and reinforcement. [Yao et al., 2005].

The dam is a clay-core-shell-wall dam with its upstream being sanded shell and its base made from gravelly coarse sand. The reservoir has been set to be in defense against earthquake of seven degrees by Richter scale. But the judgment has been made through reconnaissance that there has existed the probability of seismic liquefaction with the sanded shell in the upstream of the dam and the sanded layer in the base of it in the circumstance of earthquake. Therefore, we carried out the research to study the dynamic characteristics of gravelly coarse sand in order to provide theoretical basis for related institutions involving in the analysis of the dynamic safety of the dam and supply data for the evaluation of seismic liquefaction.

2. Samples for the experimentation

The experimental soil material was the loose soil obtained from the typical sections of sanded shell in the upstream and the sand layer at the base of the dam for Houlonghe reservoir. The characteristics of the two soils were shown in table 1. The dry density of them: the soil of the upstream sanded shell: γ_d=1.62g/cm^3, the soil of the sand layer at dam base:γ_d=1.58 g/cm^3.

3. Methods of experimentation

The DSZ-100 electromagnetic vibration triaxial apparatus was employed for the observation of the seismic behavior of the material of the dam. The sample was 3.91cm in diameter, 8cm in high, and greater than 90% in saturation. Three consolidation ratios were used in this experiment: Kc=1.0, 1.5, 2.0. The consolidation stresses were 0.05MPa, 0.10MPa, 0.15MPa, respectively. Sine wave with 1Hz in frequency was used with dynamic wave is [Yuan et al., 2004].

Method for liquefaction experiment: The

Table1 the characteristics of soils obtained from sanded shell in the upstream and sand layer at the base

sampling positions	sampling depth（m）	particle size (mm)/%					nonuniform coefficient	curvature coefficient	Name in door
		>2	2～0.5	0.5～0.25	0.25～0.075	<0.075			
upstream sanded shell	3.0	13.7	29.1	32.4	19.0	5.8	5.91	1.41	gravelly coarse sand
the sand layer at dam base	1.5	22.6	33.2	28.2	12.8	3.2	9.73	1.08	gravelly coarse sand

tested sample was prepared in such way that a given amount of dried sand by baking was mixed with water, and then boiled to be dried after thorough stirring. The process of consolidation of the sample was accomplished by applying axial stress σ_1 and lateral stressσ_3 to the sample under desired conditions and then the liquefaction test was performed by applying given axial circulation stress in the circumstance of no draining.

Method for measuring dynamic elastic modulus and damp ratio: Dynamic elastic modulus (E_d) is the ratio of dynamic-stress σ_d and dynamic-strain ε_d , which reflects the relationship between dynamic-stress and dynamic-strain during the phase of modification in shape under the action of periodically loading. Damp ratio λ is the ratio of damp coefficient c and critical damp coefficient c_{cr} , measured by cyclic triaxial test, indicating the energy-dissipation per vibrating cycle, and is therefore also called the equivalent gummy damp ratio of soil [Sun et al.,2004]. The method used for examining dynamic-elastic modulus and damp ratio in this study was as follows: the samples were consolidated with different stresses , and then the samples were respectively implemented with dynamic stresses from low grade to high grade progressively in step with 10 times per graded cycle in under the circumstance of non-draining. The resultant hydraulic pressure in the accessory small openings in the samples was dissipated after the termination of every graded loading before the implementation of the next graded loading in order to keep the valid stress constant during the process of the test.

The criterion for demolition examination at equal consolidation was set at 5% of the peak of the axial strain (double peaked value). The criterion for demolition examination at non-equal consolidation was also set at 5% of the axial halved peak value plus residual deformation.

4. Dynamic characteristics of the Materials of the dam

4.1 The characteristics of Dynamic Intensity

Dynamic intensity refers to the dynamic shearing stress leading to sample failure with a given number of circulating vibration force [Towhata et al.,1985], N_f. The relationship curve, $\sigma_d/(2\sigma_3)\sim N_f$ was displayed on uni-logarithm grapy sheet base on the results of the test. The curve was established with the results of the test when the number of circulations at 10, in viewing of that the earthquake defence intensity had been set at seven degrees by Richter scale for the dam of Houlonghe reservoir. The ratios of liquefaction-stress when N_f at 10 were shown in table 2, and the relationship curve of the dynamic shearing stress ratio $\sigma_d/ (2\sigma_3)$ of upstream sanded shell and the number of vibration destruction, N_f was shown in figure 1.

The values of dynamic stresses at different consolidation stresses were obtained from liquefaction- stress ratios when the times of

Table2 Liquefaction- stress ratio of the materials of the dam

sampling positions	Liquefaction- stress ratio $\sigma_d/2\sigma_3$		
	1.0	1.5	2.0
upstream sanded shell	0.30	0.40	0.515
the sand layer at dam base	0.32	0.43	0.535

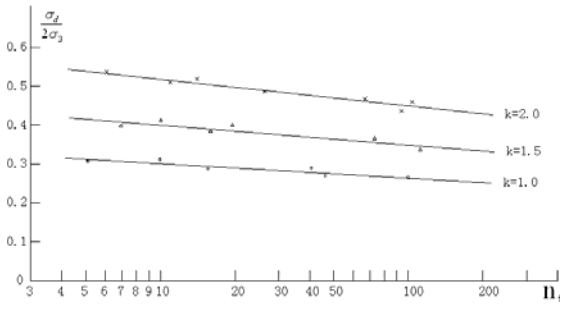

Fig.1 The relationship curve of σd/ (2σ3)

Table3 dynamic strength parameters at three different consolidation stresses of the materials of the dam

sampling positions	1.0		2.0		3.0	
	Φ_d (degree)	C_d (MPa)	Φ_d (degree)	C_d (MPa)	Φ_d (degree)	C_d (MPa)
upstream sanded shell	14.81	0	25.69	0	30.55	0
the sand layer at dam base	14.2	0	24.6	0	30.92	0

circulating force at 10, and thus then the Mohr circle could be drawn for the determination of the dynamic strength parameters. The dynamic strength parameters, Φ_d and C_d at three different consolidation stresses were shown in table 3. The Mohr circles of upstream sanded shell of the dam at different stresses were shown in figure 2.

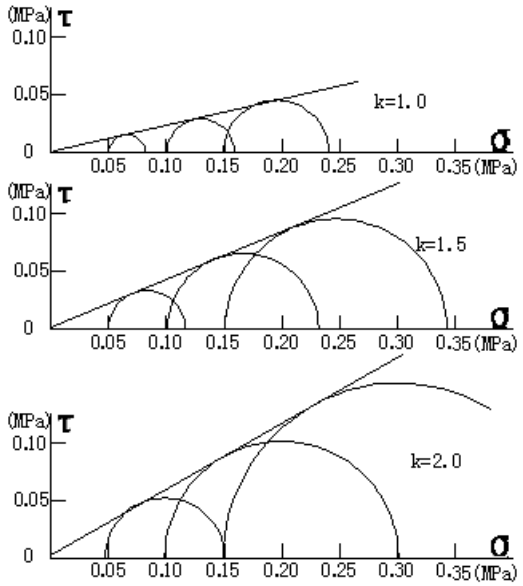

Fig.2 The Mohr circles of upstream sanded shell at different stresses (n=10)

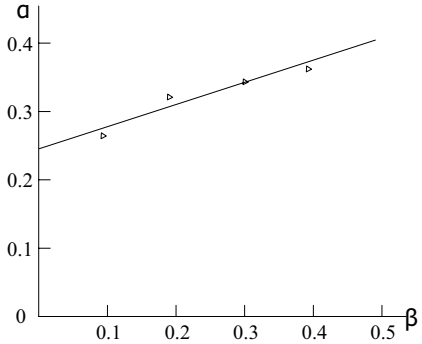

Fig.3 The relationship of α and β in upstream sanded shell

In order to perform the liquefaction analysis, the liquefaction shearing stress, τ_{fd} , under different static stresses, $\sigma_{fs,}$ had to be determined. The curve representing relationship of initial shearing stress ratio, $\beta=\tau_{fs}/\sigma_f$, with $\alpha=\tau_{fd}/\sigma_{fs}$ were obtained from the results of the test as shown in figure 3.

The shearing stress during liquefaction cycle, $\tau_{f\,d}$,resulted from the combination of a certain initial effective directed stress σ_{fs} and the initial shearing stress τ_{fs}(e.g. anti-liquefaction shear stress) could be obtained from the curve.

4.2 The characteristics of dynamic deformation

The relationship between the maximal dynamic elastic modulus E_{dmax} and the averaged effective consolidation pressure $\sigma_0^{/}$ was determined, and the relationship curve of the elastic modulus $E_{d,}$ and damp ratio λ_d against dynamic strain ε_d was established for the determination of the characteristics of dynamic deformation.

According to the results of the test, the relationship of maximal dynamic elastic modulus E_{dmax} and the averaged effective consolidation stress $\sigma_0^{/}$ was determined by the following equation.

$$E_{d\max} = kP_a\left(\frac{\sigma_0^{/}}{P_a}\right)^n$$

In the equation, $\sigma_0^{/}$ is the averaged main

effective stress when samples being consolidated, which is determined by the equation: $\sigma_0' = (\sigma_1' + 2\sigma_3')/3$; k and n are test constants relative to properties of soils used in tests. Pa is the atmospheric pressure.

$E_{dmax} \sim \sigma_0'$ relationship curve was drawn on the double logarithm coordination sheet, wherein K was the intercept of the curve on the vertical axial of the coordination, and N was the slope ratio. The values of k and n for the materials of the dam when consolidation ratio at 1 was shown in table 4.

The dynamic elastic modulus E_d decreased with the increasing of axial strain while it increased with the increasing of the consolidation stress ratio. Nevertheless, the ratio of modulus E_d and maximum of dynamic elastic modulus E_{dmax}, E_d/E_{dmax} did not change significantly with the alteration of consolidation pressure [Borden et al., 1996]. The relationship of E_d/E_{dmax} and ε_d were depicted on the halved logarithm coordination sheet based on the results of the test. The following equation was obtained after approximation of the curve for $E_d/E_{dmax} \sim \varepsilon_d$.

$$E_d/E_{dmax} = 1/(1 + \varepsilon_d/w)$$

In the equation, w is the approximation parameter.

The curve for the relationship between damp ratio λ_d and dynamic strain ε_d was depicted on the halved logarithm coordination sheet. The half logarithm squared paper. The following equation was obtained after approximation of the curve for the $\lambda_d \sim \varepsilon_d$ relationship:

Table4 k and n with the material of the dam

the material of the dam	k	n
upstream sanded shell	40	0.681
the sand layer at dam base	38.5	0.635

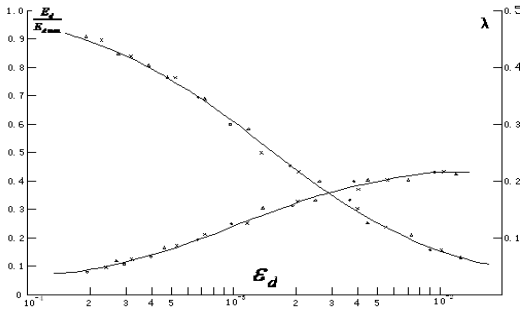

Fig.4 The respectively corresponding relationship of E_d/E_{dmax}、$\lambda_d$and$\varepsilon_d$in upstream sanded shell

Table5 Approximation parameter of elastic modulus damp ratio

the material of the dam	w	a	b
upstream sanded shell	0.001596	0.4767	0.001
the sand layer at dam base	0.001303	0.2223	0.006

$$\lambda_d = a\varepsilon_d/(b+\varepsilon_d)$$

In the equation, a and b are the approximation parameter.

The relationship curve of E_d/E_{dmax}、λ_d andε_d with the shell of the upstream of the dam was showed in figure 4. The approximation parameter for elastic modulus w with dam material and the approximation parameters for damp ratio, a and b were shown in table 5.

4.3 The characteristics of dynamic pore pressure

During the vibrating triaxial test, the changes in small opening hydraulic pressure were recorded simultaneously with computer and thus the curve for the relationship of changes in small opening hydraulic pressure with times of vibration was obtained. Data of the test was arranged with the vibration pore water pressure growth model proposed by the Institute of Water Resources, the Yellow River Committee, China ,which is denoted in the following exponential function[Li et al.,1994;Xu et al.,2006].

$$U = 1 - (1 - U_0)10^{-K\xi/(1-\xi)}$$

In the equation, ξ is the ratio of the destruction-to-times in logarithm, which could be obtained by the equation, $\xi = \log N / \log N_f$; U_0 is the relative pore pressure ratio of the first cycle.

The test constants k was determined by the following equation.

$$K = \alpha N_f^{-\beta}$$

U_0 was determined by the following equation.

$$U_0 = \gamma N_f^{-\theta}$$

N_f was determined by the following equation.

$$\alpha_d = A N_f^{-B}$$

Wherein α_d was the ratio of dynamic stress, which was determined by the equation, $\alpha_d=\sigma_d/(2\sigma_3)$. Thus, the pore pressure of any time vibration was determined by the following 7 constants, namely, A、B、γ、θ、α、β and u_f, where u_f was the averaged value of pore pressure ratio with predetermined destruction standard in the same consolidation ratio .

Different consolidation ratio and consolidation pressure has taken into consideration in this model, which is thus characterized by simplicity in expression, convenience in application, and being able to used in widespread way, etc. It revealed what inherent in the relationship of the increment of residual pore pressure with multiple factors, and hence could be used in the dynamic analysis of effective stress.

5.Conclusions

(1) The results showed in the present test with dynamic strength that the vibration-stress ratio of the material of the dam increased with the reduction of times of vibration, and the numerical points of stress ratio at different confining pressure fell relatively well into a narrowly-defined band under the same consolidation ratio and thus could be expressed as a straight line, indicating that the results were comparatively is reasonable. The results also showed that the stress ratio of each kind of dam material increased with the increment of consolidation ratio and the dynamic strength index increased significantly with the increment of consolidation ratio, indicating that the denser the dam material is, the better the anti- seismic behavior is.

(2) The results in the dynamic modulus and damp measurements showed that the dynamic elastic modulus of the dam material decreased with the increment of the strain and damp ratio increased with the increment of the strain, indicating that the sand used in the dam is non-linear in nature. The strain ranged from 10^{-4} to 10^{-2} in this test, in which modulus ratio and damp ratio were the actual values. The values of the modulus ratio and damp ratio in other ranges could be obtained through simulation curve.

(3) The model of vibration pore water pressure growth is characterized by simplicity in expression, convenience in application, and being able to use in widespread way, etc. It reveals what inherent in the relationship of the increment of residual pore pressure with multiple factors, and hence can be used in the dynamic analysis of effective stress.

Acknowledgements

This work was supported by two grants from the National Natural Science Fund of China [No.90510017 and 50679073].

References

Borden, R., Shao, L., Gupta, A., 1996.Dynamic properties of piedmont residual soils. Journal of Geotechnical and Geoenvironmental Engineering, ASCE.7, 123-127

Li,H.,Zhang,S.,1994.Study on the anti-seismic properties of Sand and Gravel in Xiaolangdi earth rockfill dam(national technology tacking report of 8th five-year plan).Institute of Hydraulic Research,YRCC.15-35.

Sun, J., Yuan, X., Sun, R., 2004.Reasonability comparison between recommended and code values of dynamic shear modulus and damping ratio of soils. Earthquake Engineering and Engineering Vibration, 24(2), 125-133.

Towhata, I., Ishihara K., 1985.Undrained strength of sand undergoing cyclic rotation of principal stress axes. Soils and Foundations, JSSMFE, 25(2), 210-218.

Xu, B., Kong, X., Zou, D., 2006.Study of dynamic pore water pressure and axial strain in saturated sand-gravel composites. Rock and Soil Mechanics.27 (6), 925-928.

Yao, K., Xu, S., 2005.Engineering Geological Investigation of Houlonghe reservoir in Rongcheng city. Shandong Provincial Institute of Water Resources, 4-14.

Yuan. Xu,C., Zhao, C.,2004. Soil lab test and in-situ testing. Tongji University Press, China, 153-272.

Marsland Press
Journal of American Science 2009:5(2) 36-42

Implementation of Improved Steganographic Technique for 24-bit Bitmap Images in Communication

Mamta Juneja, Parvinder Sandhu
Department of Computer Science and Engineering, Rayat and Bahra Institute of Engineering and Biotechnology,
V.P.O Sahauran, Tehsil Kharar, Distt. Mohali, Punjab- 140104, INDIA
91-098786-77624
er_mamta@yahoo.com

Abstract

Steganography is the process of hiding one file inside another such that others can neither identify the meaning of the embedded object, nor even recognize its existence. Current trends favor using digital image files as the cover file to hide another digital file that contains the secret message or information. One of the most common methods of implementation is Least Significant Bit Insertion, in which the least significant bit of every byte is altered to form the bit-string representing the embedded file. Altering the LSB will only cause minor changes in color, and thus is usually not noticeable to the human eye. While this technique works well for 24-bit color image files, steganography has not been as successful when using an 8-bit color image file, due to limitations in color variations and the use of a colormap.

This paper presents the results of research investigating the combination of image compression and steganography. The technique developed starts with a 24-bit color bitmap file, and then compresses the file by organizing and optimizing an 8-bit colormap. After the process of compression, a text message is hidden in the final, compressed image. Results indicate that the final technique has potential of being useful in the steganographic world. [Journal of American Science 2009:5(2) 36-42] (ISSN: 1545-1003)

Keywords: Bitmap, Colormap, Compression, LSB Based Insertion, Steganography

Introduction

Staganography is an ancient technology that has applications even in today's modern society. A Greek word meaning "covered writing," steganography has taken many forms since its origin in ancient Greece. During the war between Sparta and Xerxes, Dermeratus wanted to warn Sparta of Xerxes' pending invasion. To do this, he scraped the wax off one of the wooden tablets they used to send messages and carved a message on the underlying wood. Covering it with wax again, the tablet appeared to be unused and thereby slipped past the sentries' inspection. However, this would not be the last time steganography would be used in times of war.

In World War II, the Germans utilized this technology. Unlike the Greeks, these messages were not physically hidden; rather they used a method termed "null ciphering." Null ciphering is a process of encoding a message in plain sight. For example, the second letter of each word in an innocent message could be extracted to reveal a hidden message.

Although its roots lay in ancient Greece, steganography has continually been used with great success throughout history. Today steganography is being incorporated into digital technology. The techniques have been used to create the watermarks that are in our nation's currency, as well as encode music information in the ever-popular mp3 music file. Copyrights can be included in files, and fingerprints can be used to identify the people who break copyright agreements [5] [6] and [8].However, this technology is not always used for good intentions; terrorists and criminals can also use it to convey information. According to various officials and experts, terrorist groups are "hiding maps and photographs of terrorist targets and posting instructions for terrorist activities on sports chat rooms, pornographic bulletin boards, and other Web sites"[1].

This aspect of steganography is what sparked the research into this vast field [3] and [4]. Education and understanding are the first steps toward

security. Thus, it is important to study steganography in order to allow innocent messages to be placed in digital media as well as intercept abuse of this technology [7].

Current Usage

In modern society, steganographic techniques are used in a wide range of applications. Watermarking, a subclass of steganography, includes everything from watermarks on paper and security marks on paychecks to the hidden image of Abraham Lincoln on the five-dollar bill. Its purpose is to verify authenticity, prevent counterfeiting, or to give information about the creator. These are not the limits of steganography; it is also used in much the same manner in the digital world. Programs such as Adobe Photoshop version 4.0 or higher have the capability to embed and detect watermarks, while other programs like Stego can hide encrypted text messages in GIF images.

As hidden messages are being found and algorithms cracked, new methods of steganography are being developed. There has been a significant surge of interest since the first academic conference on the subject, the Workshop on Information Hiding, was organized in 1996 and held at the Isaac Newton Institute in Cambridge. One reason for this surge of interest is that the publishing and broadcasting industries have become interested in techniques for hiding encrypted copyright marks and serial numbers in digital films, audio recordings, books, and multimedia products. The new market opportunities due to digital distribution coupled with the fear that digital products could be too easy to copy leaves these industries in a rather large dilemma. Other motivations to study steganographic methods are due to governmental restrictions that have been placed on encryption services. People desire a way to send private messages. The controversial issue concerning this topic is that spies and criminals wanting to pass on secrets in inconspicuous data over public networks can abuse the same applications that are being developed to allow copyrights to be placed in digital media.

Least Significant Bit Insertion

One of the most common techniques used in steganography today is called least significant bit (LSB) insertion. This method is exactly what it sounds like; the least significant bits of the cover-image are altered so that they form the embedded information. The following example shows how the letter A can be hidden in the first eight bytes of three pixels in a 24-bit image.

Pixels: (00100111 11101001 11001000)
(00100111 11001000 11101001)
(11001000 00100111 11101001)

A: 01000001

Result: (0010011<u>0</u> 11101001 11001000)
(0010011<u>0</u> 11001000 1110100<u>0</u>)
(11001000 00100111 11101001)

The three underlined bits are the only three bits that were actually altered. LSB insertion requires on average that only half the bits in an image be changed. Since the 8-bit letter A only requires eight bytes to hide it in, the ninth byte of the three pixels can be used to begin hiding the next character of the hidden message.

A slight variation of this technique allows for embedding the message in two or more of the least significant bits per byte. This increases the hidden information capacity of the cover-object, but the cover-object is degraded more, and therefore it is more detectable. Other variations on this technique include ensuring that statistical changes in the image do not occur. Some intelligent software also checks for areas that are made up of one solid color. Changes in these pixels are then avoided because slight changes would cause noticeable variations in the area [9] and [10].

While LSB insertion is easy to implement, it is also easily attacked. Slight modifications in the color palette and simple image manipulations will destroy the entire hidden message. Some examples of these simple image manipulations include image resizing and cropping [11] and [12].

Bitmap File Structure

Before compression and steganographic techniques could be implemented, more information needed to be gathered about the bitmap file format. Microsoft defined the bitmap file format. In hopes of making this a popular file format, Microsoft made structures so that the information can be extracted easily from the bytes of a file. Bitmaps have two headers that contain the information needed to extract and display the image.

The first 14 bytes of the file make up the first header, which can be read into a structure called the BitmapFileHeader. The information contained in this structure can be seen in Table 1.

Table 1: Bitmap File Header Structure Items

Item Name	Size	Description
bfType	2 bytes	ASCII for "B" and "M"
bfSize	4 bytes	Size of the File in bytes
bfReserved 1	2 bytes	Reserved Equals 0
bfReserved 2	2 bytes	Reserved Equals 0
bfOffBits	4 bytes	Number of Bytes to the Picture Data

The next header in the bitmap can be read into a structure called the BitmapInfoHeader. The length of this header is determined by the first four bytes in the header, the biSize field. Generally, the length of the header is 40 bytes long. Table 2 shows the items that are contained in this structure.

Table 2: Bitmap Information Header Structure Items

Item Name	Size	Description
biSize	4 bytes	Size of the Bitmap Info Header in bytes
biWidth	4 bytes	Width of the Bitmap in pixels
biHeight	4 bytes	Height of the Bitmap in pixels
biPlanes	2 bytes	Number of Planes (Equals 1)
biBitCount	2 bytes	Number of Bits Per Pixel (1,4,8,16,24, or 32)
biCompression	4 bytes	Type of Compression (0,1,2)
biSizeImage	4 bytes	Size of the Picture Data in bytes
biXPelsPerMeter	4 bytes	Horizontal Resolution (Pixels/Meter)
biYPelsPerMeter	4 bytes	Vertical Resolution (Pixels/Meter)
biClrUsed	4 bytes	Number of Actual Colors Used
biClrImportant	4 bytes	Number of Important Colors (0 = all)

An optional colormap follows the BitmapInfoHeader in the bitmap image file. Each color in the colormap is four bytes long and is contained in a RGBQUAD structure. Table 3 shows the items within the RGBQUAD structure. The program determines whether or not a colormap exists by examining the bfOffbits field in the BitmapFileHeader. If this field is greater than the total size of the two headers, then a colormap is present.

Table 3: RGBQUAD Structure Items

Item Name	Size	Description
rgbBlue	1 byte	Blue Intensity
rgbGreen	1 byte	Green Intensity
rgbRed	1 byte	Red Intensity
rgbReserved	1 byte	Unused (Equals 0)

A colormap is used in different ways depending on the biBitCount field in the BitmapInfoHeader. If the biBitCount equals 24, the colormap is used to list the most important colors of the image, but the colormap is not actually used by the picture data. If the biBitCount equals 8, each pixel in the picture data is an 8-bit pointer to a color in the colormap. A colormap in an 8-bit bitmap has a maximum 256 colors since the pointer into it can only be 1 byte (2^8 = 256). The biBitCount field can be other values than 8 or 24, but since these are uncommon the current project does not deal with them.

Following the colormap (if a colormap exists) is the picture data. The picture data also varies depending on the value of biBitCount. If the biBitCount equals 24, then each pixel is represented by three bytes. There is exactly one byte for each intensity: red, green, and blue. If the biBitCount equals 8, each pixel is represented by 8-bits, which point to a RGBQUAD structure in the colormap.

One complication to the picture data is that each line of pixels in a picture, known as a scanline, must start on a LONG boundary. Since a LONG is four bytes in length, a LONG boundary is an address that is evenly divisible by four. The pixels in the image formats being discussed here are either 1 byte (8-bit images) or 3 bytes (24-bit images) long in the picture data. The number of bytes needed to accurately display a scanline may not be divisible by four. Since images can be any number of pixels wide, the end of the scanline may not end on a LONG boundary. In such cases, extra bytes of value zero are padded to the end of the scan line in order to make the scan line end on a LONG boundary. The next scanline can then start

on the LONG boundary as well.

Proposed Technique

After reviewing the current products on the market for steganography, it was determined that there was not a practical implementation for 8-bit images. Although network speed is increasing, and bandwidth problems are decreasing, file size is still of utmost importance and smaller file sizes are optimal in network communication. Thus, the current steganographic use of 24-bit images leads to slower communication and development of an 8-bit image format would be beneficial.

The aim of this research is to create a practical steganographic implementation for 8-bit images. A 24-bit bitmap image would be converted to an 8-bit bitmap image while simultaneously encoding the desired hidden information. An algorithm would be created to select representative colors out of the 24-bit image to create the palette for the 8-bit image. This palette would then be optimized to an 8-bit colormap that could be applied with minimal changes to the quality of the original image.

This process of compressing the image from a 24-bit bitmap to an 8-bit bitmap resulted in minor variations in the image, which are barely noticeable to the human eye. However, these slight variations aid in hiding the data. Since there would not be an original 8-bit image to compare with the stego-image, it would be impossible to discern that the slight variations caused by hiding the data are different from the slight variations caused by compression.

A practical steganographic implementation for 8-bit images enabled smaller file sizes to be utilized in steganographic communications. While also limiting the size of the hidden file, this implementation addressed issues that have been passed by in other applications, and provided a more compact vehicle for those secret communications that do not require a large cover-file.

Creating the Colormap

The colormap in an 8-bit color image has a maximum of 256, 24-bit colors. However, in order to minimize the noise added when the least significant bits are changed, a starting colormap of only 240 colors is created. Sixteen additional colors will be added to the colormap by the time the final picture is written.

In order to select the 240 original colors, the image is divided into a grid of fifteen quadrants by sixteen quadrants, as seen in Figure 1. One color is chosen from each of these quadrants by randomly selecting a set of X and Y coordinates within each quadrant. Calculations are then made to determine the index of the pixel in the array of RGBQUADS that represent the image data. (An RGBQUAD is a structure containing four bytes, one each for the red, green, and blue intensity and a reserved byte.)

Each time a color is selected from a quadrant, it is compared to every other color in the colormap, and the minimum error between any two colors is calculated. If this error is lower than a certain error level (currently set at 20), then the new color is discarded and another color is selected from the image. After five attempts to find a color from a certain quadrant that differs enough from all the other colors in the colormap, the selected color is added to the colormap and the program moves to the next quadrant.

Optimizing the Colormap

The initial colormap contains 240 colors that were picked out of the original image. These colors were chosen from the entire image but that does not guarantee that these colors are the most representative of the colors that exist in the image. Therefore, the colormap must then be optimized to provide the best 240 colors for the colors in this particular image.

The optimization algorithm uses a Linde-Buzo-Gray methodology[3]. A pixel is chosen from the original 24-bit image and its RGB values are compared to the RGB values of every color in the colormap. For each comparison an error level is calculated using the mean absolute error of the red, green, and blue component of the color. The colormap color that produces the smallest amount of error is the colormap color that is closest to the

Figure 1: Image overlaid with 15x16 grids

pixel's RGB values. The RGB values of the pixel are then added to the RGB values of the colormap color. A counter is implemented to keep track of how many pixels are assigned to each colormap color and is incremented each time a match is found. Approximately 25% of the pixels in the original image are run through this process. Once the algorithm has gone through the whole image, the RGB values of each colormap container are averaged by dividing the red, green, and blue values by the counter for that particular container. This process produces a colormap with slightly new, "better" colors in it. The process is repeated until the new colormap is considered to be optimized. To determine when the colormap is optimized, the error levels are recorded during each run and when a certain error level is attained the algorithm is finished.

Sorting the Colormap

Each pixel in an 8-bit color image is an 8-bit pointer to a 24-bit color in the colormap. Looking ahead to the LSB insertion, a pixel pointing to a red color could suddenly point to a yellow color by a simple flip of the least significant bit. In order to reduce dramatic noise such as that, the colormap was sorted so that similar colors are next to each other before the pixels are assigned to colormap colors. The sorting algorithm works as follows.

Beginning with the first color in the colormap array, the pixel that is the closest in color to the starting pixel is found using the mean absolute error measure. If the best match to a color results in an error level greater than 100 (meaning that there really was not a very good match to the color), a new color is created in the first open slot (using the sixteen extra spaces in the colormap) and this new color is used as the pair. The best-matched color is then switched with the color immediately following the starting color. The same procedure is repeated with the next color that has not been matched. Once the original 240 colors have been matched, additional colors are created to fill any of the extra sixteen positions left in the original colormap.

Assigning Pixels

After sorting the colormap, the 8-bit image is almost ready to be created. An 8-bit bitmap contains a colormap of 256 colors and contains an assignment of each pixel to a color in the colormap. To assign the pixels to a colormap color, the original 24-bit image pixels are used. A pixel is chosen from the original 24-bit image and its RGB values are compared to the RGB values of every color in the colormap. For each comparison an error level is calculated using the mean absolute error of the red, green, and blue color components. The colormap color that produces the smallest amount of error is the colormap color that gets assigned to this pixel.

Encoding the Data

The image is now ready to have data embedded into it. The encode function takes three parameters and two steps in order to complete. The data string of text, picture data, and binary data string are the three parameters for the first step in encoding the text into the image. The first step in the encoding function is to convert the ASCII text into its binary equivalent. In order to do this, each character of the text message is converted to its ordinal number (example: 'a' = 97). The ordinal number is then converted to binary using the following method called the division-remainder routine. An ordinal number is divided by two using the *mod ()* function. This function returns either a one or a zero, which is then placed in a remainder array. This is continued until the dividend is zero. The ones and zeros in the remainder array is the binary equivalent of the ASCII ordinal number. Then, once all characters have been converted in this fashion, the binary data is embedded in the image by sequentially altering the least significant bit of the image data as necessary.

Additional features

Since LSB insertion is easily attacked, repetition of the hidden message throughout the entire image will improve the integrity of the message. For example, if the image were cropped with the message embedded throughout the entire image, chances are good that the message could still be extracted from the cropped image. Repetition of the hidden message also causes the image quality to be uniform throughout instead of having noticeable areas of variations in certain sections of the image.

An encryption algorithm can also be added to this to further protect the end user's message if so desired. While embedding a message in an image will prevent most people from knowing a message exists, encrypting the message before embedding it will aid in safeguarding it from being read by someone who happens to find the message.

The encryption technique employed is a 24-bit algorithm. The user enters a number between 0 and 16,777,216 to use as the encryption key, which is converted to a 24-bit representation. The first three bytes (twenty-four bits) of the message are XORed with the 24-bit key. The next three bytes of the message are then XORed with the 24-bit key. This process is continued in a similar fashion for the remainder of the message. The following example shows how the algorithm would encrypt a 6-character message.

Message = 'abcdefg'
Key = 9,657,852
'abc' = 01100001 01100010 01100011
'def' = 01100100 01100101 01100110
9,657,852 = 10010011 01011101 11111100

$result_{abc}$ = 'abc' **XOR** 9,657,852
= 011000010110001001100011 **XOR** 100100110101110111111100
= 111111100011111110011111

$result_{def}$ = 'def' **XOR** 9,657,852
= 011001000110010101100110 **XOR** 100100110101110111111100
= 111101110011100010011010

Encrypted Message = 111111100011111110011111111101110011100010011010

Conclusion

The purpose of this research is to investigate steganographic techniques, and apply them to 8-bit images. While this research does not cover every aspect of steganographic technology, it is a good starting point for anyone interested in implementing and learning how the technology can be applied to digital images. Further developments to this could include using different picture formats, such as JPEG and GIF, to serve as the cover object. Additional features could allow other files such as other pictures or MS Word documents to be used as hidden messages. Other future endeavors could employ some of the variations of least significant bit insertion such as using two or more of the least significant bit to embed the data. This will yield a higher embedding space but also increase image degradation levels. To counteract this, the sorting of the colormap would need to be adjusted based on the number of bits used in the LSB insertion algorithm

Correspondent Author:
Mamta Juneja
Assistant Professor, CSE Department,
RBIEBT, Sahuran-mohali, Punjab, INDIA
Email:er_mamta@yahoo.com
Phone: +91-98786-77624

References

B.Schneier, "Terrorists and Steganography", 24 Sep.2001,available: http://www.zdnet.com/zdnn / tories/comment/0,5859,2814256,00.html.

Y. Linde, A. Buzo, and R. M. Gray, "An Algorithm for Vector Quantizer Design," IEEE Transactions on Communications, pp. 84-95, January 1989.

Andersen, R.J., Petitcolas, F.A.P., On the limits of steganography. *IEEE Journal of Selected Areas in Communications, Special Issue on Copyright and Privacy Protection* **16** No.4 (1998) 474–481.

Johnson, Neil F. and Jajodia, Sushil. "Steganography: Seeing the Unseen." *IEEE Computer*, February 1998, pp.26–34.

William Stallings; Cryptography and Network Security: Principals and Practice, Prentice Hall international, Inc.; 2002.[2]

Eric Cole,"Hiding in Plain Sight: Steganography and the Art of Covert Communication"

Gregory Kipper, “Investigator’s Guide to Steganography”
Stefan Katzenbeisser and Fabien, A.P. Petitcolas," Information Hiding Techniques for Steganography and Digital Watermarking”

Hiding secrets in computer files: steganography is the new invisible ink, as codes stow away on images-An article from: The Futurist by Patrick Tucker

Ismail Avcıbas,, Member, IEEE, Nasir Memon,Member, IEEE, and Bülent Sankur, Member, "Steganalysis Using Image Quality Metrics," IEEE Transactions on Image Processing, Vol 12, No. 2,February 2003..

Niels Provos and Peter Honeyman, University of Michigan, "Hide and Seek: An Introduction to Steganography" IEEE Computer Society IEEE Security &Privacy.

R. Chandramouli and Nasir Memon, "Analysis of LSB Based Image Steganography Techniques", IEEE 2001

Marsland Press
Journal of American Science 2009:5(2) 43-53

An assessment and evaluation of the ecological security in a human inhabited protected area at Korup, south western Cameroon: Linking satellite, ecological and human socioeconomic indicators

[1]Innocent Ndoh Mbue, [2]Ge Jiwen*, [1]Samake Mamadou

[1]*School of Environmental Studies, China University of Geosciences, Hongshan District, 388 Lumo Road, Hubei Wuhan, 430074, P.R. China*

[2]**Director, School of Ecology and Environmental Sciences, China University of Geosciences, Hongshan District, 388 Lumo Road, Hubei Wuhan, 430074, P.R. China.* Telephone: +862762493959

Abstract

This study attempts to identify how much understanding of ecological and human livelihood security can be gained through a binary and index model. Hereto, binary and index models of indicators of ecological security in the central zone of the Korup National Park-Cameroon are developed, taking into account the spatial variability of change in economic, social and ecological variables. Our approach is anchored in a broader conception of threats to both human well-being and ecological goods and services. The results show that, while only 1.47% of the regions cover remains unchanged, over 50% decreased barely 14 years after the creation of the park in 1986. The reasons for the decrease are mainly socioeconomic in nature. Furthermore, while the socio-economic statuses of the indigenes/villagers remain uncertain, the index of ecological security (IES) of the area has moved from slightly damaged (4.1<IES<6), to moderately damaged (2.1<IES<4) in the past decades. With increasing pressure on the land, however, sustaining livelihoods through agricultural production in the area remains a critical challenge. While community forestry, change of direction in the fight against corruption, increase finance to management of the park to step up monitoring activities could be short term remedies, we think that involuntary resettlement could be the best option for management. The results should contribute to develop and prioritize appropriate policy interventions and follow-up steps to improve the security of similar protected areas inhabited by man.
[Journal of American Science 2009:5(2) 43-53] (ISSN: 1545-1003)

Key words: Ecological security, livelihood security, binary model, index model

1. Introduction

Healthy ecosystems are essential to the well-beings of a majority of the world's poorest societies [Smith and Scherr, 2003; Sunderlin *et al*., 2007]. Unfortunately, over the past few hundred years, humans have increased species extinction rates by as much as 1,000 times background rates that were typical over Earth's history [Millennium Ecosystem Assessment, 2005]. Biodiversity is currently being lost at rates significantly exceeding those in the fossil record [Anderson, 2001], most of the loss being reported from the tropical ecosystems. Projections and scenarios indicate that the rates of biodiversity loss will continue, or accelerate, in the future. The loss is of concern due to its widespread implications for environmental security and/or ecosystem functioning [Myers *et al.,* 2000; Loreau *et al*., 2002], human well-being for all [Diaz *et al*., 2006], ethical reasons [Agar, 2001], as well as sustainable development and poverty reduction. It is estimated that some 60 million indigenous people are completely dependent on forests, while 350 million people are highly dependent, and 1.2 billion are dependent on forests for their livelihoods [World Bank, 2004]. To the extent that humankind neglects to maintain the global life-supporting ecosystems current and future generations will be confronted with increasing severe instances of environmental induced changes.

Following continuous pressure from political regimes, many governments have responded to biodiversity conservation by creating protected areas and/or nature reserves. It is in this vein that Korup national park (KNP) Cameroon was created. In this region, the belief that ecological security became secured following the creation of the park in 1986 pervades calculations of local and national policy makers, but this belief is not based on direct observation of the situation today. The living consequences in this enclaved zone of the Park include, decline in wildlife population of plants and animals, and above all, the emission of green house gases. Such insecurity situation might in the long run further insecure the people, who cannot integrate traditional markets, but need alternatives for income generation.

Because of its short history, the concept of ecological security has no universally accepted definition, parameters, and appropriate research methods [Xiao *et al*., 2002]. As far as definitions go, Scientists have adopted both broad and narrow-sense concepts of it. The broad-sense concept [Pirages and Cousins, 2005], includes natural, economic, and social ecological security. The narrow-sense concept covers the security of natural and human influenced ecosystems.
As far as methodologies go, Scholars have proposed several measurement indices that account for different requirements from the perspectives of livelihood security, ecological risk and ecological health [Yan-Zhi et *al*., 2005]. As different ecosystems and time-space dimensions require corresponding indicator systems, there is yet to be a universally accepted, well-recognized indicator system or methodology. However, given the multi-criteria nature of ecological issues, the diversity of the stakeholders involved a systematic model that can disintegrate the component parts of such an intricate unstructured problem into well-defined parts such as the Analytical Hierarchical Process [Saaty, 1990], using the "Pressure-State-Response" model [OECD, 1993] as a foundation for an indicator system seems to be feasible. In this way, one can easily understand which variable(s) has/have mostly influenced the outcomes of the situation. The Pressure-State-Response (PSR) model on the other hand, has proven to be a logical, comprehensive tool to picture environmental issues from an anthropocentric perspective.

The purpose of this study was therefore to assess and evaluate the ecological security of the central zone of Korup national park (KNP), by linking remote sensing, human socioeconomic and ecological data.

Specifically the study aims to: (a) assess and evaluate land cover change analysis to understand the locations and degree of threats to the ecological system by using satellite remote sensing data;(b) identify the socioeconomic and ecological variables that influence ecological security of the region; (c) assess the significance of the relationships between these variables and the environment that may inform the selection of conservation prescriptions, and (d) produce an index of ecological integrity map of the area.

The results should contribute to develop and prioritize appropriate policy interventions and follow-up steps to improve the security of protected area, and seek opportunities to enhance the integrity and viability of the ecological system while maintaining or expanding the diversity of livelihood options available to poor forest dependent population.

2 Materials and Methods

2.1 Study area

The study area (1,260 km^2) is located in Ndian Division, southwestern Cameroon, between latitudes 4° 54′ and 5° 28′ north; and longitudes 8° 42′ and 9° 16′ east of the equator, at the Cameroon-Nigerian border and is contiguous with the Oban National Park-Nigeria. This area was chosen because very little or no research had been carried out there because of its enclaved nature. The mean annual rainfall is in excess of 5000mm [Zimmermann, 2000].; temperatures range from 22 to 34^0C, while relative humidity averages 87% throughout the year. The highest point is Mount Yuhan- a horst, reaching 1130m. Currently, four villages are located inside the Park and 31 other villages are within 3km of the park and have about 11,500 inhabitants [Schmidt, 2004]. Shifting cultivation forms the basis of the farming system. Economic activities include hunting, collection, processing and marketing of non-timber forest products.

2.2 Field investigations and variables measured

Field work took place from February to June of 2008. Both household surveys and group

discussions were carried out using open-ended questionnaire. Our focus was on land-use changes, trends in crop yields, socioeconomic status of the indigenous people, factors that local people perceived as having been responsible for the land-use /cover changes, and management effectiveness.

Village chiefs and sub-chiefs were contacted for most of our recall data. Other stakeholders included government and staff of Korup national park.
Our sample size was 95 (age:20-85 years; women:60; Men:35; average household size:4 people), drawn at random from three villages that make up the central region of the park.(20 from *Ekundo-kundo*; 35 from *Erat*, and 40 from *Ekon1* villages).We adopted the probability proportional to the size-a multi-stage sampling methodology (clustering, stratification and simple random sampling).

2.3 Variables measured
Taking into consideration the biophysical characteristics of our study area, the following independent variables were measured: ecological indicators; socioeconomic indicators; and management effectiveness indicators.

Ecological indicators included soil characteristics (organic matter, available phosphorus, pH, nitrogen, etc.). A total of 100 soil samples were collected for analysis.
Socioeconomic indicators as well as statuses (decline, remain same, or increased) of wildlife including socioeconomic important plant species (medicinal plants, fruit and food plants), which are the main sources of livelihood for the villagers. Management effectiveness indicators included staffing situation, and legal security. Here, respondents were to answer either "yes", "mostly yes", "no" or "mostly no" depending on their judgments of the situation.

2.4 Data Analyses
ERDAS IMAGINE 9.0 was used for image processing and database creation; ArcGIS 9.2 for database creation and GIS analysis; and SuperDecision [Saaty 2003] software for analytical hierarchical processing. Satellite images were layer stacked, mosaicked, and a subset produced. Our classification scheme adopted four main broad classes: Forest; Farms and settlements; Water bodies; bare/exposed surfaces.

2.4.1 Framework for determining ecological indicators

Ecological sustainability or the process of development which is compatible with quality and security of food supplies [Smith and McDonald, 1998] was assessed based on three indicators: Soil fertility status, Risk and uncertainties (diversification and profitability from economic activities, farming, collection and sale of non wood forest products etc), and Land cover change.

Reduction of risk and uncertainty in agriculture production was modeled using the Herfinhahl index (HI) and the index of profitability (IP) of economic activities. The index is a function of the area allocated to a particular enterprise [Llewelyn and Williams, 1996]. Mathematically,

$$HI = \sum_{i=1}^{n} P_i^2 \, , 0 \le HI \le 1 \qquad (1)$$

where, P_i is the proportion of farm area allocated to a particular enterprise, in this case, the local farmer.
HI= 0 denotes perfect diversification, and if 1, perfect specialization.

Index of profitability (IP) was analyzed from household perspective, with household considered as a small business enterprise.

$$\mathrm{IP} = \left(1 - \frac{\mathrm{BEP}}{\mathrm{Sales}}\right) * 1000 \qquad (2)$$

Where,

$$\mathrm{BEP} = \left(\frac{\mathrm{FC}}{\mathrm{CMR}}\right) \equiv \left(\frac{\mathrm{FC} * \mathrm{Sales}}{(\mathrm{Sales} - \Delta \mathrm{C})}\right) \qquad (3)$$

BEP denotes the break even point, FC, the fixed costs; CMR, the Contribution Margin, and ΔC , the variable cost from economic activities. In arriving at this model, we assume that the household is a small business enterprise. The calculation is based on income from farming season (financial year). Costs of inputs were computed on the basis of respective local market prices.

Land cover change was modeled through supervised classification of satellite imageries (Landsat TM, 1986, and Landsat ETM+, 2000) of the area. The Normalize Difference Vegetation Index selected (NDVI) was used to identify the state of vegetation cover.

$$NDVI = \frac{NIR - R}{NIR + R} \equiv \frac{Band\ 4 - Band\ 3}{Band\ 4 + Band\ 3} \qquad (4)$$

Where, NIR is Near-Infrared spectral band and R is red spectral band.

2.4.2 Framework for determining economic indicators

Economic sustainability requires that development be economically feasible. Therefore, economic security was measured based on four indicators: employed members in the family, annual agricultural income and, food sufficiency. Total production multiplied by the current market price within the study area was used to calculate average household income from different sources.

2.4.3 Framework for determining social indicators

Social livelihood security was assessed in terms of the following indicators: Access of safe drinking water and sanitation; and access to market, health and educational services.

These indicators are relevant both from societal and individual perspectives. For long-term livelihood security, it is necessary to provide equity in social services to reduce the vulnerability of livelihoods.

2.4.4 Framework for determining Management indicators

A protected area obtains a value for its management for example, through the sum of all the values of all the management fields, expressed as a percentage of the optimum value. The results were ranked as unsatisfactory (<=36%), marginally satisfactory (36-50%), moderately satisfactory (51-75%), satisfactory (76-90%), or very satisfactory (91-100%) depending on its score.

2.5 Development of an indicator system for assessing ecological security

We adapted the Organization for Economic Co-operation and Development "Pressure-State-Response (PSR) Framework [OECD, 1993] as the foundation of an indicator system for assessing ecological security (figure 1).

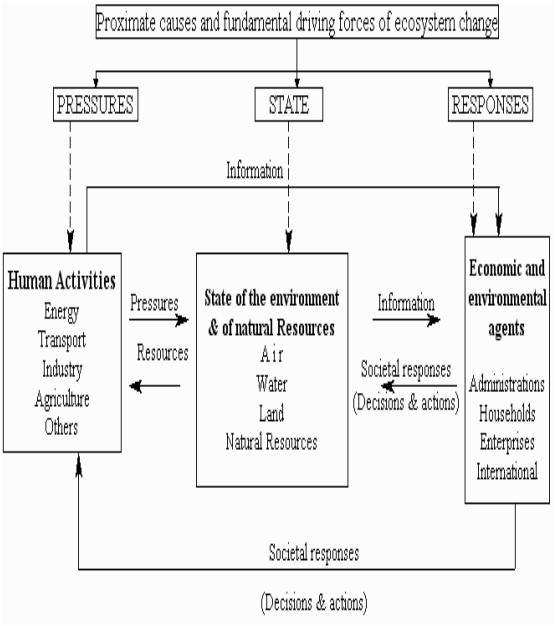

Figure 1: PSR concept model of OECD

The PSR model shows the causality between pressures on the environment and the resulting environmental degradation. The model's results thus have an obvious and intimate relationship with sustainable development. We selected three categories of factors that would be useful in assessing ecological security (natural, social, and economic factors) and that would comprehensively reflect the characteristics and situations of the regional environment.The analytic hierarchy process [Saaty, 1990] was used to decompose the factors that affect the ecosystem security into three main layers (Goal node, Criteria, and Sub-criteria node) (table 1).

Table1: Indicator system

IES=	Pressure	Population (A1)
		Hunting & collection of non timber forest products (A2)
		Farming & annual agric income (A3)
		Mean annual population growth (A4)
		Mean annual temperature (A5)
		Mean annual rainfall (A6)
	State	Soil fertility (A7)
		Land cover change (A8)
		Risk/uncertainty (A9)
		Water quality and quantity (A10)
		Access to markets & credits (A11)
		Agric diversification (A12)
		Employment (13)
		Status of fauna & non timber forest products (A14)
	Response	Staff (A15)
		Regulations (A16)
		New technology (A17)
		Behavior of households towards conservation issues (A18)
		Education & capacity building (A19)
		Research (A20)

2.5.1 Pairwise comparison

Indicators were pair-wise compared for their relative importance with respect to another element to establish priorities for the element being compared. Ratings follow the fundamental 1–9 scale [Saaty, 1997] of AHP (table 2).

Table 2. *The Fundamental Scale for Making Judgments*

1	Equal
2	Between Equal and Moderate
3	Moderate
4	Between Moderate and Strong
5	Strong
6	Between Strong and Very Strong
7	Very Strong
8	Between Very Strong and Extreme
9	Extreme
	Decimal judgments, such as 3.5, are allowed for fine tuning, and judgments greater than 9 may be entered, though it is suggested that they be avoided.

The procedure then requires that the principal eigenvector of the pair wise comparison matrix be computed to produce a best fit set of weights. These weights will sum up to one as is required by the weighted linear combination procedure. Since the complete pair wise comparison matrix contains multiple paths by which the relative importance of criteria can be assessed, it is also possible to determine the degree of consistency that has been used in developing the ratings. Saaty indicates the procedure by which an index of consistency, known as a consistency ratio (CR), can be evaluated. CR indicates the probability that the matrix ratings were randomly generated. For CR>0.1 should be re evaluated [Saaty, 1997].

2.5.2 Standardization - utility maximization mode

Ranking of alternatives is likely to be biased when attributes are measured in different units as is in our case. Hence, a multiple attribute evaluation method-utility maximization [Prato, 1999b], which involves maximizing a multiple attribute utility function, is used here:

For positive attributes or $x_{ij} \geq \min_j x_{ij}$,

$$S_{ij} = \frac{x_{ij} - \min_j x_{ij}}{\max_j x_{ij} - \min_j x_{ij}} * 100; \quad (5)$$

For $x_{ij} \leq \min_j x_{ij}$

$$S_{ij} = 1 - \left(\frac{x_{ij} - \min_j x_{ij}}{\max_j x_{ij} - \min_j x_{ij}} * 100 \right) \quad (6)$$

Where, x_{ij} is the raw value, and s_{ij} ($0 \leq s_{ij} \leq 1$), is the standardized value of the *j*th attribute for the *i*th alternative. The assumption here is that, the decision-maker is risk neutral.

It follows that, for any layer of security, the total un-security (or index of eco-security) value, IES can be estimated as:

$$IES_{ij} = \sum_{j=1}^{j=m} w_j s_{ij}; i = 1,2,...,m \quad , \quad (7)$$

Where m is the number of attributes, and w_i ($0 \leq w_j \leq 1$) is the weight for the *j*th attribute, obtained by using the AHP model $\sum_{j=1}^{j=m} w_j = 1$.

3. Results

3.1 Agricultural land-use patterns and types

A large part of the population in the Korup region depends on agriculture for their livelihoods. However, crop diversification is limited to the cultivation of Cassava, yams, plantains, bananas .Of late, the increase in prices of food crops has motivated households to increase hectares seeded to some crops especially cassava and palm trees (*Elaeis guineensis*). The identified land-use/ cover types were: cultivated areas, fallow lands (characterized by fire clearing), sparse to dense tree cover, severely eroded areas, and coarse pebbles/sand rivers with outcrops of volcanic rocks in some places. Sand in most cases was still fresh signifying erosive actions. The sparse to dense, tree cover is defined as areas with more than 40% canopy cover [Lykke, 2000].

3.2 Socioeconomic threats to the ecological system

Hunting pressure is on-going and has greatly reduced the population of animals/wildlife in the area. Apart from monkeys, it is really difficult to find other species of animals we read and hear of on papers.

Demographic changes in the central zone of KNP are fundamental to the current pressure and threats on the park. The average population

growth (following our investigation) puts Ekundo-*kundo* village at 2%, 4.5 % at *Erat* and 2.5% for *Ekon1* village. *Ekon1* and *Erat* villages are very close to neighboring Nigeria-Calabar and its environs. Hence, apart from natural population growth, positive fertility rates, etc., population growth in these areas can partly be explained by migration/immigration. This is posing serious threat to the Korup's ecological integrity.

3.2 Land cover Change (1986-2000)

Only 1.47% of land cover remains unchanged in the central zone of KNP from 1986 to date (table 3)

Table 3: Land cover change statistics of central korup from 1986 to 2000

From 1986 to 2000	Area (ha)	% change
Decrease	27946.70	49.54
Some decrease	9812.39	17.39
Increased	16527.80	29.30
Some increase	1300.44	2.31
Unchanged	829.68	1.47
Total	56417.01	100.00

An increase in population prompts the movement of new settlement into regions with fragile ecosystems; land under other uses is encroached upon by people seeking to find new lands to cultivate. From 1986 to 2000, land cover in the region has decreased by more than 50% and increased half as much.

3.3 Soil fertility status

Soils are acidic (4.7), mostly sandy (77%), low levels of nutrients and of organic matter (1.36-5.2%), and of high base saturation (Table 4).

Table4: Soil properties in the central zone of the Korup National Park

Soil properties		Unit	Range	Mean	Interpretation
Sand		%	70-84	76.95	Very high
Silt		%	10-30	20.9	Medium
Clay		%	6-21	12.55	Medium
Organic matter		%	1.36-5.2	2.52	Very Low
Organic Carbon		%	1.06-4.0	1.89	Very Low
Available Phosphorus		mg/Kg	2.02-4.48	2.73	Very low
pH	pH-water		4.25-5.01	4.60	Acidic
	pH-Kcl		3.74-4.06	3.90	Very acidic
Potassium		%	10.18-29.39	22.13	Medium
Saturate bases		%	24-39	31.85	High
Nitrogen		g/kg	0.6-2.38	1.23	Low
C/N ratio			10-32	16.12	Medium

Organic matter content not only influence soil productivity but also improves its texture and structure, reduce leaching of nutrients, increases water holding capacity, supports the activities of microorganisms, contributes to improve soil structure and productivity, and reduces erosion. Acidity makes it difficult for biomass to be recycled; thereby reducing global environmental services, as this negatively contributes to sequestrate carbon in soil.

3.4Socioeconomic indicators

3.4.1 The Index of crop diversification

The Herfindhal indices for both years (table 5) are respectively 0.309(309 per thousand) and 0.306 (306 per thousand). The crop diversification index revealed that both communities have significantly low crop diversification in their cropping systems.

Table 5: Crop diversification index for 1986 and 1996

	1986			1996		
i	x_i	h_i	h_i^2	x_{1i}	h_{1i}	h_{1i}^2
Cocoyams & Cassava	46	0.469	0.220	71	0.455	0.207
Plantains & Bananas	21	0.214	0.046	39	0.250	0.063
Palms	18	0.184	0.034	26	0.167	0.028
Cocoa	7	0.071	0.005	11	0.071	0.005
Others	6	0.061	0.004	9	0.058	0.003
Total	**98**	1.000	**0.309**	**156**	**1.000**	**0.306**

'Others' here refer to crops occupying less than 0.1ha of farmland. As shown, they make up about 6% of the total cropland.

3.4.2 Average annual incomes and Index of profitability (IP)

The average annual incomes are relatively low when compared to the current poverty rate in the country. The contribution margin and indices of security (88.75% and 78.29% for 1986 and 2000 respectively) are interestingly high and almost same for the period under study. However, per household average annual incomes hardly attains 150 000FCFA, an income far lower than the baseline of CFA269 400/yea r ≡ $1.7/day, Cameroon's poverty level. This might be so because agricultural inputs are far cheaper when compared to the current rise in food prices. With current government efforts to fight against price hikes, we do not expect such a situation to be long lasting.

3.5 Pair Wise comparison of the clusters

Pairwise comparison (table 6a-c) demonstrated here was carried out using the SuperDecisions software. We pairwise compared elements of the criteria, sub-criteria and alternative decisions for assessing and evaluating ecological security of the area.

Table 6a: Pair wise comparison of main Criteria with respect to the goal

Criteria	Pressure	State	Response
Pressure	1	5	3
State	1/5	1	3
Response	1/3	1/3	1

The inconsistency value = 0.000<0.1

Table 6b: Pair wise comparison of pressure sub-criteria of the objective

Pressure sub-criteria	A1	A2	`A3	A4	A5	A6
A1	1	1	3	5	7	9
A2	½	1	2	4	6	8
A3	1/3	1/2	1	2	5	7
A4	1/5	1/4	1/2	1	2	4
A5	1/7	1/6	1/5	1/2	1	2
A6	1/9	1/2	1/7	1/4	1/2	1

Inconsistency value = 0.0181<0.1

Table 6c: Pair wise comparison for 'state' sub-criteria of the objective

State sub-criteria	A7	A8	AC9	A10	A11	A12	A13	A14
A7	1	3	2	6	4	4	5	5
A8	1/3	1	1/2	4	2	2	3	3
A9	1/2	2	1	5	3	3	4	4
A10	1/6	1/4	1/5	1	1/3	1/3	1/2	1/2
A11	1/4	1/2	1/3	3	1	1	2	2
A12	1/4	1/2	1/3	3	1	1	2	2
A13	1/5	1/3	1/4	2	1/2	1/2	1	1
A14	1/5	1/3	1/4	2	1/2	1/2	1	1

Inconsistency ratio =0.0141<0.1

The inconsistency measure is useful for identifying possible errors in judgments as well as actual inconsistencies in the judgments themselves. Inconsistency measures the logical inconsistency of your judgments.

The judgment value pointed to 3 on the third column in table 4b for example, in the first row, for example, means that A1 (population) is more important when compared to A3 (annual agricultural income), according to the decision maker. 1/3 would mean the reverse and 1 will mean equal importance. The inconsistency index, 0.0181<0.1, shows that the judgments were quite reasonable. The State, response and the other sub-criteria were compared in a similar manner. The values from the pairwise comparison were used to produce a supermatrix from which priorities of the alternatives were obtained.

3.6 Weights of the indices –weighted and Limit super matrices

The priority weights derived from the pairwise comparisons are entered in the Unweighted Supermatrix. In a hierarchical model like this, the Weighted Supermatrix is the same as the Unweighted Supermatrix because the clusters are not weighted. Raising the Weighted Supermatrix to powers yields the Limit Matrix from which the final priority options are extracted.

The sum of products of the priority weights and the standardized values of the indicators gives the weighted score, the index of ecological security for the year concerned (table 7).

Table 7 *Standardized scores of the indicators*

	Score			Weighted scores	
Indicator Name	1986	1996	Priority weight	1986	1996
Population	0.6000	0.2857	0.0728	0.0437	0.0208
Hunting & collection of NTFP's	1.0526	0.6250	0.0625	0.0658	0.0391
Annual agric income	0.6000	0.2973	0.0409	0.0245	0.0122
Mean annual population growth rate	0.5000	0.2000	0.0186	0.0093	0.0037
Mean annual temperatures	0.2308	0.2308	0.0118	0.0027	0.0027
Mean annual rainfall	0.7668	0.7668	0.0091	0.0070	0.0070
Soil fertility(organic matter)	0.9615	1.5000	0.1107	0.1065	0.1661
Land cover change	0.6250	0.8000	0.0491	0.0307	0.0393
Risks and uncertainties	0.5000	0.0909	0.0753	0.0377	0.0068
Clean water quantity& quality	0.3750	0.6667	0.0118	0.0044	0.0078
Access to markets and credits	0.0000	0.0000	0.0301	0.0000	0.0000
Crop diversification	0.6667	0.6667	0.0301	0.0201	0.0201
Employment	0.0000	0.0000	0.0181	0.0000	0.0000
status of wildlife & NTFP's	0.4000	0.5000	0.0181	0.0072	0.0090
Staff	0.3077	0.5000	0.0145	0.0045	0.0072
Legal security& International obl'gns	0.5000	0.3333	0.0240	0.0120	0.0080
New technology	0.0000	0.1818	0.0872	0.0000	0.0159
Behavior of local people-conserv'n	0.2000	0.3000	0.0313	0.0063	0.0094
Education & capacitybuilding	0.3333	0.3333	0.0501	0.0167	0.0167
Research	0.5000	0.7500	0.0340	0.0170	0.0255

Ecological security index, U, was grouped into five classes:

- ✓ ($0<U_{ij}<2$); moderately damaged,
- ✓ ($2.1<U_{ij}<4$); slightly damaged,
- ✓ ($4.1<U_{ij}<6$); relatively damaged, and
- ✓ ($6.1<U_{ij}<8$) or secured ($U_{ij}>=8.1$).

All values are multiplied by '1000' so as to upgrade the final weight to a whole number.

3.11 Ecological safety map of the Central zone of Korup national Park

Shape files for the ecological security indices for 1986 and 2000 were created in ArCGIS 9.2 .With other shape files (points); the ecological security map (figure 2) of the area was generated.

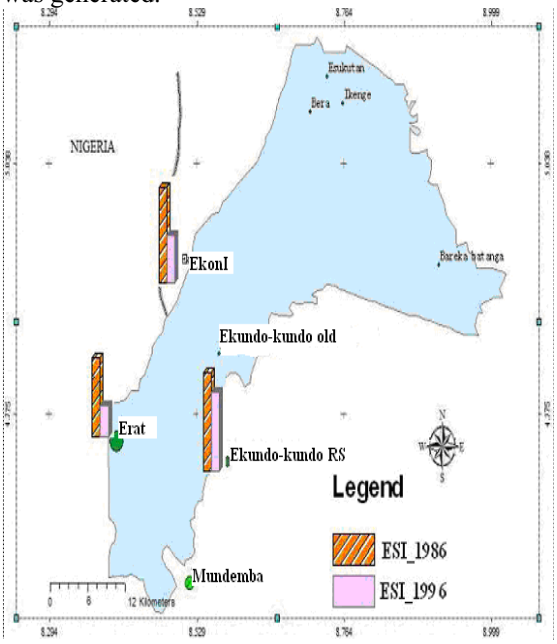

Figure 2: Index of Ecological Integrity map for the central zone of Korup national park

The taller the bar, the more secured is the ecological system and vice versa. For example, the security status of Ekundo-kundo RS (Resettlement Site), has dropped from secured (U_{ij} >=8.1) in 1986 to moderately damaged (2.1<U_{ij} <4).

4. Discussions

Ecological and livelihood security in the central zone of the Korup national park are the results of a variety of ecological, economic, social and changes.

The change in land cover is partly as a result of successional species from the old site (*Ekundo-Kundo*), following the involuntary resettlements of the early 2000.Also, it is the result of the recent extensification to palm and cocoa plantations in the entire central zone of the park, and the agro-climatic potentials are most important explanatory variables.

Herfindhal index reveals that there is diversification in the cropping system is not significant enough.We expected the poor soil quality to be a major set back to agricultural extensification. Though this is good for the environment, it is not good news as far as sustainable livelihoods is concerned.

4.1 Priority action for management

From the sensitivity analysis of our results, it is clear that population (A1) and annual agricultural incomes (A3) are most important priorities for management. The increasing population pressure associated with farming and homesteads activities raises some hypotheses. As many farmers now seem to specialize, this situation may fail to factor out in the long-run sustainability of the farm operation and thus creates uncertainty regarding its future. The increase in population density might render the area less suitable for agricultural extensification and thus people look for further encroachment into the park, let alone poaching activities.

4.2 Can we uncover driving forces of ecological and livelihood deterioration through our binary and index model?

Yes, the binary and index model developed in this study suggest some important underlying causes of ecological and livelihood deterioration that that can be related to some well-established frameworks. Soil is the base material required for the survival of plant ecosystems, and plays an important role in an ecosystem by means of its physical and chemical characteristics and its ability to regulate heat and water balances. The soils are generally acidic, low organic matter, low phosphorus content and of saturated basis. Soil structure is poorly developed, and their ability to preserve moisture and soil fertility is low. Taking into consideration the current property right regime in the area, and government action in meeting up with many of its international obligations, it is clear that food security in this area will be threatened in the long run.

Again, the population increase that has occurred in this region in recent decades is another important reason for the current ecological situation being experienced by central Korup. Human activities including building of mud houses, chopping down large quantities of woody vegetation to provide fuel, and so on, have also damaged the environment.

The creation of new agricultural land (which can be explained by socioeconomic and biophysical factors determining the marginality of the area) has significantly reduced the area of forestland and wild products. Such activities are the major

causes of poverty and environmental degradation in watersheds [Paudyal and Thapa, 2002] and may lead to further social, political and economic problems [Seddon and Adhikari, 2003].

Like elsewhere in the tropics, there seems to be widespread public ignorance of environmental issues. Over 90% of the indigenes are ignorant of the consequences of their actions. It is imperative to convince the populace and governments officials that environmental security and/or integrity matters.

High levels of political corruption exist in the area. Like in Kalimantan-Indonesian Borneo [Smith at al., 2003], local tribal leaders, military, and police are being bribed by illegal hunters. During our survey, it was observed that forces of law and order dispatched to check illegal hunting are primary consumers of wild products especially bush meat. Special police forces could be seen with hunted species of rare animals. This demonstrates that current efforts to eradicate corruption need a change of direction to achieve tangible conservation.

Poverty and lack of funding are also seen as the major driving forces of threats to ecological security of the area. A chronic lack of funding is also threatening the integrity of the ecological system. It is read and understood that forest guards exist in the region, but during our survey, only one was seen. Lack of finance hampers management efforts threatening the opportunities of the future generations from whom we are borrowing these natural resources.

4.3 Social security

4.3.1. Access to safe drinking water supply and sanitation

There is no pipe borne water supply. Streams and rivers are the main source of portable water. Indigenes bathe and drink of the same water. An outbreak of water borne diseases may cause untold consequences to human lives.

4.3.2. Access educational services

One primary school with poor infrastructure serves each village. Furthermore, environmental education which is important for conservation is lacking in schools internal curriculum.

5. Conclusion

This paper indicates the importance of understanding the dynamics of ecological change in a spatial-explicit way, their proximate and underlying driving forces, and possible impacts on human and ecological security.

Our judgment of ecological security in this paper was based on whether human activity damages the ecosystem, and whether the resulting ecosystem threatens the existence and development of humanity. Based on the calculation model described in this paper, while the socio-economic statuses of the villagers remain uncertain, the ecological security of the area has moved from slightly, to moderately damage in the past decades.

There is need to strengthen anti-poaching and law enforcement measures, update research activities, integrating poverty alleviation issues into conservation, gain local community support through creating opportunities and benefits; capacity building and environmental education. Furthermore, agroforestry will be uniquely suited to provide ecological friendly solutions that successfully combine objectives for increased food security and biodiversity conservation gains, especially by promoting greater use of native tree species in agroforestry systems. Women and children, who are the main actors in collection of non timber forest products, hunting and farming, should be a major target. This process does not end yet and our results may be considered as a first approach.

Acknowledgements

We thank the Chinese Scholarship Council for granting a scholarship and other facilities. We are also grateful to the Ministry of scientific Research of the Cameroon for granting us the research authority to carry out the research
.

Correspondence to
Professor Ge Jiwen, *Director, School of Ecology and Environmental Sciences, China University of Geosciences, Hongshan District, 388 Lumo Road, Hubei Wuhan, 430074, P.R. China.*
Telephone: +862762493959
E-mail: gejiwen2002@yahoo.com.cn

References

J.A. Anderson, Editor, *Towards Gondwana Alive: Promoting Biodiversity and Stemming the Sixth Extinction* **vol. 1**, Gondwana Alive Society, Pretoria, South Africa (2001).

Llewelyn and Williams, 1996. R.V. Llewelyn and J.R. Williams, Nonparametric analysis of technical, pure technical and scale efficiencies for food crop production in East Java, Indonesia. *Agricultural Economics* **15** (1996), pp. 113–126.

Lykke, A.M. (2000) Local perceptions of vegetation change and priorities for conservation of woody-savanna vegetation in Senegal. J. Arid Environ. 59, 107–120

M. Loreau, S. Naeem and P. Inchausti, Editors, *Biodiversity and Ecosystem Functioning: A Synthesis*, Oxford University Press, Oxford, UK (2002).

Millennium Ecosystem Assessment, 2005. *Ecosystems and Human Well-being: Biodiversity Synthesis.* World Resources Institute, Washington, DC

Myers N, Mittermeier RA, Mittermeier CG *et al.* (2000) Biodiversity hotspots for conservation priorities. *Nature* **403,** 853–8.

N. Agar, 2001, Life's Intrinsic Value: Science, Ethics and Nature, Columbia University Press, New York, USA (2001).

OECD, Group on the State of the Environment, 1993. OECD Core Set of Indicators for Environmental Performance Reviews (Environment Monograph No.83).

Paudyal and Thapa, 2002 G.S. Paudyal and G.B. Thapa, Farmland degradation in mountains of Nepal: a case study of watershed with and without external intervention, *Land Degradation and Development* **13** (2002), pp. 479–493.

Pirages, D. & Cousins, K. (Eds.) (2005). From resource scarcity to ecological security. Cambridge, MA: MIT Press

Prato, T., Hajkowicz, S., 1999. Selection and sustainability of land and water resource management systems. J. Am.Water Res. Assoc. 35, 739–752.

Rozann W. Saaty (2003). Super Decisions: Software for Decision Making with Dependence and Feedback; Pittsburgh, PA 15213

S. Díaz, J. Fargione, F.S. Chapin III and D. Tilman, Biodiversity loss threatens human well-being, *PLOS Biology* **4** (2006), pp. 1300–1305

Saaty, T. L., (1997). A scaling method for priorities in hierarchical structures. J. Math. Psycho., **15**: 234-281.

Saaty, T. L. 1990. An Exposition of the AHP in Reply to the Paper "Remarks on the Analytic Hierarchy Process", Management Science, Vol. 36, No. 3, 259-268.

Schmidt-Soltau, K. 2004. Stakeholder analysis for the Intervention of the German Financial Cooperation in the context of the Forest and Environment Sector Programme. Final report. MINEF, Yaoundé Cameroon

Seddon and Adhikari, 2003 .A conflict and food security in Nepal: a preliminary analysis, Rural Reconstruction Nepal. Kathamandu.

Smith, J., and Scherr, S. 2003. Capturing the value of forest carbon for local livelihoods. *World Development* 31(12): 2143-2160.

Sunderlin, W.D., Angelsen, A., Belcher, B., Burgers, P., Nasi, R., Santoso, L., and Wunder, S. 2005. Livelihoods, Forests, and Conservation in Developing Countries: An Overview. *World Development*, 33:1383-1402.

Turner, B.L. II, Hyden, G., Kates, R.W. (Eds.), 1993. Population Growth and agricultural Change in Africa. Univ. Press of Florida, Gainesville.

World Bank. 2004. Sustaining Forests: A Development Strategy. The World Bank. Washington D.C., USA.

Xiao, D.-N., Chen, W.-B., Guo, F.-L., 2002. On the basic concepts and contents of ecological security. Chinese Journal of Applied Ecology 13, 354–358 (in Chinese, with English summary).

Yan-Zhi Zhao, Xue-Yong Zou , Hong Cheng , Hai-Kun Jia, Yong-Qiu Wu Gui-Yong (2005). Assessing the ecological security of the Tibetan plateau: Methodology and a case study for Lhaze County. Journal of Environmental Management 80 (2006) 120–131

Zimmermann, 2000 Zimmermann, L., 2000. A comparative study of growth and mortality of trees in caesalp dominated lowland African rainforest at Korup, Cameroon

Marsland Press
Journal of American Science 2009:5(2) 54-68

Spatial Patterns of Abundance and Diversity of Socioeconomic Important Plant Species in a Human Inhabited Protected Area at Korup, Cameroon

[1,2] Innocent Ndoh Mbue , [1,2] Jiwen Ge*, [2]K. D. D. Liyanage Wasantha ,[2] Y. Nowel Njamnsi

[1]Institution of Ecology and Environmental Sciences, China University of Geosciences,
Hongshan District, 388 Lumo Road, Wuhan, China, 430074 (*Corresponding Author, Email: gejiwen2002@yahoo.com.cn)

[2]School of Environmental Studies, China University of Geosciences,
Hongshan District, 388 Lumo Road, Wuhan, China, 430074

Abstract:

We present data on sample richness, relative abundance, and community structure of economic plant species assemblage from a globally important hotspot of biodiversity- the inhabited central region of Korup National Park, southwestern Cameroon. Patterns of species diversity and spatial variability across major locations are described. We recorded 23 species, the mean richness location 13.3 (minimum: 7, maximum: 20, median: 13, standard error of the mean 3.436) which is significantly low compared to the ever increasing population. We found that population pressure and cultivation of native habitat reduces economic plants species diversity, a conclusion that has important implications in light of the rapid conversion of parts of the protected area for agriculture and fuel-wood in human inhabited protected areas of sub-Sahara Africa. The Mantel test statistic showed a significance level (P =0.001), but there is a large scatter of observations and correlation is low (r= 0.2225) among values of the gradient and ecological distance matrices. The ordination analysis revealed six axes accounting for only 30.14% of the total variance (Pseudo-F =1.78207; P<0.001, n =1000 permutations), suggesting that soil variables may not be important in the spatial distribution of plant species. These conclusions emphasize the importance of stratified long-term sampling in biodiversity studies and demonstrate that superficial levels of sampling effort can lead to erroneous conclusions regarding patterns of floristic species. Continuous existence of such protected areas, ecological integrity and sustainable human livelihoods in the areas would require that both education of the population and eco-agriculture based on the cultivation of these economic plant species be given priority. [Journal of American Science 2009:5(2) 54-68] (ISSN: 1545-1003)

Key words: Economic plant species; Ecological integrity; Sustainable human livelihoods; Korup National Park

1. Introduction

The diversity and distribution of food and medicinal plants in hotspots of biodiversity that are inhabited by poor dependent forest communities who cannot integrate traditional markets, but need alternatives for income generation need special attention in ecology. As human population density in such areas continues to increase with time, so too is increase pressure on the ecological milieu through uncontrolled degradation and conversion to other land uses, in order to meet up with the challenges of life. The resulting impacts are in the form of loss of biological resources, damage to habitats and

ecological services [Costanza et al., 1997; De Groot et al., 2002]. To the extent that humankind neglects to maintain such global life-supporting ecosystems, current and future generations will be confronted with increasing severe instances of environmental induced changes.

In the central zone of the Korup national park (KNP), Cameroon, the belief that ecological security became secured following the creation of the park in 1986 pervades calculations of local and national policy makers, but this belief is not based on direct observation of the situation today. The living consequences in the enclave central zone of the park include, decline in wildlife population of plants and animals, and above all, the emission of green house gases through environmentally harmful agricultural practices.

The preservation of biodiversity and e cosystem services of such areas requires accurate information from a wide variety of sources. Since inhabitants of such areas depend on food and medicinal plants as their main source of livelihood, information about their biodiversity and spatial distribution with respect to environmental variables is essential. Such information is needed to better predict the effects of future manipulations on biodiversity, stand development, and long-term ecosystem structure and function. This can take the form of designing alternative form of cultivations such as eco-agriculture [McNeely and Scherr, 2002], agro-forestry or analog forest [Earles 2005; Scherr and Shames 2006] that can reduce pressure on biodiversity, at the same time sustaining livelihoods and/or food security. This system shares a vision of "farming with nature," an agro-ecology that promotes biodiversity, recycles plant nutrients, protects soil from erosion, conserves and protect water [Scherr and Shames 2006].

Researchers have explored a variety of methodologies for describing the spatial distribution of diversity on large and small scales. To describe community structure and compare samples, diversity indices such as the Shannon [Shannon, 1948], the Simpson's [Simpson, 1949], etc., have been used. However, such indices have been found not to provide sufficient information to order communities in diversity [Kindt, 2006], and in some cases, when ranking differs; it is not possible to be categorical that a particular site is more diverse than another, even if the sampling regime adopted has been appropriately standardized [Whittaker et al. 2001].

Differences in vegetation cover over large areas have been linked to regional climatic gradients or to local differences in parent materials [AbdEl-Ghani 2000; Bennie et al., 2006]. Sebastiá (2004) found that soil fertility was the main environmental gradient structuring subalpine, calcareous grassland communities at the landscape scale. On the contrary, Van der Moezel and Bell (1989) found highest species richness to occur on soils with the lowest nutrient content in the mallee region of Western Australia. Hahs et al. (1999) also reported a strong negative correlation between soil nutrient concentration and species richness in sclerophyll heath vegetation in Victoria. These contradictory findings show that environmental factors act differently across scales and/or regions. One cannot therefore adopt results from other regions however similar they maybe in biophysical characteristics.

In this study, we describe the floristic diversity of food plants and medicinal plants in a human inhabited protected area; the Korup National Park (KNP) of south western Cameroon, using diversity profiles and ordination techniques.

Previous work has been taxonomic, focused on forest structure and dynamics. This study, which is the first of its kind in the region, aims to evaluate the

importance of soil factors in determining spatial patterns in the distribution of food and medicinal plants species. This involves (a) sampling the vegetation and soil variables, (b) biodiversity ordering, (c) the identification of soil variables that display patterns in distribution and (d) an assessment of the significance of the relationships between these variables and the flora that may inform the selection of conservation prescriptions.

2. Materials and methods

2.1 Study area

The study area (1,260 km^2) is located in Ndian Division, southwestern Cameroon, between latitudes 4° 54′ and 5° 28′ north; and longitudes 8° 42′ and 9° 16′ east of the equator, at the Cameroon-Nigerian border and is contiguous with the Oban National Park-Nigeria. It is believed that Korup lies at the centre of the Guinea-Congolian forest refugium, one of only two Pleistocene refugia proposed for Africa. Our study focuses on central zone of the Park. The region is of interest partly because it is inhabited by man, and because it is important for conservation since it has many rare, endemic and economic plant species.

2.2 Biophysical conditions

Based on personal investigations, region reaches elevations of up to 1130 m (peak of Mt. Yuhuan), the soil is sandy (70%-80%), and acidic (pH 3.7-4.7). The climate is characterized by a single distinct dry season from December to February and a single-peak wet season from June to October. Mean annual rainfall is in excess of 5000 mm per year [Zimmermann, 2000]. A mean annual maximum temperature of 34 ℃, and a mean minimum temperature of 23.8 ℃ have been calculated. Data for the coastal region indicates that the mean annual relative humidity is 83%, the mean daily maximum is 98% and the minimum is 66%. The flora and fauna of the Korup region is known to be part of the Hygrophilous Coastal Evergreen Rainforest that occurs along the Gulf of Biafra, and is part of the Cross-Sanaga-Bioko Coastal Forest ecoregion [Olsen et al., 2001]. This ecoregion is considered an important center of plant diversity because of its probable isolation during the Pleistocene [Davis et al., 1994] and holds an assemblage of endemic primates known as the Cameroon faunal group [Waltert et al., 2002].

2.3 Sampling design

Field work took place from February 23rd to June 15th of 2008. Thirty modified Whittaker plots (Fig. 1) [Stohlgren et al., 1995], five each per location-the buffer zone, primary forest, secondary forest, the Mt. Yuhuan, Erat, and Ekon1 were set up and surveyed.

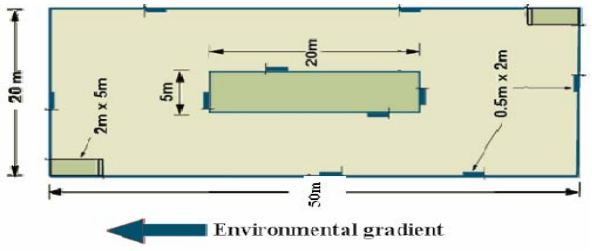

Fig. 1 Modified-Whittaker nested plot setup (adapted from Stohlgren et al., 1995)

The locations of the plots were chosen randomly so as not to create a subjective bias. Plots are placed parallel to the major environmental gradient of the vegetation type being sampled to encompass the most heterogeneity. To eliminate effects of topography, only flat areas (slope <5°) were sampled.

2.4 Variables measured

2.4.1 Soil variables

A total of 100 soil samples (5 per plot) were collected from each plot. The collections were done at the corners (4) and the center (1) with a 2.5 cm diameter soil increment core to depths of 15-20 cm

and pooled into one composite sample. For each sample, surface litter was first removed. The collected soil samples were sent to the University of Dschang, Cameroon for analysis. Some of the variables include, but not all, pH, organic matter (OM), sand, clay, silt, saturated bases (BS), percentage phosphorus, potassium, sodium, and magnesium.

2.4.2 Topographic variables

On each plot, UTM coordinates and elevation (m) were derived from a global positioning system (GPS).

2.4.3 Vegetation variables

In the smallest subplots ($1m^2$) all herbs, grasses and saplings are identified and counted (include all plants less than 50 cm in height). In the two subplots of 10 m^2, all trees and shrubs $\geqslant$ 1cm dbh are measured. In the central 20 m × 5 m sub-plot, all trees $\geqslant$ 5 cm dbh are identified and measured, while trees of (dbh) $\geqslant$10 cm not already covered by the subplots are identified and measured in the entire 1000 m^2 plot area. Cumulative plant species (i.e., additional species found in either the subplots or plot) are recorded successively in the entire sub-plots. Voucher specimens of plants were collected and sent to the National Herbarium in Yaoundé for identification. Not all specimens could be identified to species level as some genera are currently undergoing revision. Food and medicinal plants were sorted after concerting with local authorities, traditional doctors, and some experts. Food and medicinal plants include all edible and medicinal tree growth-forms encomprising trees, shrubs and ground cover.

2.5 Data analysis

BiodiversityR software developed by Roeland Kindt [Kindt and Coe, 2005], built on the free R 2.6.1 statistical program and its contributing packages such as the vegan community ecology package [Oksanen et al., 2005] was also employed.

2.5.1 Richness, abundance and density of tree species

Total species richness was determined as the total number of plant species present in each 1000 m^2 quadrat (sampling site) or each 5000 m^2 location. Total and average tree species richness and tree abundance were calculated for the survey and for separate locations. We define abundance per site or location as the observed number of tree species that were counted on that site or location. Species accumulation curves were calculated using the exact method for calculating the average number of accumulated species when sites are accumulated in a random pattern [Kindt and Coe, 2005]. They were calculated for the subset option, location so that differences in species richness could be analyzed.

2.5.2 Diversity ordering

The performance of different richness estimators varies depending on differences in richness, sampling effort, and community evenness [Colwell and Coddington, 1994], and the relative biases and inaccuracies remain poorly understood, meaning that the most robust estimates are often only for the lower and upper boundaries [O'Hara, 2005]. Hence, diversity research need not be based on single indices of diversity or evenness. As such, techniques for diversity and evenness ordering were used that produce diversity and evenness profiles. In addition, the first order Jack-knife non-parametric estimator was used. Rényi's (1970) showed that;

$$H_\alpha = \frac{1}{1-\alpha} In\left(\sum_{i=1}^{N} P_i^\alpha\right);$$

for $\alpha \in \{0, 0.25, 0.5, 1, 2, 4, 8, \infty\}$

(1)

Where (H_α) denotes Renyi diversity profile values, and P_i is the relative abundance of species i. For any

given community, H_α is a parametric measure of uncertainty in predicting the relative abundance of species. A parameter restriction ($\alpha \geq 0$) has to be imposed if H_α should possess certain desirable properties discussed in the remainder that renders it adequate in ecological research [Legendre and Legendre, 1998]. From the diversity profile, an evenness profiles, $InE_{\alpha,0}$ can be obtained, where,

$$InE_{\alpha,0} = H_\alpha - H_0 \Leftrightarrow E_{\alpha,0} = e^{H_\alpha - H_0} \quad ;$$

$$E_{\alpha,0} \cong N(0,\sigma^2) \qquad (2)$$

Shannon's index is a limiting function of the Renyi's profile function as $\alpha \to 1$; $\alpha = 2, H_2 = -In\sum P_i^2$; (log Simpson index; apparent concentration of dominance). H_0 contains information on species richness, and as $\alpha \to \infty$, this gives Berger-Parker diversity indices. It can also be dissociated into contributions of species richness, the evenness in proportion of the dominant species and the evenness in the proportions of the other species. Subsequently, the ratio, $Ln(E_1)/Ln(E_\infty)$ can be calculated. This ratio provides an indication of the evenness in distribution of the other species (excluding the dominant species). Furthermore, H_α allows for partial ranking of ecological communities in diversity such that, a community of higher diversity than a second community will have a diversity profile that is everywhere above the profile of the second community. Shannon diversity index gives more weight to rare species; Simpson diversity index gives more weight to most abundant species in a sample [Magurran, 1988].

2.5.3 Spatial variation with respect to environmental variables

The potential influence of explanatory factors on species richness and abundance of sites was analyzed by canonical correlation analysis [CCA; ter Braak, 1986]. CCA was preceded by a forward selection process. The forward selection procedure was employed to determine the amount of variance explained by each variable at time of inclusion in the model and the significance of each variable. The forward selection procedure resulted in the retention of 6 variables as significant contributors to variation in the ordination: elevation, pH, percentage of sand, clay, organic matter and Carbon: Nitrogen ratio (C: N).

Descriptive statistics of the six environmental variables, grouped by sampling locations, were calculated and differences among sites were tested by single classification ANOVA using the software program SPSS 13.0. The relationships between vegetation and environmental variables were tested using non-parametric Spearman rank correlations between each of the six environmental variables.

2.5.4 Differences in species community structure and species composition

The nonmetric multidimensional scaling (MDS) ordination was chosen because it makes fewer assumptions about the data distribution, and enables the use of a similarity index that excludes joint absences and provides a visually intuitive summary of similarity among sites [Clarke and Warwick,1994]. Similar matrices were produced using the site-standardized Bray–Curtis similarity index and square root transformed data, as well as presence–absence data. Site standardization (proportioning each species relative to the site total) reduces the contribution that differences in overall abundance make toward differences in community structure. To account for spatial heterogeneity in species richness among sites within any one location (or the importance of geographic distances among sites in determining patterns of community dissimilarity), we used the Mantel's permutation test of the rank correlation

between paired similarity matrices. This was chosen because it can be applied to variables of different logical type (categorical, rank, or interval-scale data), in our case, categorical variables (soil and vegetation variables). Differences in the multivariate community structure between habitat types were examined using an analysis of similarity test ANOSIM) [Clarke and Warwick,1994].

3. Results

3.1 Community floristic, structure and patterns

A total of 23 species of food and medicinal plants were counted in the region. The mean richness on a site was 13.3 (minimum: 7, maximum: 20, median: 13, standard error: 3.436) and the mean abundance was 44.7 (minimum: 32, maximum: 65; median: 38, standard error of the mean 8.08). Some of the structural traits for the six sites surveyed are summarized (table 1).

Table 1 Summary of the community floristic structure and patterns in the central KNP

Parameter	ALL	B	EK	ER	M	P	S
Total plot (20x50m) number	30.0	5.0	5.0	5.0	5.0	5.0	5.0
Total area sampled(ha)	3.0	0.5	0.5	0.5	0.5	0.5	0.5
Abundance(Total tallied stems):	1349.0	190.0	217.0	233.0	260.0	225.0	224.0
1. Woody stem(>=5cm)	734.0	100.0	94.0	136.0	147.0	121.0	136.0
2. Shrubs/herbs/grasses(<1cm)	615.0	90.0	123.0	97.0	113.0	104.0	88.0
Mean stems/ha	449.7	380.0	434.0	466.0	520.0	450.0	448.0
Mean species richness/site	45.0	38.0	43.4	46.6	52.0	45.0	44.8
Mean diameter/stem (cm)**	25.6	27.7	26.4	25.0	23.3	25.3	25.7
Mean basal area (m^2/ha)**	0.00126	0.00121	0.00103	0.00134	0.00125	0.00122	0.00141
Total richness	23.0	23.0	20.0	23.0	23.0	23.0	22.0
Jack.1	23.0	30.2	21.6	27.8	23.8	24.6	25.2
J	0.866	0.822	0.880	0.912	0.802	0.848	0.785

** This applies only to woody stems of dbh⩾5 cm. Richness (S) = number of species; Jack.1 is the first order Jacknife diversity index.B: Buffer zone forest site; EK: Ekon1; ER: Erat; M: Mountain forest site; P: Primary forest site; S: Secondary forest site. (Names are given just to distinguish sampling locations, for most of the forest is primary. Secondary forest here refers to the old village site of Ekundu-kundo-a former village in the park, now resettled at the peripheral zone). Erat and Ekon1 villages still remain in the park.

Stem density range from 380 ha^{-1} in the buffer zone to 520 ha^{-1} in the mountain. The first order Jack-knife estimate for the total richness for all sites combined was 23.0.

Furthermore, there is no significant difference in structural traits between the six plots (ANOVA $P < 0.002$).

The species richness-site curve (Fig. 2) approached an asymptote.

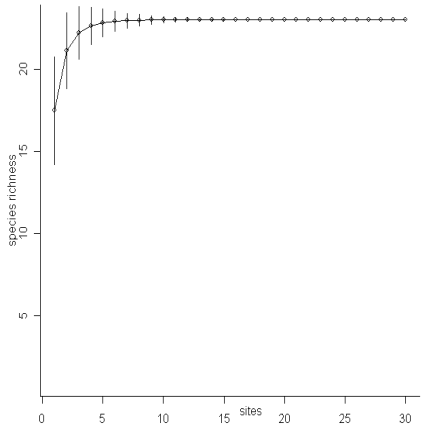

Fig. 2 Species accumulation curve based on rarefaction

At species richness=23, the curve became asymptotic with the site's axis, making comparisons among locations easier.

3.2 Diversity ordering: species richness and abundance and comparisons between locations

In terms of abundance distribution, *Anchomanes deformes* (AND,n=350), a medicinal plant, belonging to the Araceae is the most abundant (Fig. 3). This is followed by *Masularia accuminata* (n=98) and *Cola lepidopta* (n=82).

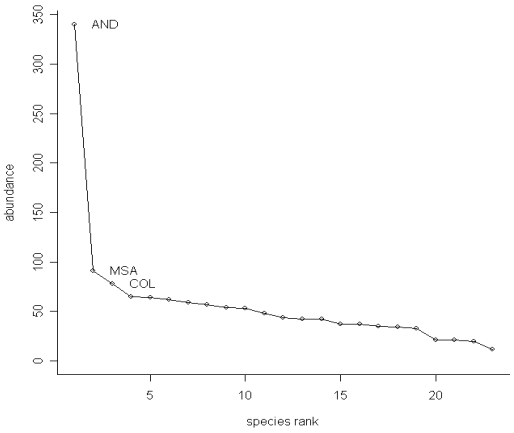

Fig. 3 Rank abundance curve for food and medicinal plants in central KNP

In terms of species richness distribution, Renyi's profile (Fig. 4) for Erat (ER) was above those of other locations.

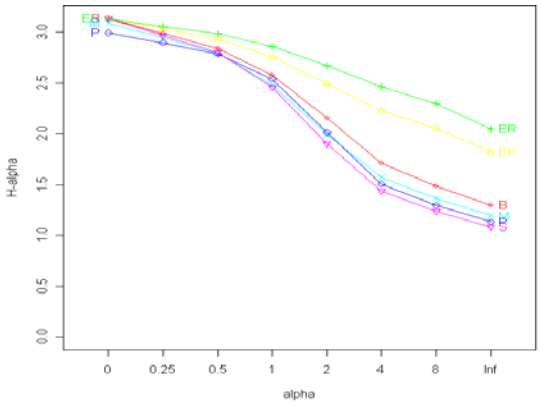

Fig. 4 Renyi's richness profiles for central Korup

Erat is therefore, relatively richest in food and medicinal plants than the other sites, closely followed by Ekon1 (EK). The intersecting profiles for the mountain (M) and secondary forest (S) makes it difficult to rank them.

In terms of evenness, the evenness profile of Erat was again above the profiles of the other locations (Fig. 5), indicating a more even distribution of species in this location than in the other locations.

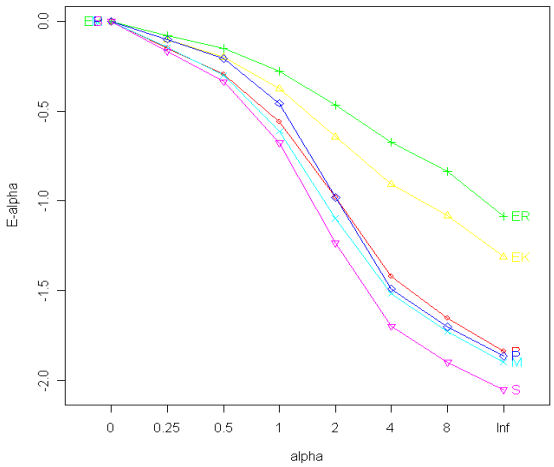

Fig. 5 Renyi's evenness profiles for central Korup

The evenness profiles for the buffer zone (B), the mountain (M) and primary forests (P) were intersecting. It is difficult in this case to rank the locations in terms of evenness distribution in these locations.

Table 2 shows the results for species richness (H_0), evenness in the distribution of the dominant species ($E\infty$), and evenness in the distribution of other species ($lnE1/lnE\infty$) for comparisons between locations of overall species diversity.

Table 2 Species diversity distribution of the dominant species, and evenness in the distribution of other species ($lnE1/lnE_\infty$) for comparisons between locations of overall species diversity

Site	0	0.25	0.5	1	2	4	8	H∞	E∞,0	E1,0	lnE1/lnE∞
B	3.1355	2.9864	2.8429	2.5787	2.1536	1.7142	1.4808	1.2958	0.1589	0.5730	0.3027
EK	3.1355	3.0344	2.9372	2.7597	2.4930	2.2297	2.0517	1.8230	0.2692	0.6868	0.2863
ER	3.1355	3.0577	2.9855	2.8589	2.6703	2.4636	2.2993	2.0488	0.3373	0.7584	0.2545
M	3.0910	2.9445	2.7903	2.4801	1.9925	1.5736	1.3623	1.1921	0.1497	0.5429	0.3217
P	2.9957	2.8964	2.7884	2.5404	2.0139	1.5063	1.2930	1.1314	0.1550	0.6342	0.2442
S	3.1355	2.9699	2.8001	2.4598	1.8999	1.4369	1.2361	1.0816	0.1282	0.5088	0.3290

NB: $E_\infty \equiv E_{\infty,0}$ and $E_{1,0} \equiv E_1$

When comparing the values of H_∞, which indicate the proportion of the dominant species, table 2 shows that Erat had the largest values for the sampled species, while the secondary forest was the

least. In direct comparisons between the locations, on the number of species sampled, Erat (ER; Ln(E∞)=-1.08669) had the least value. The ratio, Ln (E_1)/Ln(E_∞) is least for the primary forest (P). This suggests a more even distribution of other species in the primary forest. H_0, is largest in B, EK, ER and S. This suggests these locations to be richest, while the primary forest (P; H_0=2.9957) to be least rich.

Food plants were significantly more abundant in Erat and Ekon1 locations but with lower levels of relative abundance elsewhere (H = 8.88, df = 3, P = 0.03, all pairwise comparisons significant; Mann–Whitney U > 16, P < 0.05).

3.3 Differences in community structure and species composition between locations

NMDS scores of an ordination based on presence–absence data indicate that Erat, Ekon1 and secondary forest sites are segregated, but the other sites are not distinct from any of the others (Fig. 5).

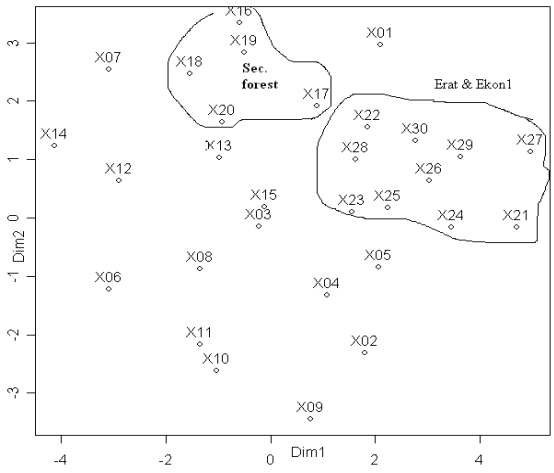

Fig. 6 Nonmetric multidimensional scaling ordination (NMS random (distmatrix, perm=1, k=2)) showing differences in the community structure among four habitats based on presence-absence data and the Bray-Curtis similarity index. A stress value of 22.14173 indicates a fair goodness of fit of the 2D configuration

This suggests that these sites host a subset of species that are also found elsewhere

3.4 Analysis of differences in species composition

The observations in the previous section are supported by the pairwise ANOSIM tests, with all comparisons of multivariate community structure among locations (ANOSIM: Global R = 0.3725, significant :< 0.001; n=1000 permutations; Bray-Curtis distance). Empirical upper confidence limits of R: 90%=0.0926; 95%=0.1140; 97.5%=0.1430; 99%=0.1954. Figure 7 shows that there is evidence for a relationship between the ecological distance and location, however the relationship is not very strong.

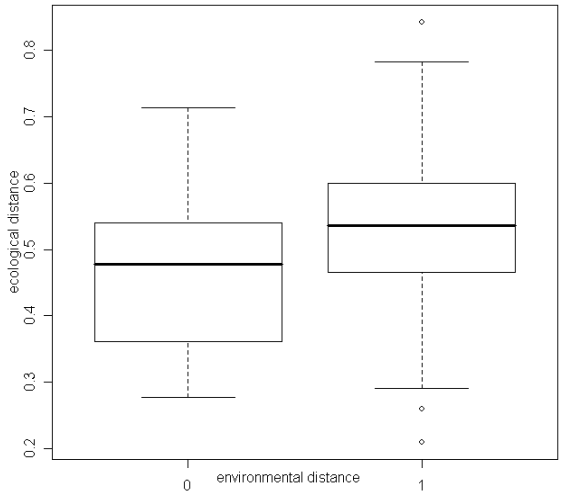

Fig. 7 Bray-Curtis distances in relationship with differences in locations for the central Korup dataset

The importance of geographic distances among locations in determining patterns of community dissimilarity (Mantle test) provided the following results: (Mantel test: permutations = 1000; statistic r: 0.2225; significance:< 0.001).Empirical upper confidence limits of r: 90%=0.0548; 95%=0.0721; 97.5%=0.0849; 99%=0.1068.

The results show that although the significance level of the correlation is quite small (P =0.001), there is a large scatter of observations and correlation is low (among values of the gradient and

ecological distance matrices). Constrained ordination technique was used to properly investigate the influence of environmental variables on species composition since these techniques provide a more comprehensive result.

3.5 Spatial variation with respect to environmental variables

Species showed some degree of spatial distribution that reflects patterns in environmental heterogeneity. Pearson-product moment correlation coefficient revealed some statistically significant correlations among the soil variables (Table 3).

Table 3 Pearson –product moment correlation coefficients (2-tail test) between environmental variables

	Clay	Sand	Elevation	C:N	pH
Sand	1.00**(0.00)				
Elevation	-0.776**(0.00)	-0.776**(0.00)			
C:N	0.399*(0.029)	0.399*(0.029)	-0.1(0.598)		
pH	-0.077(0.686)	-0.077 (0.686)	0.114(0.548)	-0.051(0.788)	
OM	0.235(0.211)	0.235)0.211)	-0.174(0.357)	0.318(0.087)	0.298 (0.109)

P values are in parentheses. C: N=Carbon/Nitrogen ratio; OM=soil organic matter; pH=soil pH.
**Correlation is significant at 0.01 level; *Correlation is significant at 0.05 level.

Clay and sand show a very strong positive correlation and vary in a similar manner with the other variables. Both have a strong negative correlation with elevation. The pH has very low correlation with respect to other soil variables.

The ordination (CCA) analysis revealed that the six axes (table 4) accounted for only 30.14% of the total variance (Pseudo-F: 3.539042; significance: 0.003, n= 1000 permutations).

Table 4: Eigenvalues extracted from canonical correspondence analysis and percentage of variation explained by each axis

	Inertia	Proportion				
Total	1.2999	1.0000				
Constrained	0.3918	*0.3014*				
Unconstrained	0.9081	0.6986				
Axis	CCA1	CCA2	CCA3	CCA4	CCA5	CCA6
Eig.values	0.1461	0.1004	0.05395	0.04362	0.02611	0.02165
Accounted (%)	11.24	18.96	23.112	26.467	28.476	30.142
Intraset correlation coefficients						
Clay	-0.56987	-0.3172	-0.54625	-0.00952	0.1522	0.5028
Sand	0.102533	0.5757	0.56499	-0.28089	0.1619	-0.4819
Elevation	-0.908243	-0.3090	0.17015	0.12513	0.1105	-0.1516
C:N	0.021487	0.3286	-0.56300	0.32387	0.2914	-0.6208
pH	-0.004273	-0.4306	-0.02631	0.28147	0.8398	-0.1717
OM	0.217706	0.3239	0.57086	0.53923	0.2092	0.4332

The ordination diagram (Fig. 8) and intra-set correlation coefficients (Table 4 above) showed that the canonical axes were related to different environmental gradients: axis 1 and 3 were related to decreasing clay (r = -0.56987 and -0.54625 respectively), and increasing clay in axis 6 (r=0.5028). Elevation decreased significantly in axis 1 (r = -0.908243); while axis 5 was related to an increasing soil pH (r = 0.8398)

The most important gradient is the elevation-clay continuum (Fig. 8), increasing along a gradient south east or from the right to left.

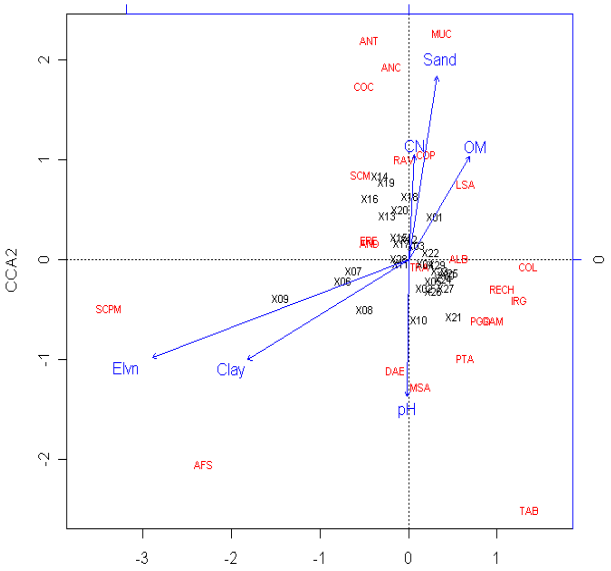

Fig 8 Canonical correlation analysis for central KNP

AFS: *Afromomum sp.*; SCPM: *Scyphocephallum mannii*; DAE:

Dacryodes edulis; SCM: *Schumanniophyton magnificum*; MUC: *Musanga cecropioides*; ANT: *Angylocalyx talbotii*; PTA: *Pycnanthus angolensis*; COC: *Cola chlamydantha*; ANC: *Annickia chlorantha*; COP: *Cola pachycarpa*; COL: *Cola lepidopta*; IRG: *Irvingia gabunensis*; RECH: *Recinodendron heudelotii*; ALB: *Alstonia boonei*; POGA:*Poga oleosa*;RAV: *Rauvolfia vomitoria*; TAB: *Tabernaemontana brachyantha*; LSA: *Lasianthera Africana*, MUC: *Musanga cecropioides*, COP: *Cola pachycarpa.*

The arrows representing the environmental variables indicate the direction of maximum change of that variable across the diagram. Similarly, sand, C:N and OM increase north east, while pH increases southward.

The length of the arrow is proportional to the rate of change, so a long pH arrow indicates a large change and indicates that change in pH is strongly correlated with the ordination axes and thus with the community variation shown by the diagram. In this case the strong correlation between sites X08 to X12 (Mountain), elevation and % clay content is unsurprising.

The most important gradient is the elevation-clay-sand continuum, with sand increasing on lowlands gentle-slopes. Clayey soils have higher concentrations of nitrogen and most cations, including aluminum ions. Clays have more binding sites for cations, largely because clay content is positively correlated with organic matter, which is an important determinant of cation exchange capacity in soils with clays of low activity.

Soil pH did not show any strong association with any of the axis. Some plant species show strong association with soil variables while some did not. For example, *Lasianthera africana, Cola pachycarpa; Musanga cecropioides, and Rauvolfia vomitoria are related with C:N ratio, OM,* and sand. However, a majority of the species seems not to have a significant correlation with soil variables.

A posteriori tests however did not produce consistent groupings of locations. Only elevation and sand showed significant differences between forest locations. Sites were significantly different among with respect to soil variables in one-way MANOVA (df=20, 329, Wilks' l = 0.182; F = 11.055; P= 0.001). Generally, the soils were quite sandy, clayey, acidic and similar across the entire region.

4. **Discussion**

4.1 Brief description of vegetation in central Korup

Though there are many economic plant species, our attention was focused on food and medicinal plants since this form a major source of household income and food. No evidence of industrial timber logging could be found in the area.

The central zone of Korup National Park contains a very rich flora, with many plant species that are poorly known or have very limited distribution. Due to lack of information on distributions and taxonomy, it is impossible to describe species as "endangered" or, "threatened"; instead, the term "rare" is used to indicate species of concern to forest management. Rare food plants in the buffer zone, secondary forest, mountain and primary forest areas include (but not all), *Coula edulis*, *Elaeis guineensis*, *Monodora* spp., *Poga oleosa*, *Scorodophloeeus zenkeri*, *Baiillonella toxisperma*, *Recinodendron heudelotii*, *Afrostyrax lepidophyllus*, *Garcinia kola*, *Poga oleosa*, *Recinodendron heudelotti*, *Tetracarpidium conophorum*, *Tetrapleura tetraptera*, and *Treculia africana.* However, most of these food plants are found in substantial quantities in Erat and Ekon1 area and yield substantial income to the households.

Other forest fruit trees of importance include, but not all, *Cola lepidopta*, *Cola pachycarpa*, *Dacryodes edulis*, *Irvingia gabonensis*, *Trichoscypha acuminata.* These plants are unevenly distributed in the area. *Gnetum africana* for

example can hardly be seen in the buffer zone, secondary, mountain and primary forest.

The conversion of forest in some of the locations (Erat and Ekon1) for farmland is one of the primary threats facing the conservation of this important biome. Consideration of the relative biodiversity value of the entire region is severely limited by a paucity of data from other areas. It is unfortunate that the deployment of an intensive sampling campaign is both time demanding and financially costly, and accordingly many recent studies of amphibian diversity in the area have not been based on a statistically defined methodology.

4.2 Spatial patterns of food and medicinal plants relative to abundance and diversity

We found that patterns of overall food and medicinal plants relative abundance in our samples were strongly influenced by the distribution of the two dominant species (*Anchomanes deformes*-a medical plant), which were present all over the central zone of KNP. In contrast, a number of other species in this study also displayed peaks of relative abundance both within specific locations (*e.g.,* most food plants are found in the forest around Erat and Ekon1 while most medicinal plants were concentrated elsewhere). The botanist, who currently works with the *Smithsonian* project observed that the central zone has a little more different kinds of species than further south. This observation has important implications for the design of both biodiversity assessment and population monitoring studies.

In line with little or low similarity in species richness in the different locations, we observed significant differences in the composition (presence – absence data) of the both food and medicinal plants assemblages. In particular, Erat-Ekon1 and the secondary forest habitats exhibited distinct differences in community structure, and species composition. This suggests that they are comprised of a nested subset of the larger species pool found within the wider landscape.

4.3 Diversity and evenness profiles

As diversity profiles and evenness profiles generally show a sample size-dependent accumulation pattern (influenced by the underlying species abundance distribution), comparisons of diversity between various studies are only meaningful if based on the same sample size to neutralize the influence of sample size on diversity [Rennolls and Laumonier; 1999].

We observed increasing ranges of diversity and evenness profile values associated with increasing scale. Similar observations on the variation of the Shannon (scale 1) and Simpson (scale 2) diversity indices resulted in recommendations to use the Shannon diversity index for comparisons among sites, as this index would be more sample-size efficient in yielding significant differences [Gimaret-Carpentier; 1988]. However, where the evenness in the species abundance distribution differs among sites (a factor eliminated by choice of a species abundance distribution model [Magnussen; 1995], comparisons based on the Simpson index may be more efficient. Especially where species abundance distributions are not known *a priori*, we recommend analyses based on accumulated Rényi diversity profiles, also because calculation of several profile values does not pose major computational difficulties. Calculation of Rényi diversity and evenness profiles allows separating the influence of species richness and the evenness on diversity. Our methodology of calculating average profiles, therefore, allows for separation of the effects of three factors that influence diversity: richness, evenness and sample size.

4.4 Comparison of overall diversity in the different locations

Results for ln (E∞) did not yield a consistent pattern. In some cases, the dominant species was less evenly distributed, while in other cases the reverse pattern could be observed.

The intersections of diversity profiles indicate situations of partial ordering in our data set and difficulties to order most groups in diversity. Similarly, the intersecting evenness profiles is an indication that many groups cannot be ranked in evenness. However, the slow decrease in the joined curve of sites such as in Erat and Ekon1 locations as α is increases are associated with greater evenness in the community. Elsewhere, diversity profiles decrease rapidly between α=0 and α=2, indicating the presence of rare species or low equitability/evenness. Samples from the Erat had the highest diversity and evenness respectively, both because of the unlimited total number of species present (both at low value at α=0 and at α=3). On the contrary, the secondary forest location had all time least species richness and evenness.

Analysis of differences in diversity among areas allows the prioritization of activities. However, an understanding of the underlying factors for differences among diversity may be crucial to select priority areas. For instance, we observed a relationship between proximity to forests on the evenness of the dominant species. However, as proximity to forest is obviously correlated with other factors such as altitude, rainfall, and population density, we could not separate the influence of proximity to forests from these co-varying factors.

4.5 Spatial variation with respect to environmental variables

Three species were shown here to have clear distribution patterns within the patch, and similar distribution patterns were found for other species. Patterns in species distribution were similar to those for environmental variables, and CCA suggested relationships between species occurrence and some of these environmental variables. In general the known habitat preferences of these species support the interpretation that for some species, at this scale, distributions are strongly influenced by environmental variables. Resource limitations prevented a larger area from being sampled, and the range of species and environmental variables that could be included was restricted. It is not known if results would be influenced strongly by inclusion of a greater number of species, and it is not known if findings for the central region are typical of other patches in regions.

Soil nutrients such as Phosphorus, Potassium, and Calcium etc, present in reasonable quantities, were unfortunately found in this case to be uncorrelated with species richness in our forward process modeling. We are also astonished that pH and organic matter had very little influence on species richness. These suggest that species richness is not correlated with soil fertility and pH of the area. Our conclusion joins those of Van der Moezel and Bell (1989) who found highest species richness to occur on soils with the lowest nutrient content in the Mallee region of western Australia, and Hahs et al. (1999) who reported a strong negative correlation between soil nutrient concentration and species richness in sclerophyll heath vegetation in Victoria. Adam et al. (1989) also found a strong negative relationship between soil phosphorus concentration and species richness in the coastal plant communities of New South Wales.

At a broader scale, Margules et al. (1987) found that the diversity of *Eucalyptus* species in southeastern Australia was related to mean annual rainfall, mean annual temperature and solar radiation. These salient factors, including slope, angle, rocks, stoniness and other landscape characteristics, were unfortunately left out in this

study because of resource limitations. Also, resource limitations prevented a larger area from being sampled, and the range of species and environmental variables that could be included was restricted. It is not known if results would be influenced strongly by inclusion of a greater number of species, and it is not known if findings for this patch are typical of other patches in the Korup national park.

4.6 Implications of results for conservation planning and food security

In our household survey, we noticed that important food /economic and medicinal plants such as *Gnetum africana*, *Garcinia kola*, *Poga oleosa*, *Irvingia gabunensis*, *Cola chlamydantha* and *Baillonella toxisperma* are either fast declining, scarce or absent. This partly explains the reason for continuous hunting and environmental unfriendly agricultural practices-clearing the grass with fire, encroaching into the forest as farmland is becoming limited due to the growing population. If government cannot meet up with the cost of resettlement, then environmental education and agricultural diversification (eco-agriculture/analog foretstry), using the economic crops could be important for conservation purposes and food security.

By identifying foods and medicinal plants of lower relative diversity (the rare species), priority can be given to these use-groups for diversification. The lack of evenness in the distribution of these species showed that diversity could be increased substantially in many use-groups by targeting evenness, rather than targeting richness. Like Kindt et al. (2006) suggested, evenness increment could be achieved by encouraging farmers to establish trees in more even numbers (influencing the demand for tree germplasm) or by more species-even germplasm distribution (influencing the supply of tree germplasm).

5. Conclusion

The data presented here indicate that patterns of diversity in food and medicinal plants can vary significantly across ecological scales. Importantly, we found that cultivation of these plants reduce their numbers, increase pressure on the nature reserve, and may lead to food and environmental insecurity in future, everything being equal, a conclusion that has important implications in light of the rapid conversion of tropical forests for agriculture and fuel wood across much of sub-Saharan Africa [Mittermeier et al., 2003]. In addition to the consequences of cultivation for food and medicinal plants communities in the region, the fact that species composition differ among major habitat types means that conservation planners need to give adequate consideration to landscape scale variability in order to ensure maintenance of regional diversity. We have shown that superficial levels of sampling effort, such as a narrow focus on a particular area, can lead to erroneous conclusions regarding patterns of diversity in the region. Simple ecological data such as those presented here are of importance to conservation in the face of growing threats to biodiversity. The fact that few research projects have the time or resources to deploy sufficient levels of sampling effort remains a major problem for conservation.

Amongst the variables considered in this study, the variables that contributed significantly to explain the differences between vegetation units were elevation, clay and sand content. We were able to document differences in diversity among the different locations. Our results could be interpreted in terms of the global biodiversity conservation value of one location over the other. In this context, we want to stress the importance of studying differences in composition among locations, investigating genetic diversity and reproductive ecology of component species, and sampling species diversity in natural

ecosystems adjacent to the agroecosystems that we sampled, to evaluate their conservation value.

6. Acknowledgments

We thank the Chinese Scholarship Council for granting a scholarship and other facilities. We are also grateful to the Ministry of Scientific Research of the Cameroon for granting us the research authority to carry out the research. Also a word of gratitude goes to the International Co-orporation Office for all the care and advice.

7. Correspondence Author

Profesor Dr. Jiwen Ge, Director, Institution of Ecology and Environmental Sciences, China University of Geosciences, Hongshan District, 388 Lumo Road, Wuhan, 430074, China. E-mail: gejiwen2002@yahoo.com.cn

8. Submission date: January, 03rd, 2009; **Revised date**: March 15th, 2009

9. References

Abd, El-Ghani M. M., 2000. Floristic and environmental relations in two extreme desert zones of western Egypt. Global Ecology and Biogeography 9, 499-516.

Bennie, M.O., Hill, R. Baxter, Huntley, B., 2006. Influence of slope and aspect on long-term vegetation change in British chalk grasslands. Journal of Ecology 94, 355-368,

Clarke, K.R., Warwick, R.M., 1994. Change in marine communities: An approach to statistical analysis and interpretation. Plymouth Marine Laboratory, Plymouth, UK.

Colwell, R.K., Coddington, J.A., 1994. Estimating terrestrial biodiversity through extrapolation. Philosophic Trans R. Soc. Lond. B. 345,101-118.

Costanza, R., d'Arge, R., de Groot, R., Farber, S., Grasso, M., Hannon, B., Limburg, K., Naeem, S., O'Neill, R.V., Paruelo, J., Raskin, R.G., Sutton, P., van den Belt, M., 1997. The value of the world's ecosystem services and natural capital. Nature 387, 253-260.

De Groot, R.S., Wilson, M.A., Boumans, R.M.J., 2002. A typology for the classification, description, and valuation of ecosystem functions, goods, and services. Ecological Economics 41, 393-408.

Earles, R., 2005. Sustainable Agriculture: An Introduction Publication of ATTRA, the National Sustainable Agriculture Information Service. USA.

Gimaret-Carpentier, Pélissier., R., Pascal, J. P., Houllier, F.,1998. Sampling strategies for the assessment of tree species diversity. Journal of Vegetation Science, 161-172.

Hahs, A., Enright, N. J., Thomas, I., 1999. Plant communities, species richness and their environmental correlates in the sandy heaths of Little Desert National Park, Victoria. Aust. J. Ecol. 24, 249-57.

Kindt, R., Coe, R., 2005. Tree diversity analysis. A Manual and Software for Some Common Statistical Methods for Biodiversity and Ecological Analysis. World Agroforestry Centre (ICRAF)

Legendre, P., Legendre, L., 1998. Numerical Ecology. Elsevier Science BV, Amsterdam. 853 pp.

Magurran, A.E., Henderson, P.A., 2003. Explaining the excess of rare species in natural species abundance distributions. Nature 422, 714-716.

Margules, C. R., Nicholls, A. O., Austin, M. P. , 1987. Diversity of *Eucalyptus* species predicted by a multi-variable environmental gradient. Oecologia 71, 229-32.

McGill, B.J., 2003. A test of the unified neutral theory of biodiversity. Nature 422, 881-885.

McNeely, J. A., Scherr, S. J., 2002. Ecoagriculture: Strategies to Feed the World and Save Wild Biodiversity. Island Press, Washington. 323 pp.

Mittermeier, R. A, Mittermeier, C. G, Brooks, T. M, Pilgrim, J. D, Konstant, W. R, da Fonseca, G. A. B., Kormos, C., 2003. Wilderness and biodiversity conservation. Proc Natl. Acad. Sci. USA 100,10309-10313.

O'Hara, R. B., 2005. Species richness estimators: How many species can dance on the head of a pin? J. Anim. Ecol. 74, 375-386.

Oksanen, J., Kindt, R., O'Hara, R. B., 2005. Vegan: Community Ecology Package version 1.6-9. http://cc.oulu.fi/~jarioksa/.

Rényi, A., 1970. Probability Theory, North Holland, Amsterdam.

Kindt,R., Damme, P. Van Simons, A. J., 2006. Tree diversity in western Kenya: using profiles to characterize richness and evenness. Biodiversity and Conservation 15, 1253-1270.

Rennolls, K., Laumonier, Y.,1999. Tree species-area and species-diameter relationships at Three Lowland Rain Forest Sites in Sumatra. Journal of Tropical Forest Science 11,784-800.

Hayek, L.-A.C., Buzas, M. A.,1997. Surveying Natural Populations. Columbia University Press, New York.

Ricotta, C., Avena, G. C., 2002. On the information-theoretical meaning of Hill's parametric evenness. Acta Biotheor 50, 63-71.

Scherr, S.J., Shames,S. ,2006. Agriculture: a threat or promise for biodiversity conservation. Arborvitæ, The IUCN/WWF Forest Conservation Newsletter.

Sebastiá, 2004. Role of topography and soils in grassland structuring at the landscape and community scales. Basic and Applied Ecology 5 , 331-346.

Shannon, C., 1948. A mathematical theory of communication. Bell Syst. Tech. J. 27,.379-423.

Simpson, E.H., 1949. Measurement of diversity. Nature 163, 688.

Stohlgren, T. J., Falkner, M. B., Schell, L. D., 1995. A modified Whittaker nested vegetation sampling method. Vegetatio 117,113-121.

Ter Braak, C. J. F., Smilaur P., 2002. CANOCO reference manual and CanoDraw for Windows user's guide: software for canonical community ordination (version 4.5): 500 pp. Ithaca, Microcomputer Power.

Van der Moezel, P. G., Bell, D. T., 1989. Plant species richness in the mallee region of Western Australia. Aust. J. Ecol. 14, 221-6.

Waltert, M., Lien, Faber K., Muhlenberg, M., 2002. Further declines of threatened primates in the Korup Project Area, South-west Cameroon. Oryx 36, 257-265.

Whittaker, R. J., Willis K. J., Field, R., 2001. Scale and species richness: towards a general, hierarchical theory of species diversity. Journal of Biogeography 28, 453-470.

Zimmermann, L., 2000. A Comparative Study of Growth and Mortality of Trees in Caesalp Dominated Lowland African Rainforest at Korup, Cameroon.

Marsland Press
Journal of American Science 2009:5(2) 69-82

Analog forest's contribution to biodiversity conservation; a biodiversity assessment of an analog forest on a private property in south-western wet zone of Sri Lanka

[1]Wasantha K.D.D. Liyanage, [2]Saman N. Gamage, [1]Lai Xulong, [1]Julia Ellis Burnet

[1]School of Environmental Studies, China University of Geosciences, 388, Lumo Road, Wuhan, Hubei, 430074，P.R. China.
[2] Department of Zoology, Faculty of Science, University of Colombo, Colombo 03, Sri Lanka

Abstract

Most natural ecosystems in the wet zone are severely fragmented and interspersed between human managed agro ecosystems and home gardens. There is growing evidence that traditional agro-ecosystems contribute to sustain the regional biodiversity of many invertebrate and vertebrate species. Analog forests, as a concept, is accepted by agronomists and conservationists, bringing profits on a long-term, sustainable basis. Bangamukanda Estate is an example of an 18 hectares plantation (tea, rubber and cinnamon) that has been converted into an analog forest. The objective of the study was in assessing the current biodiversity in this 30-year-old analog forest with special reference to vertebrate species and major plants. A total of 197 plants species were recorded of which 63 were endemic to Sri Lanka. A sum of 207 vertebrates species belonging to 79 families were observed during the study period. From those, 48 species were endemic to Sri Lanka. The findings of the survey clearly highlight the contribution of analog forest systems towards sustaining a rich biodiversity. In addition, analog forest systems can be used to link the forest patches in the wet zone.
[Journal of American Science 2009:5(2) 69-82] (ISSN: 1545-1003)

Key words: Analog forest, biodiversity, critically endangered, fragmentation

1. Introduction

Among all the biological resources of Sri Lanka, forests are ecologically remarkable, environmentally indispensable, socio-economically invaluable and culturally inseparable from the Sri Lankan traditional way of life (Pemadasa, 1996). From a biological point of view, wet zone forests are more important than others. The lowland wet zone of the island has been identified with highest incidence of biodiversity of Sri Lanka (Pethiyagoda, 1994), and a high percentage of endemism. However, a majority of these species are listed as threatened (IUCN, 2004). Even though Sri Lanka's biodiversity is thought to be very high, at present only a small fraction of Sri Lanka's biodiversity is known to science (Nekaris *et al.*, 2005). Also, little information is available regarding the affects of habitat disturbance on the fauna of Sri Lanka. Sri Lanka also has one of the densest human populations in Asia; which has resulted in much of its original forests being cleared for settlements, cultivation, and production of timber. Hence, the lowland forests of the wet zone, which harbours 90% of the 830 endemic flowering plants, have suffered the greatest loss (Gunatilleke and Gunatilleke, 1990). A

burgeoning population, demand for subsistence land and a high proportion of endangered and endemic species within the wet zone of Sri Lanka have resulted in its being declared a critically endangered eco-region; designated as one of the world's 11 biodiversity 'hyperhot' hotspots in demand of extensive conservation investment (Brookes *et al.*, 2002; Nekaris *et al.*, 2005).

These wet zone ecosystems harbour a high percentage of endemic and globally threatened species of animals as well. According to the previous studies conducted by Senanayake and Moyle (1981); Erdelen (1989); Kortmulder *et al.* (1990) and Pethiyagoda (1994), 29 endemic fish species are present in this region of which 20 are restricted to this area. Pethiyagoda and Manamendra-Arachchi (1998) and Manamendra- Arachchi and Pethiyagoda (2005) noted that most of Sri Lanka's amphibian fauna is faced with the risk of extinction due to the loss and fragmentation of their habitat as well as habitat quality degradation due to pollution. Many species known from 19th century museum collections are not recorded during present surveys and are probably extinct (Meegaskumbura *et al.*, 2002). Two primate taxa, *Semnopithecus vetulus nester*, and *Loris tardigradus nycticeboides* are endemic to the south-western wet zone forests of Sri Lanka and categorized as a critically endangered species and it's also listed as one of the top 25 endangered primates in the world due to habitat loss (Mittermeir *et al*. 2006). The loss and fragmentation of forest habitats by human land use are recognized as important factors influencing the decline of forest-dependent fauna. Many forest dependant mammal species, other than bats, are particularly sensitive to habitat loss and fragmentation due to their highly specific habitat requirements, and in many cases they have limited ability to move through and utilize the land use matrix (McAlpinea *et al.*, 2006).

In recent decades, sustainable farmers and researchers around the world have responded to the extractive industrial model with ecology based approaches variously called eco-agriculture, agro-forestry or analog forest (Earles, 2005). Non-farmed portions of the mainly agricultural landscapes can provide patches of habitat for forest wildlife and form corridors that connect protected areas and allow species to continue genetic contact with populations as would have occurred if not isolated (Scherr and Shames 2006). There is growing evidence that traditional agro-ecosystems contribute to sustain the regional biodiversity of many invertebrate and vertebrate species (Lawler, 2001).

Vast extents of Sri Lanka's biodiversity rich lands that were transformed into mono-crop plantations during the colonial era are regenerating in many places due to various reasons, both natural and anthropogenic. Bangamukanda Estate is an example of an 18 hectares plantation land (tea, rubber and cinnamon) that has been deliberately reclaimed as an analog forest as a direct result of the far sighted, land use policy of Sri Lanka during 1970 -1977, which introduced crop diversification in uneconomic tea plantations. Bangamukande Estate is situated in Pitigala, Galle, Sri Lanka. The land is formed into an undulating terrain that consists of a series of ridges and valleys with an altitudinal range from 100m to 300m. It has an intricate network of small streams, which drain into the Benthara River. In 1904 ancestors of the

present owner planted agricultural mono-crops such as cinnamon, rubber, and tea. This practice was continuing up to 1973. It was changed in 1973 and 12 hectares of cinnamon and tea land was transferred to analogue forest using a government subsidy, under crop diversification of uneconomic tea lands. The remaining rubber field of 6 hectares is presently been allowed to regenerate into forestland while been cropped (Wimalasuriya, 2006).

Analog forest is a tree-dominated ecosystem that is analogous in structure and function to the original climax and sub-climax community. With time, the natural succession of any undisturbed forest community is to increase in diversity and stability until a highly complex ecosystem or Climax State is reached. When an ecosystem is designed to mimic the indigenous Climax State, the efficiency and dynamics of the natural processes can be replicated; such forests are referred to as analog forests. As well to their ecological distinctiveness, analog forests are considered to provide economic benefits. A wide range of supplies can be produced that may include: fruit, nuts, herbs, cut flowers and cut-foliage, pharmaceuticals and timber. Furthermore, this type of concept can be used to link the fragmented forest patches in the wet zone of Sri Lanka.

Therefore, the main objective of this study was to assess the biodiversity of this analog forest with special reference to the vertebrate fauna and major plant species.

2. Materials and methods

Bangamukande Estate (BKE) is situated in Niyagama Divisional Secretate Area in Galle District of Southern Province of Sri Lanka, at 06^0 20' 46" N - 080^0 16' 26" E, The average annual rainfall, average temperature and relative humidity are 2300mm, 28^0C and 90% respectively. Approximate distances from BKE to the larger forest complexes are as follows:

To South 4 km Polgahakande-Malabure forest reserve

To East 1 km Hiniduma forest reserve

To Southwest 8 km Beraliya forest reserve

To Southeast 100 m Bangamukanda proposed forest

To Southeast 8 km Kannaliya-Dediyagala-Nakiyadeniya forest reserve

To Northeast 12.5 km Sinharaja forest reserve World Heritage site

To North 11 km Kalugalkande Forest Hermitage and reserve

Figure 1 shows the location of BKE and surrounding forests.

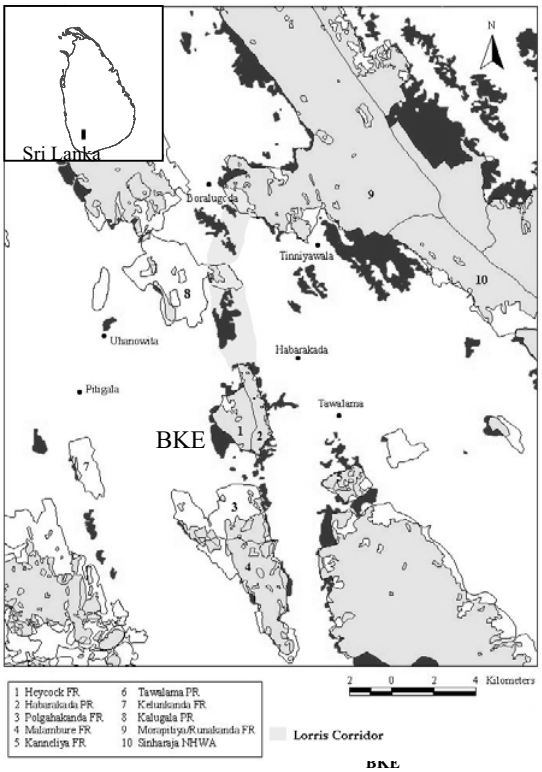

Figure 1: **Location of Bangamukanda Estate (BKE) and surrounding Forests**

Surveys were carried out dividing BKE into 4 plots, in relationship to different levels of regeneration. Vegetation sampling used the Quadrant method; in addition each quadrant of 400 m^2 was subdivided in to 25 grids of 4m x 4m quadrants. Within each quadrate, all plants equal to and above 1 m in height and 2 cm in girth size were listed. Individuals with (CBH)>10cm were measured and recorded as trees. Vines occurring on trees were described qualitatively.

Different methodologies were used to assess the vertebrate fauna in BKE, including systematic line transect surveys of primates, recording of the presence of animal species whenever they were seen, and a trapping regime for rodents (Shermann traps), arboreal rodents (Chardonnet traps) and slender lorises (live mammal traps). Invertebtrates were excluded from the survey and fish were only sampled at two sites. Amphibians, many of which occur in the treetops and reptiles were only sampled opportunistically. The following methods were applied for sampling different taxa:

2.1 Herpetofauna

Quadrate sampling was the main method used for herpetofauna. It involves placing small quadrates at randomly selected sites within a habitat and thoroughly searching these squares for presence of herpetofauna (Heinen, 1992). A total of 18 quadrates (8 x 8 m) were placed at randomly selected points of each study site. When placing quadrates, areas with a deep slope or areas adjacent to tree-fall gaps were omitted. A polythene fence (45cm height) was placed along the sides of the quadrate to prevent animals from escaping. At least two people were engaged in all sampling sessions. Sampling involved sorting through all leaf litter in the plot, tree trunks, branches, under stones and logs (Heinen, 1992). In addition, fixed line transects were also used to assess the herpetofauna.

2.2 Avifauna and Mammals

A fixed line transect method was used assess avifaunal and mammal richness of the study site (Sutherland, 1996). Day and night surveys were conducted between August 2003 and April 2006. Field observation was carried out at 6.30 am to 9.00 am and 4.00 pm to 6.00 pm. Furthermore, night observations were carried out between 7.00 pm to 10 pm and 2.00 am to 6.00 am. Headlamps were used to spot animals at night and red lights were used to prevent the animals from been frightened. Nocturnal animals were identified according to colour, size and shape of eye shine and eye movement. Transects were surveyed by one or two people at a speed of 0.5 to 1 km/hr, depending on time of the day at which survey was conducted (day or night) and depending on the terrain and weather conditions.

2.3 Identification

Vertebrates species were identified using the most recent taxonomic keys or guides available such as; Freshwater fish: Pethiyagoda (1991), Pethiyagoda (1998); Amphibians: Dutta and Manamendra-Aarachchi (1996), Manamendra-Arachchi and Pethiyagoda (1998), Manamendra- Arachchi and Pethiyagoda (2005), Meegas- kumbura and Manamendra-Arachchi (2005); Reptiles: De Silva (1990), Pethiyagoda and Manamendra-Arachchi, (1998); Birds: Henry (1978), Kotagama and Fernando (1993); Mammals: Phillips (1980), Corbet and Hill (1992), Groves (2001). Furthermore, Bambaradeniya eds. (2006) was used for

confirmation of nomenclature.

3. Results

A total of 197 plants species were recorded (Appendix 1) of which 63 (39%) were endemic while 75 species are used for medicinal purposes. From animal species recorded (Appendix 2-6), 207 vertebrates species belonging to 79 families were observed from which 48 species are endemic to Sri Lanka (table 1). The species list is composed of amphibians (17 species), snakes (25 species), tetra pods reptiles (17 species), fish (23 species), birds (90 species) and mammals (34 species). Fresh water fish had the highest number of endemism (48%). The overall endemism was also high (23%).

Table 1: Recorded number of vertebrate species, families and endemism % in the each group during the study period.

Taxa	No. of Species	No. of families	No. of spp. Endemic & %
Plants	**197**	**63**	**63 (39%)**
Fish	23	8	11 (48%)
Amphibians	17	4	7 (24%)
Snakes	25	5	6 (24%)
Tetrapod Reptiles	17	5	7 (41%)
Birds	90	39	12 (13%)
Mammals	34	18	5 (15%)
Total Vertebrates	**207**	**79**	**48 (23%)**

Table 2 shows the conservation status of several threatened species found in the study site of which two were vulnerable, five were endangered, one was critically endangered and one was data deficient.This critically endangered frog (*Philatus nemus*) is a newly described species and previously it was only found in Hiniduma forest reserve of Sri Lanka.

Table 2: Conservation statuses of some threaten species, which were found in Bangamukanda Estate.

Species	Conservation status
Polipedates longinasus	Endangered
Polypedates eques	Endangered
Philatus nemus	Critically-Endangered
Nanophrys ceylonensis	Vulnerable
Lepidocephalichthys jonklaasi	Endangered
Sicyopus jonkalaasi	Data deficient
Loris tardigradus tardigradus	Endangered
Semnopithecus vetullus vetullus	Endangered
Macaca sinica aurifrons	Vulnerable

4. Discussion

The results indicate that the BKE analog forest is an agro-ecosystem that sustains a high species richness of plants and vertebrate fauna. A variety of methods targeting different groups enabled the documentation of BKE biodiversity as expressed in terms of species richness. The total vertebrate richness shows the BKE maintains high species diversity. In addition to the species richness, the study site is providing niches for a large number of endemic vertebrates. The results clearly show that agro-forestry systems are closer to natural conditions in maintaining high biodiversity. Furthermore, the study site is providing niches for 9 globally threatened species of which one is critically endangered. This clearly shows the importance of this ecosystem. Most birds and mammals species used the estate as a

temporary refugia or feeding area, while they move from one forest patch to another. Thus, these results demonstrate the advantages of using such type of systems for connecting forest patches in the country.

5. Conclusion

According to the results can conclude the analog forest systems are sustaining high level of vertebrate diversity and endemism. As a concept, the analog forestry systems are biodynamic and environmentally friendly (Earles, 2005). The results were agreed to this concept. The findings of the survey clearly highlight the contribution of the analog forest systems towards sustaining a rich biodiversity. Further, such agro-ecosystems can be used to link the forest patches in the area.

Acknowledgements

We wish to acknowledge Mr. Sunil Wimalasuriya and members of LORRIS (Land Owners Restore Rainforests In Sri Lanka) and BEOG (Bangamukande Environmental Observation Group) for invaluable assistance provided in the field. We thank the Chinese Scholarship Council for granting a scholarship and other facilities. Also a word of gratitude goes to the International corporation office of the China University of Geosciences for all the care and advice.

References

Bambaradeniya, C.N.B. (Edited). (2006). Fauna of Sri anka: status of Taxonomy, Research & Conservation. The World Conservation Union, Colombo, Sri Lanka & Government of Sri Lanka. Viii + 308pp.

Brookes, T.M., Mittermeier, R.A., Mittermeier, C.G., Da Fonseca, G.A.B., Rylands, A.B., Konstant, W.R., Flick, P., Pilgrim, J., Oldfield, S., Magin, G. & Hilton-Taylor, C. (2002) Habitat loss and extinction in the hotspots of biodiversity. *Conservation Biology.* 16(4): 909-923.

Corbert, G.B. & Hill, J.E. (1992). Mammals of the Indomalayan Region: A systematic Review. *Oxford University, Oxford, UK*.

De Silva A. (1990). Colour Guide to the Snakes of Sri Lanka. *R & A Publishing Ltd., Avon, England*, 130pp.

Dutta, S.K., & Manamendra-Arachchi, K. (1996). The Amphibian fauna of Sri Lanka. *Wildlife Heritage trust of Sri Lanka, Colombo*, 280pp.

Dutta, S.K., & Manamendra-Arachchi, K. (1996) The Amphibian fauna of Sri Lanka. *Wildlife Heritage Trust of Sri Lanka, Colombo.* 280 P.

Earles, R. (2005). *Sustainable Agriculture*: An Introduction Publication of ATTRA, the National Sustainable Agriculture Information Service. USA.

Erdelen, W. (1989) Aspects of the biogeography of Sri Lanka. *Forschungee Aug. Ceylon.* 3: 73-100.

Groves, P.C. (2001). Primate Taxonomy. Smithsonian Institution Press, Washington D.C.

Gunatilleke, I.A.U.N. and Gunatilleke, C.V.S. (1990). Distribution of floristic richness and its conservation in Sri Lanka. *Conservation Biology*, 4(1): 21-30.

Henry, G.M. (1971). A guide to the Birds of Ceylon (Sri Lanka) with 30 half-tone plates of which 27 are coloured and 136 black and white drawings. (2nd edition). *K.V.G. de Silva & Sons, Kandy, Ceylon (Sri Lanka)*. 457pp.

Heinen, J.H. (1992). Comparisons of the leaf litter herpetofauna in abundoned cacao plantaions and primary rain forest in Costa Rica: some implications for faunal restoration. *Biotropica* 24(3): 431-439.

IUCN (2004) IUCN red list of threatened

species, 2004. http://www.iucn.org

Kortmulder, K., Padmanadhan K.G. & de Silva, S.S. (1990). Pattern of distribution and endemism in some cyprinid fishes, as determined by the geomorphology of South-west Sri Lanka and soth Kerala (India). *Ichthyol. Explor. Freshwater.* 1(2): 97-112.

Kotagama, S.W. & Fernando, P. (1992). A field guide to the birds of Sri Lanka. *Wildlife Heritage Trust of Sri Lanka, Colombo 8, Srilanka*. 226pp.

Lawler, S. P. (2001). Rice fields as temporary wetlands: A review. *Israel J. of Zoology*, 47 (3), 513-528.

Manamendra-Arachchi, K., & Pethiyagoda, R. (1998). A synopsis of Sri Lankan Bufonidae (Amphibia: Anura) with discription of new species. *J. South Asian Nat. Hist*., 3(1), 213-247.

Manamendra-Arachchi, K., & Pethiyagoda, R. (2005). The Sri Lankan shrub-frogs of Genus *Philautus* Gistel., 1848 (Ranidae: Rhacophorinae), with discription of 27 new species. *The Raffles Bulletin of Zoology*, Supplement No. 12: 163-303.

McAlpinea, C.A., Rhodesa, J.R., Callaghanc, J.G., Bowena, M.E., Lunneyd, D., Mitchellc, D.L., Pullara, D.V. & Possingham, H.P. (2006) The importance of forest area and configuration relative to local habitat factors for conserving forest mammals: A case study of koalas in Queensland, Australia. *Biological Conservation* 132: 153-165.

Meegaskumbura, M., Bossuyt, F., Pethiyagoda, R., Manamendra-Arachchi, K., Bahir, M., Milinkovitch, M.C., & Schneider, C.J. (2002) Sri Lanka: An Amphibian Hot Spot. *The Ecology.*

Meegaskumbura, M., & Manamendra-Arachchi, K. (2005). Description of eight new species of shrub frogs (Ranidae: Rhacophorinae: *Philautus*) From Sri Lanka. *The Raffles Bulletin of Zoology*, Supplement No. 12: 305-338.

Mittermeier, R.A., Valladares-Pádua, C., Rylands, A.B., Eudey, A.A., Butynski, T.M., Ganzhorn, J.U., Kormos, R., Aguiar, J.M., and Walker, S. (2006). Primates in Peril: The World's 25 Most Endangered Primates, 2004–2006. *Primate Conservation*. 20: 1–28

Nekaris, K.A.I., Liyanage, W.K.D.D. & Gamage, S.N. (2005) Influence of forest structure and floristic composition on population density of the red Slender Loris (*Loris tardigradus tardigradus*) in Masmullah proposed forest reserve, Sri Lanka. *Mammalia.* 69(2): 201-210.

Pemadasa, M.A. (1996) The green mantle of Sri Lanka. *National Library Services Board, Sri Lanka.* 242 P.

Pethiyagoda, R. (1991) Fresh water fishes of Sri Lanka. *Wildlife Heritage Trust of Sri Lanka.* 362p

Pethiyagoda, R. (1994) Threats to the indigenous fresh water fishes of Sri Lanka & remarks on their conservation. *Hydrobiologia.* 285: 189-201.

Pethiyagoda, R. (1998). *Freshwater fishes of Sri Lanka*. Wildlife Heritage Trust, Colombo. xiv+362pp.

Pethiyagoda, R. & Manamendra-Arachchi, K. (1998) Evaluating Sri Lanka's amphibian diversity. *Occasional Papers, Wildlife Heritage Trust, Colombo.* 2:1-12.

Pillips, W.A.A. (1981). Manual of the Mamals of Sri Lanka. *Wildlife and Nature Protection Society of Ceylon (Sri Lanka). Colombo*. Vol. I, II, & III.

Scherr, S.J. & Shames, S. (2006). Agriculture: a

threat or promise for biodiversity conservation. *Arborvitæ* The IUCN/WWF Forest Conservation Newsletter.

Senanayake, F.R., & Moyle, P.B. (1981) Conservation of freshwater fishes of Sri Lanka. *Biological Conservation.* 22: 181-195.

Sutherland, J.W. (1996). Ecological census techniques. *Cambridge University Press.UK*. 336pp.

Wimalasuriya, S.H. (2006) Resurrecting Razed Rainforests. *Part 1*. Wimalasuriya Property Developers, Colombo, Sri Lanka. 35 pp.

Appendix 1: List of plants species observed at BKE (*denotes endemic species)

ORDER: Angiospermae

Family: Acanthaceae

1. *Strobilanthes calycina*
2. S. cordifolium
3. *Asystasia gangetica*
4. *Justicia adhatoda*
5. *Ecobolium ligustrinum*

Family: Anacardiaceae

6. *Semecarpus mooni*
7. **S. nigro-viridis*
8. *S. subpeltata
9. **Mangifera Zeylanica*
10. *Mangifera indica*
11. **Campnosperma Zelanica*

Family: Annonaceae

12. **Xylopia championii*
13. **Cyathocalyx zeylanica*
14. X. *Parvifolia*

Family: Apocynaceae

15. *Alastonia macrophilla*
16. A.*Scholaris*
17. *Pagiantha dichotoma*

Family: Araceae

18. *Pathos scandens*

Family: Asclepiadaceae

19. *Tylophora indica*

Family: Bombacaceae

20. *Bombax ceiba*
21. *Ceiba pentandra*
22. **Cullenia zeylanica*

Family: Burseraceae

23. **Canarium zelanicas*

Family: Campanulaceae

24. *Lobelia nicotinifolia*

Family: Celastraceae

25. **Bhesa zelanica*

Family: Clusiaceae

26. *Calophyllum thwaitesii*
27. *C. trapazifolium*
28. *C. bracteatum*
29. *C. soulattr*i
30. C. *inophyllum*
31. *Garcinia terpnophylla*
32. *G. quaesita*
33. *G.. morella*
34. *Mesua ferrea*

Family: Combretaceae

35. *Terminalia bellirica*

Family: Concolvulacea

36. *Operculina tuepethum*
37. *Ipomoea obscura*

Family: Connaraceae

38. *Rourea minor*

Family: Dilleniaceae

39. *Dillenia triquetra*
40. **D. retusa*
41. *Schumacheria castaneifolia*

Family: Dioscoreaceae

42. *Dioscorea spicata*

Family: Dipterocarpacea

43. **Diptherocapus zelanicas*
44. D. *hispidus*
45. D. gardneri
46. *Shorea megistophylla*
47. *Stemonoporus canaliculatus*

48. *Vateria copallifera*

Family: Ebanaceae

49. *Diospyros atrata*
50. *D. quaesita*

Family: Elaeocarpaceae

51. *Elaeocarpus subvillosus*

Family: Euphorbiaceae

52. *Bridelia retusa*
53. **B. moonii*
54. *P. indicus*
55. *Croton officinalis*
56. *Chaetocarpus castanocarpus*
57. **Fahrenheitia zelanicas*
58. *Macaranga peltata*
59. *Digina*
60. *Hevea braziliensis*
61. *Aporosa cardiosperma*

Family: Fabaceae

62. *Albizia falcataria*
63. *Pericopsis mooniana*
64. *Humboldtia laurifolia*

Family: Flacourtiaceae

65. **Scolopia schreberi*
66. **Erithrospermum zeylanicum*
67. **Homalium Zeylanicum*

Family: Hippocrateaceae

68. *Salacia reticulata*

Family: Lamiaceae

69. *Pogostemon heyneanus*

Family: Lauraceae

70. *Cinnamonum verum*
71. *C. dubium*
72. *Multiflorum*
73. *Litseifolium*
74. *L. gardeneri*

Family: Leguminosae

75. *Adenanthera aglaosperma*
76. *Pongamia pinnata*
77. *Quassia inidica*
78. *Dalbergia pseudosis*
79. *Puereria phasioloides*

Family: Liliaceae

80. **Sansevieria zelanica*

Family: Loganiaceae

81. **Strychnos cinnamomifolia*
82. *Gaerinera vaginans*

Family: Melastomataceae

83. **Axinandra zeylanica*
84. **Osbeckia octandra*
85. *O, aspera*
86. *Melastoma malabathricum*
87. *Lijndenia capitellata*

Family: Meliaceae

88. **Dysoxylum championi*i
89. *Swinitenia macrophylla*
90. *Toona sinensis*

Family: Menispermaceae

91. *Coscinium fenestratum*
92. *Tinospora malabarica*
93. *Cyclea burmanni*

Family: Minomiaceae

94. *Hortonia floribunda*

Family: Moraceae

95. **Artocarpus nobilis*
96. *A. heterophyllus*
97. *A.altilis*
98. *Ficus elastica*
99. *F. hispida*
100. *F. nervosa*
101. *F. fergusonii*
102. *F. tsiela*

Family: Myristicaceae

103. **Horsfieldia iryaghedhi*
104. *H. iriya*
105. **Myristica dactyloides*

Family: Myrtaceae

106. *Syzygium firmum*
107. *S. opperculatum*
108. **S. makul*
109. *S. aromaticum*

Family: Ochnaceae

110. **Ochnacseae jabotapita*
111. *O. lanceolata*

Family: Olacaceae

112. **Olax zeylanica*

Family: Oleaceae

113. *Olea glandulifera*

Family: Orchidaceae

114. *Dendrobium maccarthiae*

Family: Palmae

115. *Areca catechu*
116. *Caryota rivalus*
117. **C. zeylanicus*
118. *C. urenus*

Family: Pandanaceae

120. *Pandanus thwaitesii*
121. **P. Zeylanicus*

Family: Passifloraceae

122. *Adenia palmate*

Family: Piperaceae

123. *Piper sylvestre*

Family: Poaceaegramineae

124. *Ochalandra stridula*
125. *Bamboosa valgaris*

Family: Potamogetonaceae

126. *Potamegeton roxburgianus*

Family: Rhamnaceae

127. *Ziziphus oenoplia*

Family: Rhizophoraceae

128. *Anisophyllea cinnamomoides*
129. *Carallia brachiata*

Family: Rosaceae

130. *Gaertnera vaginans*
131. *Hedyotis fruticosa*
132. *Mussaenda frondosa*
133. **Prunus walkeri*

Family: Rubiaceae

134. *Canthium dicocum*
135. *Ophiorrhiza mungos*

Family: Rutaceae

136. **Micromelum minutum*
137. *Acrenychia pedunculata*
138. *Euodia lunuankenda*

Family: Sapindaceae

139. *Harpullia arborea*
140. *Filicium decipiens*
141. *Dimocarpus longan*
142 *Nephelium lappaceum*

Family: Sapotaceae

143. *Isonandra compta*

Family: Simaroubaceae

144. *Quassia indica*

Family: Smilacaceae

145. **Smilax zelanica*

Family: Staphyleaceae

146. *Turpinia malabarica*

Family: Symplocaceae

147. *Symplocos cochinchinensis*

Family: Theaceae

148. *Camellia sinensis*

Family: Thymelaeaceae

149. *Gyrinops walla*

Family: Tiliaceae

150. *Berrya cordifolia*
151. *Microcos paniculata*
152. *Grewia orientalis*

Family: Verbenaceae

153. *Tectona grandis*
154. *Vitexr pinnata*
155. *Lantana camara*
156. *Clerodendrum infortunatum*

Family: Vitaceae

157. *Seratia pecata*

Family: Zingiberaceae

158. *Costus sepicious*

ORDER: Gymnospermae

Family:Cyatheaceae

159. *Cyathea hookeri*
160. Paathara
161. Kekilla

<u>Appendix 2: List of fresh water fish observed at BKE</u> (*denotes endemic species)

Order: Elopiformes

Family: Aplocheilidae

1. *Aplocheilus werneri* Werner's killifish

Family: Anguillidae

2. *Anguilla icolor* Level finned eel

Family: Bagridae

3. *Mystus gulio* Long whiskered catfish
4. *Mystus keletius* Yellow catfish

Family: Balitoridae

5. **Schistura notostigma* Banded mountain loach

Family: Cobitidae

6. **Lepidocephalichthys jonklaasi* Jonklas loach
7. *Lepidocephalichthys thermalis* Common spiny loach

8. *Danio malabaricus* Giant danio
9. *Esmos thermoicos* Flying barb
10. **Garra ceylonensis* Stone sucker
11. *Puntius amphibious* Scarlet-banded barb
12. *Puntius bimaculatus* Redside barb
13. **Puntius cumingii* Cuming's barb
14. **Puntius nigrofasciatus* Black ruby barb
15. **Puntus sinhala* Filamented barb
16. **Puntius tittaya* Cherry barb
17. *Rasbora daniconius* Striped rasbora
18. **Rasboroidus vaterifloris* Golden rasbora

Family: Gobiidae

19. *Awaous melanocephalus* Scribbled goby
20. **Sicyopus jonkalaasi* Lipstick goby

Family: Belontiidae

21. **Belontia signata* Comb-tail

Family: Channidae

22. *Channa gachua* Brown snakehead
23. **Channa orientalis* Smoothbrested snakehead

Appendix 3: List of amphibians observed at BKE (*denotes endemic species)

Order: Apoda

Family: Ichthyophiidae

1. *Ichthyophis glutinosus* Common yellow-band cecillian

Order: ANURA

Family: Bufonidae – terrestrial frogs

2. Bufo melanostictus Common house toad
*3. *Bufo atukoralei* Athukorala's toad

Family: Ranidae – aquatic frogs

4. Rana aurantiaca Golden frog
5. R.ana temporalis Bronzed frog
6. Fejervarya kirthisinghe Kirtisinghe's frog
7. Fejervarya limnocharis Common paddy field frog
8. Hoplobatrachus crassus Jerdon's bull frog
9. Nanophrys ceylonensis Sri Lankan rock frog
*10.*Lankanectus corrugatus* Corrugated water frog
11.Euphlyctis hexadactylus Indian green frog
12.Euphlyctis cyanophlyctis Skipper frog

Family: Rhacophoridae – arboreal frogs

*13.*Polypedates eques* Saddled tree frog
14. Polypedates cruciger* Common hourglass treefrog
*15.*Polipedates longinasus* Long-snouted tree frog
*16.*Philatus. folicla* Anthropogenic shrub frog
*17.*Philatus. nemus* Southern shrub frog

Appendix 4: List of reptiles observed at BKE

Order: Serpentes

Family: Boidea

1. *Python molurus* Rock python

Family: Elapidae

2. Naja naja naja Indian cobra
*3. * Bungarus ceylonicus* Ceylon krait

Family: Colubridae

4. **Xenochrophis asperrimus* Checkered keel back
5. *Xenochrophis piscator* Checkered keel back
6. **Baloniphis ceylonensis* Sri Lankan Keelback
7. **Aspidura brachyorrhos* Boie's roughside
8. *Amphiesma stolata* Buff-stripped keel back
9. *Oligodon sublineatus* Streaked Kukri Snake
10. *Ahaetulla nasutus* Green vine snake
11. *Boiga ceylonensis* Sri Lanka cat snake
12. *Boiga forsteni* Forsten's catsnake
13. *Chrysopelea ornata* Gold & black tree snake
14. *Dendrelaphis bifrenalis* Bronze back
15. *Dendrelaphis tristis* Common bronze back
16. *Dryocalamus nympha* Bridal snake
17. *Coelognathus helena* Trinket snake
18. *Lycodon aulicus* Wolf snake
19. *Lycodon striatus* Shaw's wolf snake
20. *Ptyas mucosus maximus* Rat snake
21. *Oligodon arnensis* Common kukri

Family: Uropeltidae

*22. *Cylindrophis maculata* Pipe snake

Family: Viperidae

23. *Hypnale hypnale* Hump-nosed viper
24. **Trimeresurus trigonocephalus* Green pit viper
25. *Daboia russellii* Russell's viper

Order: Sauria

Family: Agamidae

1. Calotes calotes	Green garden lizard
2. Calotus versicolor	house lizard
*3. *Calotus liolepis*	Whistling lizard
*4. *Ceratophora aspera*	Rough-horn lizard
*5. *Otocryptis wiegmanni*	Kangaroo lizard
*6. *Lyriocephalus scutatus*	Hump-nosed lizard

Family: Scincidae

7. Mabuya carinata	Rat snake skink
*8. *Nessia burtoni*	Three-toe snakeskink
*9. *Lankascincus fallax*	Common Lanka skink
*10. *Lankascincus gansi*	Gans's lanka skink

Family: Varanidae

11. Varanus bengalensis	Land monitor
12. Varanus salvator	Water monitor

Family: Gekkonidae

13. Cnemaspis podihuna	Small Day Gecko
14. Hemidactylus frenatus	Asian House Gecko
15. Hemidactylus brooki	Brooke's House Gecko
16. Gehyra mutilata	Four-clawed Gecko

Family: Trionychidae

17. *Lissemys punctata*	Flapshell turtle

<u>Appendix 5: List of birds species observed at BKE</u> (*denotes endemic species)

Order: Pelicaniformes

Family: **Phalacrocoracidae**

1. *Phalacrocorax niger*	Little cormorant

Order: Ciconiformes

Family: Ardeidae

2. *Bubulcus ibis*	Cattle egret
3. *Egretta garsetta*	Little egret
4. *Ardeola grayii*	Indian pond heron

Order: Falconiformes

Family: Accipitridae

5. *Ictinaetus malayenisi*	Black eagle
6. *Haliastur indus*	Brahmini kite
7. *Spizaetus cirrhatus*	Changeble hawk eagle
8. *Spilornis cheela*	Crested serpent eagle
9. *Accipiter bandius*	Shikra

Order: Galiformes

Family: Phasianidae

10. **Gallus lafayetii*	Sri Lankan junglefowl
11. **Galloperdix bicalcarata*	Sri Lankan spurfowl

Order: Gruiformes

Family: Rallidae

12. *Amaurornis phoenicurus*	White breasted water hen

Order: Columbiformes

Family: Columbidae

13. *Chalcophaps indica*	Emerald dove
14. *Ducula aenea*	Green imperial pigeon
15. *Treron bisenta*	Orange breasted green pigeon
16. *T. Pompadora*	Pompadour green pigeon
17. *Streptopelia chinensis*	Spotted dove

Order: Psittaciformes

Family: Psittacidae

18. *Psittacula krameri*	Rose ringed parakeet
19. *P.cyanocephala*	Plum headed parakeet
20. **Loriculus beryllinus*	Sri Lankan hanging parrot

Order: Cuculiformes

Family: Cuculidae

21. *Eudynamys scolopacea*	Asian Koel
22. *Centropus sinensis*	Greater coucal
23. **C chlororhynchus*	Green billed coucal

Order: Strigiformes

Family: Tytonidae

24. *Bubo nipelensis*	Spot bellied eagle owl
25.**Glaucidium castanontum*	Chestnut backed owlet

Family: Strigidae

26. *Strix letogrammica*	Brown wood owl
27. *Ketupa zelanicas*	Brown fish owl

Order: Caprimulgiformes

Family: Podargidae

28. *Batrachostomus monilieger*	Frog mouth

Order: Apodiformes

Family: Apodidae

29. *Cypsiurus balasiensis*	Asian palm swift

Family: Hemiprocnidae

30. *Hemiprocne coronata*	Crested tree swift

Order: Trogoniformes

Family: Trogonidae

31. *Harpactes faciatus*	Malabar trogon

Order: Coraciformes

Family: Alcedinidae

32. *Ceyx erithacus*	Oriental dwarf kingfisher
33. *Alcedo atthis*	Common kingfisher
34. *Halcyon smyrnensis*	White breasted kingfisher

Family: Meropidae

35. *Merops philippinus*	Blue tailed bee-eater

36. *Merops leschenaultia* Chestnutheaded bee-eater
Family: Coraciidae
37. *Eurystomus orientalis* Dollar bird
Family: Bucerotidae
38. **Ocyceros gingalensis* Gray hornbill
Order: Piciformes
Family: Capitonidae
39. *Megalaima zelanica* Brown headed barbet
40.**M. rubricapilla* Crimson fronted barbet
41.**M, flavifrons* Yellow fronted barbet
Family: Picidae
42. *Chrysocolaptes lucidus* Greater flamback
43. *Pitta brachyura* Indian pitta
44. *Dendrocopos nanus* Pigmy woodpecker
45. *Dinopium benghalense* Red backed woodpecker
Order: Passeriformes
Family: Motacillidae
46.*Dendronantus indicus* forest wagtail
Family: Hirundinidae
47. *Hirundo daurica* Red rumped swallow
Family: Campephagidae
48. *Pericrocotus flammeus* Scarlet minivet
49. *P. cinnamomeus* Small minivet
Family: Pycnonotidae
50. *Hypspetes leucocephalus* Black bulbul
51. **Pycnonotus melanicterus* Black crested bulbul
52. *Pycnonotus cafer* Red vented bulbul
53. *Pycnonotus luteolus* White browed bulbul
54. *Iole indica* Yellow browed bulbul
Family: Passeridae
55. *Lonchura striata* White-rumped Muniya
56. *Lonchura punctulata* Scaly-breasted Muniya
Family: Irenidae
57. *Chloropsis cochinchinensis* Blue winged leafbird
58. *Chloropsis aurifrons* Gold fronted leafbird
59. *Aegithina tiphia* Common iora
Family: Laniidae
60. *Lanius cristatus cristatus* Brown shrike
Family: Muscicapidae
61. *Muscicapa daurica* Asian brown flycatcher
62. *Terpsiphone paradisi* Asian paradise flycatcher
63. *Hypothymis azurea* Black-naped Monarch
64. *Copsychus saularis* Oriental magpie robin
65. *Cyornis tickelliae* Tickell's blue flycatcher
Family: Rhipiduridae
66. *Rhipidura aureola* White browed fantail
Family: Sittidae
67. *Sitta frontalis* Velvet fronted nuthatch
Family: Silviidae
68. *Orthotomus sutorius* Common tailerbird
69. Phylloscopus trochiloides Greenish tree warbler
70. P. magnirostris Large-billed leaf warbler
71. *Turdoides affinis* Yellow billed babbler
72. *Rhopocichla atriceps* Dark fronted babbler
73. **Pellorneum fuscocapillum* Brown capped babbler
74. Pomatorhinus horsfieldii Scimitar Babbler
Family: Paridae
75. *Parus major* Great tit
Family: Dicaeidae
76. *Zosterops palpebrosa* Oriental white-eye
77. **Dicaeum vincens* Legge's flowerpecker
78. *Dicaeum erythrorhynchos* Small flowerpecker
Family: Nectarinidae
79. *Nectarinia zeylanica* Purple rumped sunbird
80. *Nectarinia lotenia* Long billed sunbird
81. *Nectarinia asiatica* Purple sunbird
Family: Zosteropidae
82. Zosteropes palpebrosus Small white-eye
Family: Sturnidae
83. *Acridotheres tristis* Common myna
84. *Gracula religiosa* Hill myna
85. **G ptilogenys* Sri Lankan myna
Family: Oriolidae
86. *Oriolus xanthornus* Black headed oriel
Family: Dicruridae
87. *Dicrurus caerulescens* White bellied drongo
88. *Dicrurus paradisius lophorhinus* Crested drongo
Family: Artamidae
89. *Artamus fuscus* Ashy wood swallow
Family: Corvidae
90. *Crovos macrohynches* Jungle crow

Appendix 6: List of mammals observed at BKE (*denotes endemic species)

Order: Chiroptera **Family: Pteropidae**

1. Cynopterus sphinx Short-nosed fruit bat

2. *Pteropus giganteus* Flying fox

Family: Emballonuridae

3. Taphozous melanopogon Black-bearded sheath-tailed bat

Family: Rhinolophidae

4. Rhinolophus rouxi Rufus horseshoe bat

5. *Hipposideros lankadiva* Great leaf-nosed bat

Family: Vespertilionidae

6. Pipistrellus ceylonicus Kelaart's pipistrel

7. *Kirivoula pictus* Painted bat

Order: Primata

Family: Loridae

8.**Loris tardigradus tardigradus* S.L.Red slender Loris

Family: Cercopithecidae

9. **Macaca sinica aurifrons* Dusky toque macaque

10.**Semnopithecus vetullus vetullus* Purple faced leaf monkey

Order: Rodentia

Family: Sciuridae

11. Funambulus palmarum Palm squirrel

12. Funambulus layardi Flame-striped jungle squirrel

13. Funambulus sublineatus Dusky-striped jungle squirrel

14.Ratufa macroura melanochra Black and yellow giant squirrel

Family: Muridae

15. Bandicota indica Malabar bandicoot

16. Mus booduga Field mouse

17. *Mus musculus* Indian house mouse

18.Rattus rattus Common house rat

19.Vandeleuria oleracea Long-tailed tree mouse

Family: Hystricidae

20. *Hystrix indica* Porcupine

Order: Pholidota

Family: Manidae

21. *Manis crassicaudata* Indian Pangolin

Order: Lagomorpha

Family: Leporidae

22. *Lepus nigricollis* Black-Napped Hare

Order: Carnivora

Family: Viverridae

23. Viverricula indica Ring-tailed civet

24.Paradoxurus hermaphroditus Palm cat

25.**Paradoxurus zeylonensis* Golden palm civet

Family: Herpestidae

26. Herpestes brachyurus Brown mongoose

27. *Herpestes smithii* Black-tipped mongoose

Family: Felidae

28. Prionailurus rubiginosa Rusty-Spotted Cat

29. Panthera pradus kotiya Leopard

30.Prionailurus viverrinus Fishing cat

Family: Mustelidae

31. *Lutra lutra* Otter

Family: Canidae

32. *Canis aureus* Jackal

Order: Artiodactyla

Family: Suidae

33. Sus scrofa Wild boar

Family: Tragulidae

34. Moschiola meminna Mouse deer

Marsland Press
Journal of American Science 2009:5(2) 83-90

Estimation for Groundwater Balance Based on Recharge and Discharge: a Tool for Sustainable Groundwater Management, Zhongmu County Alluvial Plain Aquifer, Henan Province, China

[1]Y. Nowel Njamnsi, [2]Innocent Ndoh Mbue
[1]School of Environmental Science, China University of Geosciences, Department of Hydrology and Water Resources, Lumo Road 388, Wuhan- Hubei, Zip Code 430074. P.R China.
[2]School of Environmental Science, China University of Geosciences, Department of Hydrology and Water Resources, Lumo Road 388, Wuhan- Hubei, Zip Code 430074. P.R China.

Abstract:
This study evaluates and estimates groundwater resources of the Zhongmu County China for the period between, 1980 and 2007, which is the main resource for agricultural and domestic water supply. Our approach is centered on quantitative estimation of two main parameters-input and output. Recharge and discharge components have been quantified based on inflows, outflows and changes in the aquifer groundwater storage. Inflow to the system includes groundwater recharge from precipitation lateral groundwater inflow, irrigation infiltration, influent seepage from rivers. Discharge from the system includes effluent seepage to rivers, evaporation losses, groundwater lateral outflow, and groundwater extraction. Our results show that the average total annual discharge of the area ($19928\times10^4 m^3/a$) exceeded total average annual recharge ($21984.70\times10^4 m^3/a$), implying that the system is in deficiency – an indication of unsustainable water withdrawal. Abstraction of groundwater could be minimized by providing sufficient canal irrigation water to the farmers. We further recommend the institution of a groundwater regulatory framework to optimize groundwater use on sustainable basis, provision of drinking water wells with a recharge structures and a ban on the construction of irrigation wells / tube wells within a distance of 200metres or less (depending on scientific criteria) of the drinking water supply well. [Journal of American Science 2009:5(2) 83-90] (ISSN: 1545-1003)

Key words: Groundwater resource evaluation, recharge, discharge, water balance, sustainable use, Zhongmu County.

1. Introduction

Water is an essential natural resource for sustaining life and environment. The available water resources are under pressure due to increased demands with an ever increasing population and the time is not far when water, which we have always thought to be available in abundance and as a free gift of nature, will become a scarce commodity. From a volume perspective, most water use in Zhongmu is appropriated from groundwater. Rapid development of economy and increase of population bring more and more acute contradiction between the water supply and water demand, especially for agricultural purposes, has increase rapidly in recent times, and both surface water (including rivers, lakes, and springs) and groundwater have been exploited [Li-Tang ,et al,2007]. China's total water use was $579.5\times10^6 m^3$ in 2006, with 63.2% of agricultural use, 23.2% of industry use, 12.0% of domestic use, and 1.6% of ecological and environmental uses (supplied by the man-made measures) [MWRC, 2006]. Utilization ratio of agricultural water accounted for 75.7% (referred to as the proportion of water consumption to water use). About 90% of the

agricultural water was consumed by farmland irrigation.

In order to properly evaluate the degree of significance and impact of groundwater development in Zhongmu, any scientific evaluation must focus strictly on Zhongmu's conditions. One means of objectively evaluating the relative significance of changes in water demands in Zhongmu is to employ water budget methodology. Water shortage has become a main factor in restricting sustainable socio-economic development. Agriculture is an important part of the local economy national well-known garlic production base and a major water consumer. Groundwater is the major water-supply source to agricultural in Zhongmu County, and in some towns it's even the only water supply source. About 90% of groundwater yield per year in Zhongmu County is used in Agricultural irrigation. The statistical data show that 83.57% of total surface water use ($22.9\times10^6 m^3$/yr) and 64.61% of total groundwater use ($6.10\times10^6 m^3$/yr) were consumed in agricultural irrigation during the period from 1998 to 2006 [BSZ, 1998-2006]. That means agriculture consumed 78.7% of the total water use in the provinces of Yellow River Basin every year.

In this paper, based on making full use of hydrology and hydrogeology data and predecessor's research results in the past 20 years, groundwater quantity assessment in Zhongmu County was carried out in order to offer scientific basis in the course of establishing the sustainable development use plan of groundwater resources. Then, according to the assessment results, the rationality of management and development of groundwater in Zhongmu County was analyzed.

Available water resources per capita are decreasing as a result of population growth. Groundwater basins constituting Zhongmu are very scarce and vary in quantity and quality. Recharge of renewable water aquifers is generally highest in the mountainous northern part of the country where precipitation is greatest. Most surface water belongs to poor grade water quality (grade V or below V in Chinese terminology, of which grade I is best and grade V is only applicable to agriculture irrigation). The surface waters have been polluted badly because of direct discharge of industrial and domestic wastewater. So, groundwater is the most important water supply source for urban and rural areas. Continuation of groundwater overexploitation at these high levels will lead to mining these sources as well as deteriorating the quality of abstracted water, which will lead at the end to an extensive damage of the aquifers.

2. Objectives

The main objectives of the study are to:

(i) Identify and quantify all recharge and discharge components of groundwater;

(ii) Calculate the average annual groundwater balance; and

(iii) Prepare recommendation for sustainability of groundwater use for irrigated agriculture.

3. Physiography and Location of Study Area

Zhongmu County lies in the heart of Henan, on the southern alluvial flood plain of the Yellow River, between Zhengzhou and Kaifeng. It is located in the middle latitude belt and stretches from north latitude 113°46' to 114°12' and east latitude 34°26' to 34°56', total area of 1416.6 km^2 with a length of 55km in the north-south direction and a width of 35 km in the east-west extension and a population of 680,000. It has jurisdiction over 11 towns, 6 countries and 431 villages, with a population density of 476 persons per square kilometer in 2002. The study area is rather flat region; west-high and east-low, with the hill land and piedmont in the west and plain in the east, an altitude 85m, a gentle slope (1/2,000-1/10,000) to north slight undulation in the piedmont part.

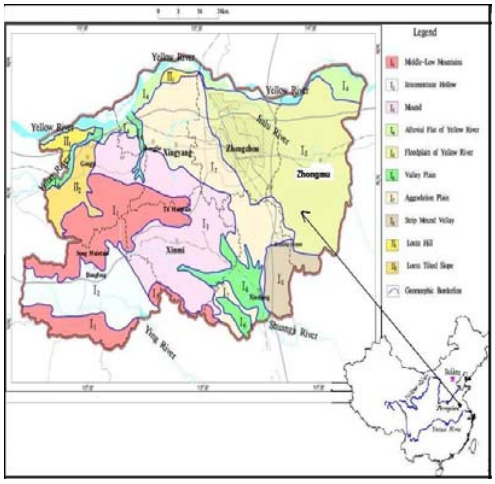

Figure 1. Location of Zhongmu County

Climatically, Zhongmu belongs to the typical mid-latitude temperate continental monsoon climate, four distinct seasons. It is cold in the winter and hot in the summer and the dry and moist season is obvious. It is warm in the spring and cool in the autumn. The sunshine duration in the whole year is about 2366 hours, with average annual temperature of 14.4°C. January, whose average temperature is 4.6°C, is the coldest month of the year, and July is the hottest with an average temperature of 32.1°C. The annual average rainfall is 640.9 mm and the frost-free period is 240 days. Zhongmu County, with rich water resources, 9 main Rivers Jialu, Qili, Zhangbagou, xiaoqin, Dilixiaoqing, Damenggou, Shigou, Yunliang, Shuikuigou rivers of various sizes that respectively belongs to the two great river systems of the Yellow River and the Huaihe River. Mean annual evaporation is 1492.6mm. The average relative humidity of the year is 67%. It is 113.5 meters above the sea level on average. Of the 1416.6 square kilometers, 930.600 mu of it is farmland, which covers 43% of the total area. Woods covers an area of 319000 mu which forms 1470 of the total area. 20000 mu is covered by water. It has a population of 659.000; 321000 laborers which constitute 49.37% of the total population. The number of social laborers stands at 220000 which form 58.5% of the laborers and 33.67% of the total population.

4. Geology and Hydrogeology

In most parts of Zhongmu County, the phreatic water is principally stored in the Holocene Yellow River alluvial plain aquifer, whose lithology consists of coarse grained main stream- facies or very fine grained flood plain facies or marginal facies. These have been distributed in an interlacing manner. Groundwater occur in various natural geological environments according to the depth of burial, the characteristics of the water- bearing medium, the tectonic structure, the dynamic conditions and the geophysico-chemical environment. On the basis of this we can subdivide the aquifer system as follows: shallow aquifer (unconfined aquifer less than 60 m deep), intermediate aquifer (confined aquifer 60~300 m deep), deep aquifer (confined aquifer 300~800 m deep) and super-deep aquifer (confined aquifer deeper than 800 m) [Li, G. R, Wang, X. G., Guo, Y. Q., 2005].

The shallow aquifers have abundant groundwater because they can be easily recharged by precipitation, irrigation, rivers, and reservoirs. The confined aquifers, on the other hand, have abundant groundwater because of their huge extent and volume. In Zhongmu County based on the geomorphology, aquifer type, groundwater dynamics, hydrochemistry and influence of human activities, the groundwater can be classified as shallow groundwater subsystem in piedmont plain. The Quaternary sediments consists chiefly coarse grained sands, and gravel bearing medium to coarse sands. The aquifers gradually becomes finer grained with low permeability as we move away from the mountains and shallow groundwater in the central plain as we move further from the mountain.

In the north of Zhongmu County, the

phreatic water mainly stored in the Epi-Pleistocene and Neocene aquifers below the surface in 40m depth. Therefore, distribution regularities, genetic types, lithology, thickness and water abundance closely related to the local relief condition. The south and west mountain areas are characterized by karstic water in Carbonate systems, water in fractured systems in hard rock and clastic rock. Fractured rock systems generally have deep groundwater table depth and are relatively difficult to exploit. The lithology textures of the shallow aquifers in the study area have a great bearing on their transmissivity and yield. Aquifers systems with less than 60m in depths can be divided in the following four types:

(i) Monolayer type; the aquifers are thick, coarse grained and have good transmissivity.

(ii) Double type; aquifers of this type are located in the areas where the main stream facies is covered by flood plain facies deposits of the Yellow river accounting for 60-70%of the total area. The aquifers thus have a “double “ structure with and upper finer grained part and a lower coarser grain part, with the upper part forming and aquitard composed of clayey sand and sandy clay, and the lower part a stable sand aquifer. Their specific well yields are commonly less than 5-10 m^3/hour/m, transmissivity approximately 500m^2/day in near- main- stream facies zones and 200 m^2/day in other areas.

(iii) Multilayer type; aquifers of this type are located in the peripheral facies zones of alluvial fans of the Yellow river. The main sand aquifer is absent, and this type is composed of alteration of silt, clayey sand and sandy clay, with poor transmissivity. Specific yield are commonly less than 5m^3/hour/m. Transmissivity coefficient is about 50m^2/day.

5. Methodology

Based on general hydrogeologic principles, a groundwater budget was prepared to estimate the amount of groundwater inflow, outflow and change in storage. Water balance techniques have been extensively used to make quantitative estimates of water resources and the impact of man's activities on the hydrologic cycle. On the basis of the water balance approach, it is possible to make a quantitative evaluation of water resources and its dynamic behavior under the influence of man's activities. The study of water balance is defined as the systematic presentation of data on the supply and use of water within a geographic region for a specified period. With water balance approach, it is possible to evaluate quantitatively individual contribution of sources of water in the system, over different time periods, and to establish the degree of variation in water regime due to changes in components of the system.

The basic concept of water balance is:

The amount of water entering a control volume during a defined time period (inflow, I), minus the amount leaving the volume during the time period (discharge, Q), equals the change in the amount of water stored (ΔS) in the volume during that time period.

$$\boldsymbol{I - O = \Delta S}$$

$$\left(\underbrace{P_{pt} + I_r + G_{in} + R_i}_{\text{inflow, I}} \right) - \left(\underbrace{R_e + G_{out} + E_l + G_{ex}}_{\text{outflow, O}} \right) = \Delta S$$

Where:

Inflow (I) consists of; precipitation (P_{pt}) lateral groundwater inflow (Gin), irrigation infiltration (I_r), influent seepage from rivers (R_i).

Outflow (O) consists of; effluent seepage to rivers ... (R_e), evaporation losses (E_l), groundwater lateral outflow, and groundwater extraction (G_{ex}) and ΔS change in ground water storage.

5.1. Recharge Components

Natural recharge of the area is from direct precipitation, influent seepage from rivers, and irrigation waters which in a broad sense [Simmers, 1988] defined groundwater recharge as "an addition of water to a groundwater reservoir". Modes and mechanisms of recharge were classified by the same author into four broad categories:

• Downward flow of water through the unsaturated zone reaching the water table;

• Lateral and/or vertical inter-aquifer flow;

• Induced recharge from nearby surface water bodies resulting from groundwater abstraction; and

• Artificial recharge such as from borehole injection or man made infiltration ponds.

The different mechanisms are further described [Beekman et al., 1996; Selaolo, 1998; de Vries & Simmers, 2002; Lerner et al., 1990; Lloyd, 1986] by enhancing the classification based on the origin of the incoming water, movement of water in the unsaturated zone, aerial extent on which recharge acts upon, and time scale of the recharge occurrence.

(a) Precipitation inputs

Rainfall occurs in the area mainly during the monsoon months. The average annual rainfall was calculated as 580.30 mm. The surface area covered by the aquifer is approximately 1393.00 km^2 The annual groundwater recharge due to monsoon rainfall has been estimated with the help of the following equation:

$$Q_P = P \times \alpha \times n \times F \times 0.1$$

Where:

Q_P = annual precipitation infiltration recharge ($10^4 m^3/a$),
P= annual precipitation (mm), α is precipitation infiltration coefficient,
n= precipitation valid infiltration coefficient (0.8 value was adopted for the study);
F = aquifer area, calculation area (km^2).

(b) **Lateral groundwater inflow**

The Groundwater in Zhongmu County is recharged by lateral inflow from the north, southwest and west. Computation formula is the following:

$$Q_{OR} = T \times I \times L \times t \times 0.001$$

Where:

Q_{OR}= annual groundwater lateral flow recharge quantity ($10^4 m^3/a$),
T= hydraulic conductivity (m^2/d);
I= average hydraulic gradient (‰),
L= the length of calculated section (km),
t= recharge days per annual (d/a). (365days was adopted for the study)

(c) **Influent seepage from rivers**

The area under study has an extensive river network which recharges the groundwater. There is Jialu River which is the main River flowing across Zhongmu County was used. The computing formula of recharge from Jialu River：

$$Q_{sr} = q \times l \times t \times 0.1$$

Where:

Q_{sr} = annual river infiltration recharge quantity ($10^4 m^3/a$);
q = infiltration volume per unit river length (m^2/d);
l = river length in Zhongmu County (km);
t = wet days per year (d/a).

(d) **Irrigation infiltration**

Recharge from surface-water irrigation is the largest component of aquifer. Computing formula of irrigation leakage recharge capacity is:

$$Q_{IR} = \beta \times Q_I$$

Where:

Q_{IR} = agricultural irrigation leakage recharge ($10^4 m^3/a$),
β = irrigation leakage coefficient,
Q_I = annual irrigation water volume ($10^4 m^3/a$).

5.2. Discharge Components

The total amount of groundwater withdrawn artificially or naturally from aquifers is termed groundwater discharge.

1. Artificial groundwater discharge

(i)**Groundwater extraction** (Q_{ex})

The artificial withdrawal of groundwater from shallow aquifer is by means of dug wells. These withdrawals are mainly for domestic industrial and agricultural purposes.

According to statistical data from water conservation office and water conservancy between 1980 and 2007, industrial exploitation quantity (Q_{IE}= 829.60x$10^4$$m^3$/a), agriculture exploitation quantity (Q_{AE}11096.00 x$10^4$$m^3$/a) and domestic consumed water quantity (Q_{DE} 936.51 x$10^4$$m^3$/a) were calculated in each computing unit. Given a sum total of Q_t =12862.11 x$10^4$$m^3$/a.

2. Natural groundwater discharge

The major sources of natural groundwater discharges are:

(i) Effluent seepage to rivers, (ii) evaporation losses, (iii) lateral out flow.

Evaporation intensity method was adopted to calculate evaporation quantity:

$$Q_E = \varepsilon \times F$$

Where:

Q_E = annual phreatic evaporation quantity ($10^4$$m^3$/a),

ε = phreatic water evaporation intensity (m/a),

F = evaporation area ($10^4$$m^2$). Evaporation area was determined according to evaporation limit depth (3m).

6. Change in Groundwater in Storage

Aquifers in the Zhongmu alluvial Plains are generally unconfined, the change in water in storage in the aquifers can be estimated using the water-level change maps and the average specific yield of the aquifer indifferent sub areas which ranges between -0.05 m/a and -0.19 m/a .

The expressions of groundwater reserves variable in shallow aquifer is as following:

$$\Delta W = 100 \times (h_2 - h_1) \times \mu \times \frac{F}{t}$$

Where:

ΔW =Groundwater reserves variable in shallow aquifer (10^4 m^3/a);

h_1 =the groundwater table at the beginning of the calculating time (m);

h_2 =the groundwater table at the end of the calculating time (m);

μ =Specific yield in range of stage of shallow groundwater;

F =Calculated area (1393.00km^2);

t =Length of calculating time (a).

7. Results and Discussions

The annual groundwater budget is summarized in table1, showing the range of annual calculations between 1980 and 2007.

Table 1. Summary of water balance calculations for the Zhongmu County(1980-2007).

1. Recharge Components			
Recharge from Rainfall			11201.86 x$10^4$$m^3$/a
River Recharge			271.98 x$10^4$$m^3$/a
Irrigation recharge			3058.85 x$10^4$$m^3$/a
Groundwater lateral inflow			5395.20 x$10^4$$m^3$/a
Total Aquifer Recharge			19927.89x$10^4$$m^3$/a
2. Discharge Components			
Evaporation losses			6580.34x$10^4$$m^3$/a
Groundwater lateral outflow			1112.72 x$10^4$$m^3$/a
Groundwater Pumping	Industrial pumping	829.60x$10^4$$m^3$/a	12862.11x$10^4$$m^3$/a
	Agriculture pumping	11096.00x$10^4$$m^3$/a	
	Domestic consumption	936.51x$10^4$$m^3$/a	
Effluent seepage to rivers			1429.53 x$10^4$$m^3$/a
Total Discharge			21984.70 x$10^4$$m^3$/a
Change in Storage			-2056.11 ×$10^4$$m^3$/a

According to table 1, we know the multi-annual average recharge quantity of groundwater is 19927.89×104m3/a from 1980 to 2007 in Zhongmu County, the multi-annual average discharge quantity is 21984.70×104 m3/a, and the multi-annual average loss quantity is 1527.52×104 m3/a.The groundwater table is of downtrend in Zhongmu County, which expresses that the groundwater balance is at minus situation in this area at present.

In the studied area, the dug wells are fully penetrating. Monitoring data from 17 groundwater observation wells in were used to calculate the average groundwater reserves variable in shallow aquifer from 1980 to 2007 at every computing unit.

Thus, using the expressions of groundwater reserves variable, the deficit groundwater of the area is then calculated to be -1527.52X104m3/a

8. Conclusion

Sustainable groundwater resources development implies use of groundwater as a

source of water supply, on a long term basis, in an efficient and equitable manner sustaining its quality and environmental diversity. Zhongmu County area has been prepared to estimate the inflows and outflows to the groundwater system. Zhongmu is blessed with abundant and clean water resources that are sufficient to sustain the level of growth projected into the future. Based on a variety of calculations and available data, the gross annual average recharge of groundwater is 19927.89×104m3/a from 1980 to 2007 and a gross annual average discharge of groundwater is 21984.70 x104m3/a resulting to a dramatic deficiency of -2056.11×104m3/a in the water balance. The main reasons of the minus balance of the phreatic water are overexploitation and inadequate recharge. The safe yield of ground water aquifers is a quantity of water that may be harvested on a sustainable basis and is equivalent to annual replenishment/recharge. Continuing overdraft exceeding the safe yield will require conservation practice implementation to reduce demand, and increase water use efficiency. In some areas, conservation will not reduce ground-water use to the safe yield of the aquifer and land-use changes will be inevitable. This raises question about the sustainability of groundwater use in the area. There should be a balance in recharge and discharge components to maintain an equilibrium in the area. Groundwater is an important natural resource with high economic value and sociological significance. It is important that this resource be utilized in such a manner that a permanent depletion of the resource in both quantity and quality aspects is avoided and that any other environmental impacts. Given the sensitivity of the water balance to processes like artificial recharge, further work towards improving the reliability of calculated values is important.

Recommendations

- ✧ Abstraction of groundwater could be minimized by providing sufficient canal irrigation water to the farmers.
- ✧ A groundwater regulatory framework needs to be developed to optimize groundwater use on sustainable basis.
- ✧ By providing all drinking water wells with a recharge structure.
- ✧ By banning construction of irrigation wells / tube wells within a distance of 200metres or less (depending on scientific criteria) of the drinking water supply well.

Acknowledgements

We thank the Chinese government scholarship, without which this work will not have been realizable. We are also indebted to the ministry of higher education, Cameroon for initiating this wonderful cooperation with the government of the Peoples Republic of China.

References

Beekman, H. E., Gieske, A. & Selaolo, E. T. (1996) GRES: Groundwater recharge studies in Botswana 1987-1996. Botswana Journal of Earth Sciences, 3:1–17.

Bureau of Statistics of Zhengzhou (BSZ) (1998-2006). Bulletin of water resources of Yellow River, 1998-2006. (In Chinese)

Bureau of Statistics of Zhongmu County (BSZ) (2002). Statistical Year Book of Zhongmu 1991-2001. (in Chinese)

China Geologic Survey Bureau. Series of national groundwater resource and its environmental problem survey assessment technique requirement (2) [R].2003.

de Vries, J. J. & Simmers, I. (2002) Groundwater recharge: An overview of processes and challenges. Hydrogeology Journal, 10(1):5–17.

Environmental School, China University of Geosciences. Groundwater resources survey and appraisal report for Zhongmu county, Zhengzhou city[R].2005.

Lerner, D. N., Issar, A. & Simmers, I. (1990) A guide to understanding and estimating natural recharge, I. A. H publication: International contribution to hydrogeology, vol. 8. Verlag Heinz Heisse, 345 pp.

Li, G. R, Wang, X. G., Guo, Y. Q., 2005. Concentrated Groundwater Development Status of middle aquifer in Zhengzhou Municipal Area. Yellow River, 27 (5): 44-46. (In Chinese).

Li–Tang H., Chong-X., Chen, J., Jimmy Jiao and Zhong-Jing W., 2007. Simulated groundwater interaction with rivers and springs in the Heihe river Basin Hydrol. Process DOI:10.1002/hyp.6497

Li, G. R, Wang, X. G., Guo, Y. Q., 2005. Concentrated Groundwater Development Status of middle aquifer in Zhengzhou Municipal Area. Yellow River, 27 (5): 44-46. (In Chinese).

Lloyd, J. W. (1986) A review of aridity and groundwater. hydrological processes, 1:63–78.

Lohman, S.W., 1979, Ground-water hydraulics: U.S. Geological Survey Professional Paper 708, 70 p.

Ministry of Water Resources of the People's Republic of China (MWRC) (2006). Bulletin of water resources in China.(in Chinese)

Selaolo, E. T. (1998) Tracer studies and groundwater recharge assessment in the eastern fringe of the Botswana Kalahari -the Lethlakeng - Botlhapatlou area. Ph.D thesis, Free University.

Simmers, I., ed. (1988) Estimation of natural groundwater recharge, NATO ASI series C, Mathematical and physical sciences, vol. 222. Reidel, Dordrecht

Marsland Press
Journal of American Science 2009:5(2) 91-96

Primary Phytochemical Analysis Of *Kappaphycus Sp.*

[1]p. Rajasulochana, [2]R. Dhamotharan, [3]P. Krishnamoorthy
[1] Research Scholar & Lecturer, Industrial Biotechnology Dept., Bharat University, Chennai
[2] Reader, Dept. Plant Biology & Plant Biotechnology, Presidency College, Chennai
[3] Head and Dean academic, Dept. Bioinformatics, Bharat University, Chennai.
E-mail: prajasulochana@yahoo.co.in, Telephone: 91-9444222678

ABSTRACT: *Kappaphycus sp*., an edible seaweed from the sea coast of Rameswaram, India was analysed for its primary phytochemical analysis. Chemical composition was carried out for estimation of proteins, fatty acids, β-carotene and sterol compounds. β-carotene was estimated through high performance liquid chromatography where as fatty acids and sterol compounds were determined using gas chromatography technique. From the standard graph, the protein was estimated as 0.169gm/ml indicating that the protein content is quite high in red algae. Sterols were estimated on the basis of chromatographic peak areas for each with respect to total sterol peak area. The predominant sterol identified is cholesterol. From the qualitative analysis of β-Carotene, it was observed that one compound is present in large besides other impurities. Results of this study suggest the utility of *Kappaphycus sp.* for various nutritional products for use as health food or nutraceutical supplement.[Journal of American Science 2009:5(2) 91-96] (ISSN: 1545-1003)

Key word: Kappaphycus sp, Antibacterial, Protein, Fatty acid, Sterol, β-carotene

1. Introduction

Marine organisms are a rich source of structurally novel and biologically active metabolites. Secondary or primary metabolites produced by these organisms may be potential bioactive compounds of interest in the pharmaceutical industry. Seaweeds have some of the valuable medicinal value components such as antibiotics, laxatives, anticoagulants, anti-ulcer products and suspending agents in radiological preparations. Fresh and dry seaweeds are extensively consumed by people especially living in the coastal areas. From the literature, it is observed that the edible seaweeds contain a significant amount of the protein, vitamins and minerals essential for the human nutrition [Fayaz et al., 2005]. Marine sources are receiving much attention mainly because of the contents of functional ingredients such as polyunsaturated acids, β-Carotene and their pigments Carotenoids, sulphated polysaccharide (antiviral), and sterols (antimicrobials). Among the different compounds with functional properties, antioxidants are the most widely studied. Sterols are an important family of lipids, present in the majority of the cells. Because of different routes of synthesis, sterols from plants, fungi and animals show marked differences. Brazilian red algae have been found to have phenolic substances. Oxidative stress is an important factor in the genesis of pathology, from cancer to cardiovascular and degenerative disease. Marine algae are the excellent source of bioactive compounds such as carotenoids, dietary fibre, protein, essential fatty acids, vitamins and minerals [Viron et al., 2000, Sanchez-Machado et al., 2002, Fayaz et al., 2005]. Fayaz et al. (2005) suggested the utility of *Kappaphycus alvarezzi* for various nutritional products including antioxidant for use as health food or nutraceutical supplement. Sanchez-Machado et al. (2004) found that the predominant sterol was desmosterol in red seaweeds (87-93% of total sterol content). Tasende (2000) confirmed that fatty acids and sterol of algal class, families and sometimes even species are characteristics to those particular taxa and could be useful as chemotaxonomic. Cholesterol generally plays a structural role in the cell membrane [Nabil and Cosson, 1996]. Clinical studies have demonstrated that dietary intake of plant sterols (as part of the normal diet, or as a supplement) may help reduce blood cholesterol levels [Dunford and King, 2000]. Sterols are thus among the nutritionally important lipids that need to be routinely determined in foods. Plant sterols have been quantified by gas chromatography [Govindan and Hodge, 1993, Jeong and Lachance, 2001] or by HPLC with UV detection [Indyk, 1990] or evaporative light scattering detection. However, few studies have presented techniques for parallel determination of different sterols. Further, it is observed that gas chromatography/mass spectrometry techniques are widely employed for identification of sterols. Microalgal metabolites have attracted attention for two main reasons, first, because they are the source of toxins in harmful algal blooms and secondly because they are a potentially rich source of new drug candidates. Many of the microalgal metabolites have chemical structure and possess interesting biological activity. Present investigation aims at estimation of proteins, β-carotene, fatty acids and sterol compounds from *Kappaphycus sp*.

2. Materials and methods

Sample was collected from the sea coast of Rameshwaram, Tamil Nadu, India in the form of dry and living sample. Algae samples were cleaned at epiphytes and necrotic parts were removed. Samples were rinsed with sterile water to remove any associated debris. Sample was kept under sunshade for 7 days. After drying the sample, it was ground thoroughly to powder form. The powder was then used for the primary estimation of proteins, fatty acid, β-carotene, sterol compounds and antimicrobial test. This powder was stored in cold conditions in an airtight container and analysis was carried out within three months of processing. Total protein content, fatty acids, sterols and beta carotene analysis in *Kappaphycus sp*. were determined by the respective methods.

2.1 Quantitative estimation of proteins

One gram of sample was taken and homogenized in a prechilled mortar and pestle with ice cold Tris buffer (0.1M pH-7). The extract was centrifused at 8000 rpm for 10 minutes and the supernatant was collected. It was added with 10% TCA (twice the volume) and kept overnight at 40°C. The sample was centrifuged at 8000 rpm for 10 minutes and the pallet was collected, dissolved in Tris buffer and was used for the estimation of protein. The final protein extract was used to measure the absorbance at 595nm.The absorbance was recorded 3 times by taking 1ml each at 595 nm. It is found out to be 0.316, 0.312 and 0.320. The average was taken as 0.316.

2.2 Analysis of fatty acid composition

Dried samples (2.50 g) were extracted with trichloromethane-methanol (2.1v/v) in a soxhelt apparatus for 48 h. The extract was evaporated under vacuum. Ethanol with 6% KOH was added to the residue and the reaction mixture was saponified by refluxing at 100^0C for 1 h with pyrogallol. The mixture was cooled, concentrated under reduced pressure and thereafter H_2O and ethanol were added and extraction with ether was repeated three times. The aqueous alkaline fraction was acidified with 6N HCl to pH 1 and then extracted several times with hexane. The organic fraction was dried over anhydrous Na_2 So_4 and evaporated under reduce pressure.

The fatty acid fraction was dissolved in methanol-H_2 So_4 (97.5:2.5 v/v) with pyrogallol methylated. The fatty acid methyl esters were extracted with hexane:ether (2:1 v/v). The organic fraction was dried over anhydrous Na_2 So_4 and concentrated under vacuum. The fatty acid methyl esters were purified by silica thin layer chromatography (TLC) and analyzed on a Varian 3400 CX gas chromatograph equiped with a flame ionization detector and a OV-1 Interchin column (30 m X 0.32mm). The column temperature was programmed from 180 to 200^0 C at a rate of 1 ^{0}C min^{-1} and from 200to 240^0 C at a rate of 2^0C min^{-1}. The injection temperature was 270 ^{0}C and the detector temperature was 300^0C. The gas carrier was helium at a pressure of 1 bar. Methyl esters were identified by comparison of the retention times with those of heptadecanoic acid and by comparison with authentic standards.

2.3 Analysis of sterol composition

Dried samples (2.50g) were extracted in 2:1 (v/v) dichloromethane-methanol using a Soxhlet apparatus for 24 h. The extract was concentrated under reduced pressure and fractionated, in order to obtain total sterols, by preparative TLC on Silica gel plates (0.25 mm)developed in the first dimension in 92:8 (v/v) hexane-ethyl acetate (18 cm length of run) to separate steryl esters (SE), and, in a second dimension in 90:10:0.5 (v/v) dichloromethane-methanol-water(12 cm length of run) to separated free sterols (FS), acylated steryl glycosides (AGS) and steryl glycosides (GS) (*27*). The SE, FS, AGS and GS bands were located according to Rf values of standards simultaneously chromatographed: cholesterol palmitate, cholesterol (Sigma), Cholesterol-3-0-6-palmitol, palmitoyl-glucopyranoside and cholesterol-3-0-glucopyranoside (Matreya, Pleasant Gap, USA). Spots of standars were visualized with Liebermann-Burchard reagent (Rf=0.95, 0.07, 0.05 and 0.35 respectively). The different bands were scrapped off and eluted with dichloromethane SE and FS with 2:1 (v/v) dichloromethane-methanol for AGS and GS. The SE were saponified by 1 h reflux with 6% (w/v) methanolic KOH with 0.5% (w/v) pyrogllol. The AGS and GS were separately hydrolyzed in a 1% (v/v) ethanolic $H_2SO_4$by refluxing for 4 h. Sterols were dried in a stream of nitrogen gas and purified by silica gel TLC plates developed in dichloromethane with colesteryl acetate as the standard. Identification was determined as mentioned above. Resulting total steryl acetates were analyzed on a Carlo Erba 2900 gas chomatograph coupled with a Jeol JMS-D300 mass spectrometer. Gas chromatography was carried on 30 m x 0.32 mm fused silica capillary column with a 0.1 mm film of DB5. The column was operated at a pressure of 0.5 bars of helium. Temperature was increased from 260 to 278^0 C at a rate of 2^0 C min^{-1} then to 300^0 C at a rate of 5^0C min and held at 300^0 C for 10 min. The injector temperature was held at 275^0 C and the detector temperature 300^0 C. Electronic impact mass spectra was measured at 70 eV and an ionization temperature of 150^0C. Identifications were based on the retention times of the steryl acetates relative to cholesterol acetate and their mass spectra. For quantification, 5 a cholestane was added to each

sample as internal standard. Relative abundances of sterols were calculated by measurements of spectra which were proportional to content.

2.4 Extraction of β-carotene

β-carotene was extracted following the method described by Hart and Scott (1995) with some modifications. In this method triplicate samples of approximately 5 g were taken for – β-carotene extraction. The samples were extracted with tetrahydrofuran/methanol (1:1, THF:MeOH) followed with petroleum ether (40±60◦C) and antioxidant, 0.1% butylated hydroxytoluene. (BHT). During the extraction, 10% NaCl was added to give a better separation between the organic and aqueous phase. The aqueous phase was extracted twice with peteroleum ether and the washings were added together. Saponification was performed with addition of 40% KOH/MeOH to.
tetrahydrofuran/methanol (1:1, THF:MeOH) followed with petroleum ether (40±60◦C) and antioxidant, 0.1% butylated hydroxytoluene. (BHT). During the extraction, 10% NaCl was added to give a better separation between the organic and aqueous phase. The aqueous phase was extracted twice with peteroleum ether and the washings were added together. Saponification was performed with addition of 40% KOH/MeOH to the extract, with a flow of nitrogen gas and was kept in the dark at room temperature for an hour. Saponification eliminated chlorophyll pigments and hydrolyzed carotenoids esters which would interfere in the HPLC chromatographic process. The carotenoid was extracted from the KOH/MeOH phase with petroleum ether and washed with distilled water until pH was neutral. The extract was dried by rotatory vacuum evaporation and was diluted again with petroleum ether and dichloromethane to a volume of 5 ml. **β**-carotene content in the sample extract was determined by reverse phase high performance liquid chromatography (HPLC) method. Recovery experiments were also performed in which standard solution of beta-carotene was added to the tested sample.

2.5 High performance liquid chromatography Separation of β-carotene

Quantitative analysis on the amount of β -carotene present was performed using HPLC μa reverse phase column, Waters m-Bondapak C18 column (30cmX3.9 mm i.d.) operated at 30^{o}C. The column was preceded by a Waters Guard-Pak pre-column module housing a disposable Guard-Pak pre-column insert packed with the same material as that in the analytical column. A Waters 510 pump was used to deliver the mobile phase which was a ternary mixture of acetonitrile, methanol, dichloromethane MeCN:MeOH:DCM) 75:20:5 v/v/v, containing 0.1% BHT and 0.05% trie-thylamine (TEA), a solvent modifier and prepared fresh daily. The flow rate was 1.0 ml/min. Solvents for liquid chromatography were of HPLC grade. All solvents for use as the mobile phase in HPLC were filtered through a 0.45 mm cellulose membrane filter and degassed using an ultrasonic bath. β -carotene standard was purchased from Sigma Chemical Company and a concentration 0.2 mg/ml was prepared diluted in the mobile phase and 20 μl injected into HPLC. Peak responses were determined at 450 nm with a variable wavelength programmable photodiode array UV detector (Waters 994) and Waters 520 printer plotter. β-carotene peak was identified by its retention time and compared with that of pure β-carotene standard. Twelve sample extracts were analyzed. Thin layer chromatography (TLC) and UV± vis absorption spectrophotometry were also used to aid in the identification of β -carotene.

Statistical Analysis

For all analysis (fatty acid, sterols), the mean and standard deviation of replicate trials were performed and values were reported as ±SEM.

3. RESULTS AND DISCUSSION

3.1 Quantitative analysis of Protein

Quantitative analysis of protein was carried out and the values of optical density corresponding to standard concentration are provided in Table 1. From Table 1, it can be observed that the protein content is quite high in red algae. It can serve as functional food with vital nutritional and biological values.

Table 1 Standard Concentration versus Optical Density table for Protein

OD value for the protein at 595 nm	
Concentration of protein(μg)	**Optical Density(OD)**
10	0.101
20	0.111
30	0.122
40	0.132
50	0.143
60	0.149
70	0.157
80	0.164
90	0.169
100	0.175

From the standard graph the protein was estimated as 0.169gm/ml (Table 1). Fayaz et al. (2005) mentioned that the protein content is 16.24±0.04 in *Kappaphycus alvarezzi,* were determined by standard AOAC methods.

The difference could be due to geographical and seasonal variations. Strong variations of protein content were observed according to the season in the following species; palmariapalmata, 22.0%±1.3, porphyra, 25.8%±1.5, chondruscrispus, 25.5%±1.1, gracilaria, 22.5%±1.1.

3.2 Analysis of Fatty acid composition

Fatty acid analysis shows that the compounds present in *Kappaphycus sp*. are, Caproic acid, Caprylic acid, Methyl heptanonaite, Butanoic acid, Ethanoic acid, Octadecic acid, Octadecatrienoic acid, 4-Methylo atanonaite (Fig. 1). The relative percentages of identified fatty acids are presented in Table 2. From the identified eight fatty acids, Caprylic acid contributes highest composition. The relative quantity of Octadecatrienoic acid is in lesser quantity among all identified fatty acids. The composition of fatty acid may be useful for taxonomic purposes.

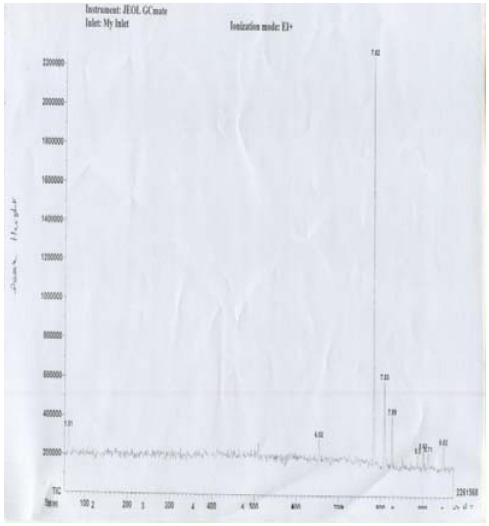

Fig. 1 Fatty Acid Estimation (Gas Chromatography)

Table 2 Relative levels of fatty acid in *Kappaphycus sp*.

Fatty acid	Mean±S.E.
Caproic acid	32±1.15
Caprylic acid	82±1.64
Methyl heptanonaite	26±0.123
Butanoic acid	15±1.123
Ethanoic acid	11±0.28
Octadecic acid	11.1±0.12
Octadecatrienoic acid	6.1±0.058
4-Methylo atanonaite	9±0.18

Fayaz et al. (2005) conducted experiments on red algae and found that gas chromatography analysis of sample extract showed the presence of fatty acid mainly containing heptadecanoic acid is 34.24%. This difference may be due to environmental effect. The quantitative estimation of the fatty acid content of c.crispus revealed that gametophytes had larger amounts of fatty acid (0.71±0.01) than sporophytes (0.622±0.004) (*11*). Many micro algae have been shown to be a good source of LCPUFA (*32*). An investigation on the fatty acid content of brown algae from Indian coast has shown the presence of only nine fatty acids, palmitic acid as the major constituent and the absence of lauric acid in the alga is notable and distinct [Dhamotharan, 2002]. Jaysankar and Kulandaidelu (1999) have shown variations in the levels of fatty acid in different variations and species of gracilaria. Dhamotharan (2002) have shown quantitative variations in the fatty acid content of sargassum collected during winter and monsoon months.

3.3 Estimation of Sterols content

Table 3 shows the percentage sterol composition of the seaweeds analysed, estimated on the basis of chromatographic peak areas for each with respect to total sterol peak area. Sterols in the non-saponifiable fractions of the seaweed samples were identified by comparison of retention times and UV absorption spectra with those obtained for corresponding standards (cholesterol, Methylenecholesterol, stigmasterol, camposterol, and β-sistosterol). For determination of retention times, the reference standards were injected both individually and as a mixture (Fig. 2). From Table 3, it can be observed that the predominant sterol is cholesterol. Cholesterol has previously been found to be present at high concentrations in Caribbean red seaweeds (Govindan and Hodge, 1993) and similar observations were reported by Beastall et al., (1971). The content of stigmasterol is less among all the sterols identified in *kappaphycus sp*. Rao et al. (1991) have shown similar variations in the sterol content of the algae. Goad and Goodvin (1972) observed that the proportion of cholesterol and desmosterol can vary sample to sample in a given species with some samples containing only cholesterol or both c27 sterols. Sanchez-Machado (2004) determined in canned or dried brown seaweed and red seaweeds. The predominant sterol was fucosterol in brown seaweeds (83 to 97% of total sterol content) and desmosterol in red seaweeds (87 to 93% of total sterol content) [Dhamotharan, 2002].

Rival variation in sterol composition among different seaweeds possibly reflecting physiological differences under or environmental influences. Marine algae have shown to be good source of unsaponofiable, non toxic sterols that have medicinal value [Orcut, 1970]. The studies of Combaut et al., (1985) have shown cholesterol to be the predominant sterol of red algae and fucosterol in brown algae. Rao et al., (1991) have shown higher levels of sterols in dried samples of three species of sargassum as compared to fresh and frozen samples. In the present study, according the relative distribution

of sterols cholesterol content is high. Stigmasterol is less.

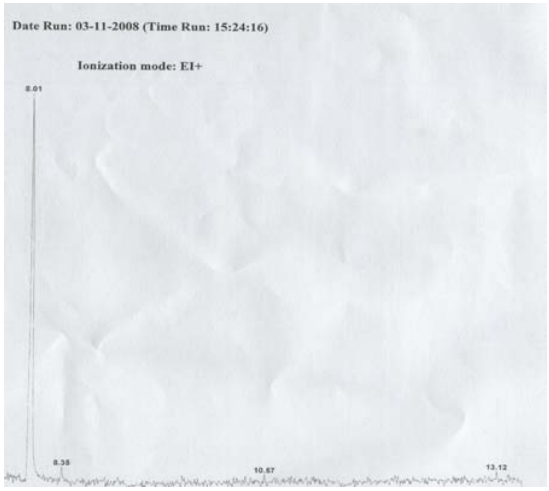

Fig. 2 Sterol Estimation (Gas Chromatography)

3.4 Analysis of β-Carotene

From HPLC result of β-Carotene shows that one compound is present in large besides other impurities (Fig. 3). The red colour of these algae results from the pigments phycoerythrin and phycocyanin; this masks the other pigments, Chlorophyll *a* (no Chlorophyll b), β-carotene and a number of unique xanthophylls. The main reserves are typically floridean starch, and floridoside; true starch like that of higher plants and green algae is absent. The walls are made of cellulose and agars and carrageenans, both long-chained polysaccharide in widespread commercial use. There are some unicellular representatives of diverse origin; more complex thalli are built up of filaments. Fayaz et al., (*1*) determined HPLC chromatogram of β-Carotene in extracted sample of *Kappaphycus alvalerez*. It showed the β-Carotene peak (RT=9.11/minute). The concentration of β-Carotene was 5.26 mg/100 gm sample. In the present study, the β-Carotene peak is observed to be 12.94 /minute. The concentration of β-Carotene is 2.5 mg/50 gram sample. Difference between the RT values of the above study and in the present study may be due to the influence of environmental conditions of the habitat over the physiology and biochemistry of the algae in the marine eco system, which indicates by the seasonal and geographical variations observed in the proximate composition of the algae. Dave et al. (1987) and Dhamotharan (2002) have studied 29 genera of red algae from Gujarat coast of India and showed monthly variations in their crude protein levels. Variations may be due to seasonal and biochemical composition of the algae.

Table 3. Relative distribution of Sterols

Sl. No.	Sterol	Mean± S.E.
1	Camposterol	1.03±0.11
2	Cholesterol	83.44±0.33
3	Stigmasterol	0.44±0.02
4	β-Sistosterol	0.75±0.03
5	Methylenechole sterol	0.65±0.01

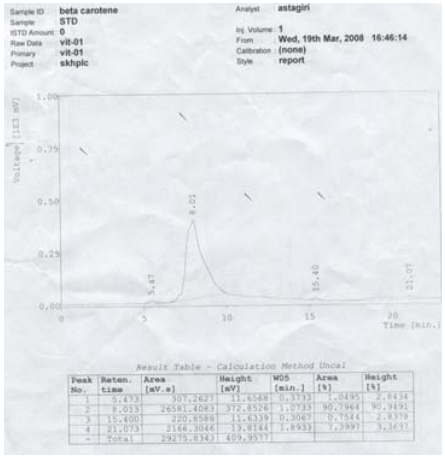

Fig. 3 β-Carotene Estimation (HPLC)

4. Conclusion

Investigation was carried out on primary metabolites of *Kappaphycus sp*. The metabolites include proteins, fatty acids, sterols and β-Carotene. From the studies, it is concluded that the *Kappaphycus sp*. located in the sea coast of Rameswaram, India, can be used as antibacterial product and serve as a food product, since it contains rich proteins, exhibits high cholesterol content, presence of one large compound of β-Carotene and variety of fatty acids. From the findings, it is also observed that the primary metabolites produced by these organisms may be potential bioactive compounds of interest in the pharmaceutical industry. Results of this study suggest study that the utility of *Kappaphycus sp.* for various nutritional product for use as health food or nutritional supplement. The remarkable differences between our results and the results obtained in the previous studies may be due to several factors. Because of the intraspecific variability, occasionally related to seasonal variations as observed in the literature and at the same time test materials have trace impurities. Finally, we conclude that macro algae from the coast of Tamilnadu are potential source of bioactive compounds and should be investigated for antibiotics. However, further work is required to identify the bioactive compounds which will show antioxidant activity against fungi and viral related pathogens..

References

Beastall GH, Rees HH, Goodwin TW., 1971. Sterols in prophyridium cruentum. Tetrahedron Lett., 4935-4938.

Beveridge THJ, Li TSC, Dover JCG., 2002Phytosterol content in American ginseng seed oil. J. Agric. Food Chem 50, 744–750.

Bhaskar N, Miyashita K., 2005. Lipid composition Padina tetratomatica (Dictyotales,Pheophyta), a brown seaweed of the west coast of India. Indian J. Fish 52, 263-268.

Combaut G, Yacoubou A, Piovetti L, Kornprobst JM. , 1985. Sterols of the Senegalese brown alga *Padina vickersiae*", Phytochemistry 24, 2131-2132,

Dave, M.J.; Parekh, R.G.; Doshi, Y.A.; Chauhan, V.D, 1987. Protein contents of Red seaweeds from Gujarat coast. Seaweed Res. Utiln 10, 17-20.

Dhamotharan R., 2002. An investigation on the bioactive principles of Padina tetrastromatica Hauck and Stoechospermum marginatum (C. Ag.) Kuetz. with respect to antimicrobial and biofertilizer properties. PhD Thesis , University of Madras.

Dunford NT, King JW., 2000. Phytosterol enrichment of rice bran oil by a supercritical carbon dioxide fractionation technique. J. Food Science 65, 1395–1399.

Goad LJ and Goodwin, T.W., 1972. Byosinthesis of plant sterols. Prog. Phytochem 3, 113-198.

Govindan M, Hodge JD, Brown KA, Nunez Smith M., 1993. Distribution of cholesterol in carribbean marine algae. Steroids 58, 178-180.

Hart DJ, Scott KJ., 1995. Development and evaluation of an HPLC method for the analysis of carotenoids in foods, and the measurement of the carotenoid content of vegetables and fruits commonly consumed in the UK. Food Chemistry 54, 101-111.

Indyk HE., 1990. Simultaneous liquid chromatographic determination of cholesterol, phytosterols and tocopherols in food. Analyst 115, 1525–1530.

Jayashankar R and Kulandaivelu G., 1999. Fatty acid profile of marine red alga Gracilaria sp. (Rhodophyta, Gigartinales). Indian Journal Mar. Sci. 28, 74-76.

Jeong WS, Lachance PA., 2001. Phytosterol and fatty acids in fig (Ficus carica, var. Mission) fruit and tree components. J. Food Science 66, 278–281.

Mohamed Fayaz, Namitha KK, Chidambara Murthy KN, Mahadeva Swamy M, Sarada R, Salma Khanam, Subbarao PV, Ravishankar GA., 2005. Chemical composition, Iron Vioavailability and Antioxidant Activity of *Kappaphycus alvarezzi* (Doty). J. Agric. Food Chem 53, 792-797.

Nabil S, Cosson J., 1996. Seasonal variations in sterol composition of Delesseria sanguinea (Ceramiales, Rhodophyta). Hydrobiologia 326/327, 511–514.

Orcutt DM., 1970. Sterols of *Oocystis polymorpha* , a green alga. Steroids 16, 429-446.

Rao PS, Srinivasa Rao P, Karmakar SM., 1991. Chemical investigations of Indian Phaeophyceae. 3. Total sterol content from different species of Sargassum. Seaweed Res. Utiln 14, 15-19.

Sanchez-Machado DI, Lopez-Hernandez J, Paseiro-Losada P, Lopez-Cervantes J., 2004. An HPLC method for the quantification of sterols in edible seaweeds. Biomed. Chromatogr. 18, 183-190.

Tasende MG., 2000. Fatty acid and sterol composition of gametophytes and saprophytes of Chondrusb Crispus. Scientia Marina 64(4), 421-426.

Viron C, Saunois A, Andre P, Perly B, Lafosse M. , 2000. Isolation and identification of unsaturated fatty acid methyl esters from marine micro-algae. Analytica Chimica Acta 409, 257-266.

Marsland Press
Journal of American Science 2009:5(2) 97-104

Vegetation coverage influence on rainfall-runoff relation based on wavelet analysis

[1]Jinchi Zhang, [2]Jiang Jiang, [3]Daoping Liu, [4]Donald L. DeAngelis
[1]College of Forest Resource and Environment, Nanjing Forestry University
Nanjing, China, 210037
[2]Department of Biology, University of Miami, Coral Gables, Florida 33124-0421 USA
[3]State Forestry of Administration, Beijing, China, 100117
[4]U.S. Geological Survey, Florida Integrated Science Center, Department of Biology
University of Miami, Coral Gables, Florida 33124-0421 USA

Abstract:
This investigation proposes a new approach for establishing rainfall-runoff-forest coverage relationship by wavelet-based analysis. First, the Db4 discrete wavelet transform is used to decompose the rainfall and runoff time series to obtain wavelet coefficients at multi-resolution level. The results show that trends of rainfall and runoff were similar. However, runoff did not always follow rainfall, as it was also influenced by other factors. Second, these wavelet coefficients are applied to model. The results show that potential impacts of forest coverage on hydrological response are of significant importance in Lao Shi-Kan watershed. Runoff decreases along with the increase of vegetation coverage. [Journal of American Science 2009:5(2) 97-104] (ISSN: 1545-1003)

Key word: Wavelet transform; Rainfall; Runoff; Vegetation Coverage; Trends

1. Introduction

Vegetation, especially in the case of forests, plays an important role in regulating runoff, as it reduces dramatically surface water volume, runoff velocity and peak discharge (Karvonen et al., 1999; Pizarro et al., 2005). Many studies showed that the variation in runoff is attributed to the vegetation cover and land use management changes (Bryan and Campbell, 1986; Kosmas, et al., 1997; Newson, 1985).Removal of forest coverage causes important changes in the hydrological balance of a watershed, although the magnitude of the response is highly variable and unpredictable (Anderson, 1990). Increased forest coverage, replacing pasture areas, can trigger a reduction of annual flow of up to 40% (Bosch and Hewlett, 1982). It is therefore essential to study the relationship of rainfall, runoff and forest coverage.

The establishment of a clear rainfall–runoff–forest coverage relationship is difficult due to the large number of variables which affect the process. It's more challenging to quantify the impact of vegetation change on rainfall-runoff relations for large basins where the interactions between land use, climatic characteristics and underlying hydrological process are more complex and dynamic [Bultot et al, 1990]. Pizarro et al. (2005) studied runoff coefficients, and their relation to vegetation coverage and water yield in the Purapel River basin, as influenced by land use and the replacement of native forest by plantations. Since hydrology is controlled and influenced by complex factors, distributed or semi-distributed

rainfall-runoff models are developed, which consider spatial heterogeneity [Beven, 1992; Jain 2004]. A kind of model include only rainfall, runoff and vegetation coverage will be more useful for those who could not get detail data, and simply want to predict how vegetation coverage affect rainfall-runoff relationship. Most methods and models available for analyzing and simulating the rainfall-runoff process involve hydrological time series with the original data [Croke and Nethery, 2006; Kothyari, et al, 2004; Labat, et al, 2002]. For time series data, periodical change caused by noise or some mechanism should be determined. We need find a method to eliminate noise and reflect real trend of hydrological data.

Wavelet analysis has been applied in the investigation of the rainfall–runoff relationship (Partal and Murat, 2006; Zhang, et al, 2006). The distinct feature of a wavelet is its multi-resolution characteristic, which is becoming an increasingly important tool to process images and signals. Since a wavelet is a localized function both in time and frequency domain, it can be used to represent an abrupt variation or a local function vanishing outside a short time interval adaptively [Morlet et al, 1982; Kumar and Georgiou, 1993]. So, in the field of hydrology, use of wavelets could be essential in the analysis of rainfall and runoff.

Using this framework, the present paper analyzes the influence of changes in forest coverage on the runoff over a period of 43 years from 1962 to 2004, in the watershed of Lao Shi-Kan in the Anji of China. This article is organized as follows. First, the original hydrological time series, including rainfall and runoff, is decomposed into detail and approximation by discrete wavelet transform. Then, the relationship of rainfall-runoff is developed which include vegetation coverage. Finally, the results are discussed and conclusions drawn.

2. Method

2.1Wavelet transform

In recent years, there has been an increasing interest in the use of wavelet analysis in a wide range of fields in science and engineering. Wavelet transform analysis, developed during the last two decades, appears to be a more effective tool than the Fourier transform (FT) in studying non-stationary time series (Torrence and Compo, 1998 ; Wang, et al, 2004). Of course, this provides an ideal opportunity to examine the process of energy variation in terms of where and when hydrological events occur.

Assuming a continuous time series $f(t)$, $t \in [\infty,-\infty]$, a wavelet function $\psi(t)$ that depends on a non-dimensional time parameter t can be written as

$$\psi(t) = \psi(a,b) = |a|^{1/2}\psi\left(\frac{t-b}{a}\right),$$

where t stands for time, a for the time step in which the window function is iterated, and b for the wavelet scale. $\psi(t)$ must have zero mean and be localized in both time and Fourier space. The continuous wavelet transform (CWT) is given by the convolution of $f(t)$ with a scaled and translated $\psi(t)$,

$$W_f(a,b) = |a|^{-1/2}\int_{t=-\infty}^{\infty} f(t)\overline{\psi}\left(\frac{t-b}{a}\right)dt$$

The lower scales refer to a compressed wavelet, and these allow us to trace the abrupt changes or high frequency component of a signal. On the other hand, the higher scales composed by the stretched version of a wavelet and the corresponding coefficients represent slowly progressing occurrences or low-frequency components of the signal.

Calculating the wavelet coefficients at every possible scale is a fair amount of work, and it generates a lot of data. If one chooses scales and positions based on powers of two (dyadic scales and positions), then the analysis will be much more efficient as well as accurate. This transform is called discrete wavelet transform (DWT).

Assuming $a = a_0^{\,j}$, $b = kb_0 a_0^{\,j}$ $a_0 > 0$ and $a_0 \neq 1, b_0 \in R$, then DWT has the form as

$$W_f(j,k) = a_0^{-j/2} \int_{-\infty}^{\infty} f(t)\overline{\psi}\left(a_0^{-j}t - kb_0\right)dt$$

The discrete wavelet transform decomposes the input hydrological time series into detailed signal, and an approximation, so the original hydrological time series is expressed as a combination of wavelet coefficients, at various resolution levels.

2.2 Rainfall-runoff relationship

After rainfall begins, precipitation can be intercepted by forest ecosystem, until the interception capacity is exceeded. Once their storage capacity is exceeded, runoff can begin. Many predictive models have been developed to predict canopy interception. Horton (1919) found that interception loss is proportional to the amount of precipitation (*P*). Due to canopy storage capacity is not filled during small rainfall events, Merriam (1960) suggested a relationship which included an exponential term to consider amount of precipitation. Rutter (1971, 1975) and Gash (1979) move away from empirical regression approach to physical and analytical model.

We did not try to analyze these models any further, because the models are focus on canopy or litter interception. However, precipitation intercept by whole ecosystem contain canopy interception, litter water-holding capacity and soil water storage. We develop the relationship according to Merriam's idea, which is exponential regression.

Precipitation that captured by vegetation eventually either evaporates or used in plant transpiration and returned to the atmosphere. So we denote *IT* here, as rainfall interception by whole forest ecosystem, which contain canopy interception, litter interception, soil water storage and evaporation. Regardless variation of vegetation characteristics, *IT* varies with the amount of precipitation (*P*).

$$\frac{dIT}{dP} = \exp(-K \cdot P)$$

When rainfall amount P approach zero, initial interception rate may attain 1. Interception rate decreased exponentially with increasing gross rainfall amounts. When the rainfall amount surpasses the maximum interception capacity of the forest system, then the excess amount of rainfall drains and is no longer intercepted by the forest.

Where K stands for the speed at which the rainfall interception rate decreases progressively with the rainfall amount, has a close correlation with vegetation coverage. We carry out the integration of the above equation and yields:

$$IT(P) = \frac{1}{K}\left(1 - e^{-KP}\right)$$

When $P \to \infty$, we obtain the possible maximum rainfall interception loss (*ITM*):

$$ITM = \frac{1}{K}$$

According to the water volume balance, runoff (Q) can be defined as

$$Q = P - IT = P - \frac{1}{K}\left(1 - e^{-KP}\right)$$

ITM is determined by land cover and the roughness and soil in watershed (Toba, 2005;

Wang, 2005). Vegetation cover represents one of the most powerful factors influencing *ITM*, since it modifies and moderates many others. Dense vegetation coverage has a higher interception storage capacity than rock or pavement.

We assuming $ITM = b\alpha + c$, where α is vegetation coverage, refers to the ratio of area of afforested land to total land area (According to State Forestry Administration (SFA) of China). *c* represents water storage by surface and soil, when vegetation coverage is 0%. *b* is *ITM* increase rate in the direction of vegetation coverage. So runoff can be described as function of rainfall and vegetation coverage.

$$Q(P,\alpha) = P - (b\alpha + c)\left(1 - e^{-\frac{P}{b\alpha + c}}\right)$$

3. Results and discussion

3.1 Study basin

This work demonstrates the feasibility of applying the wavelet-based method to model the relationship of rainfall, runoff and vegetation coverage by selecting the Lao Shi-Kan watershed located in 119°53′-119°14′E, and 30°52′-30°23′N, northern Zhenjiang as the study area. The area of the watershed of Lao Shi-Kan is 258 km^2, as displayed in Fig.1. The mean annual precipitation in these watersheds is 1714.2 mm; the mean annual runoff is 226 million m^3. As for temperatures, the annual mean corresponds to 15℃, with maximum and minimum of 40.8℃ and -17.4℃, respectively. There are four rainfall stations and one hydrologic station in the basin (Fig.1).

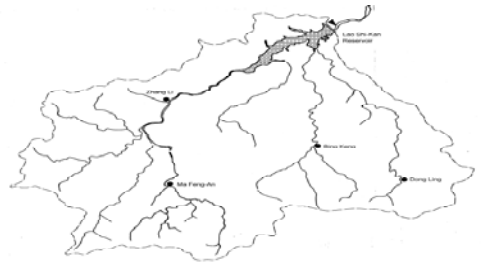

Fig.1 The map of Lao Shi-Kan watershed showing the study area, Anji Zhejiang

The time series of yearly mean rainfall and runoff were obtained from the hydrology stations of Anji, Zhejiang. The length of record is 43 years, from 1962 to 2004. But one of the rainfall stations, Bing-Keng, missed data from 1996 to 2001. The problem of missing data was solved by interpolation of neighboring points.

3.2 Trend analysis results of wavelet transform

In this section, we used DW transform coefficients at three decomposition levels. By using discrete wavelet components of time series, we aimed to find which periodicities are mainly responsible for trend of the series.

The original signal f (t) is decomposed into series of approximations and details by db4 wavelet. Db4 wavelet is simple and compact. It is suitable to detecting a sudden change of the error signal due to amplitude mutation. The process consists of a number of successive filtering steps. The original signal is first decomposed into an approximation (a1) and accompanying detail (d1), then the first level approximation (a1) is decomposed into an approximation (a2) and accompanying detail (d2). The decomposition process is then iterated, with each successive approximation being decomposed in turn, so that the original signal is broken down into many lower-resolution components.

The time series of the DW transform coefficients represent rainfall and runoff variations. The time series of multi-resolution levels are generated and are presented in Fig. 2. The top panels in Fig.2 represent the original time series of annual total rainfall (mm) and runoff (mm). The time series of DW coefficient give the contributions to total annual rainfall and runoff in each year. Time series of first level mode (a1, d1), second level mode (a2, d2), and third level mode (a3, d3) are presented in other lower panels of Fig.2.

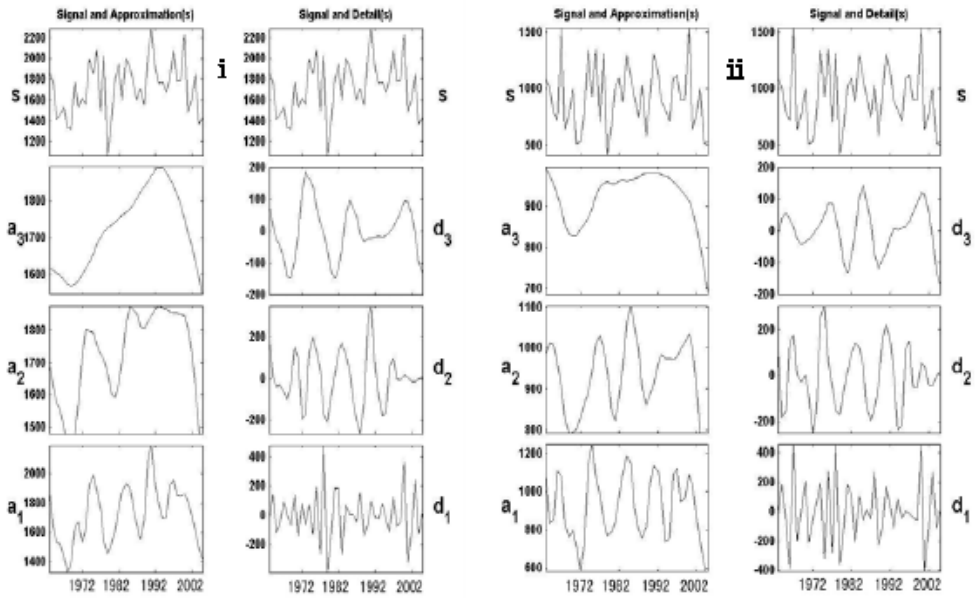

Fig.2 Top panel, rainfall (ⅰ) and runoff (ⅱ) series for the period 1962–2004 for Lao Shi-Kan station. Other lower panels: time series of first level (a1, d1), second level (a2, d2), third level (a3, d3)

From the first level of approximation (a1), we can see that the rainfall and the runoff trends are similar on the whole. The second level (a2) shows a decreasing trend during 1973-1980, however the runoff increased continuously until 1977. From the third level (a3), we find that rainfall had a slowly decreasing trend during 1962-1967. Runoff also decreased during this period of time. Rainfall started to increase during the years 1968~1993; the rainfall dropped rapidly after year 1993, the turning point being in 1993. But runoff started to increase after year 1968, increased gently until year 1977, and then had a declining trend. The third level approximation (a3) show clear relationship between rainfall and runoff, which is not linear and change along time. Detail explanation will be presented next section.

3.3 Rainfall-runoff affect by vegetation

First, we compared the graphs of the original data used in the rainfall-runoff relationship (Fig.3A) and the wavelet coefficients (Fig.3B).

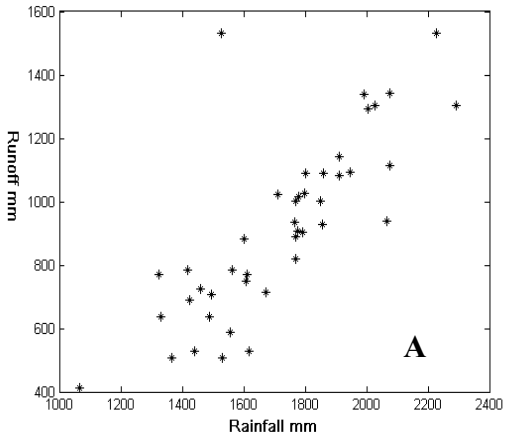

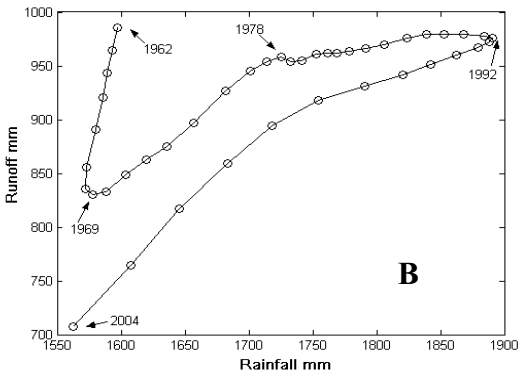

Fig.3 Runoff and the rainfall relational graphs; the original data (A) and wavelet coefficients (B) were

It is very difficult to find the real relations of rainfall-runoff in the original data; so some scholars use a simple linear model to fit it. Applying wavelet coefficients of third level approximation, we can see that rainfall and runoff do not have a unique relationship, and thus cannot fit directly into a simple linear model. This is because the forest coverage differed during different periods. 1970s runoff was much higher than that of the 1990s under the same rainfall, because the 1990s forest coverage was higher than the 1970s.

Next we want to incorporate vegetation coverage data to rainfall-runoff relationship. Due to the difficulty of forest assessment, it is impossible to get vegetation coverage each year. Six nation forest censuses have done since 1950s. The recorded data of forest resources in the basin of Lao Shi-Kan are listed in Table 1. Vegetation coverage changed significantly during last 40 years, especially when the catchment was enclosed and became a natural reserve on 1985, vegetation coverage increased drastically.

The percentages of vegetation coverage in Table 1 only represent the average levels over those periods. In contrast to approximately 40 years of detailed data on rainfall and runoff, the percentages of vegetation coverage are available for only six time periods. Lacking vegetation coverage for each year, model parameter estimation will be more difficult. In order to avoid unnecessary error, this article estimates parameters as follows:

1. Classify rainfall and runoff data into six groups, according to correspondingly years of the six forest censuses. Calculate average rainfall and runoff during these periods.
2. Estimate the initial model parameters by Nelder-Mead method.
3. Hind casting corrected value of the vegetation coverage use rainfall and runoff data as inputs. This will generate 43 years vegetation coverage.
4. Classify new corrected vegetation coverage into six groups, use these six paired data estimate parameters again.
5. Repeat processes 3 and 4, until the estimated parameters don't change.

Following the above process, a Matlab code is developed to estimate parameters, yielding the result b=1346.8, c=16.9. After the computer programming, the simulation produces the relations as shown in Fig.4.

Fig. 5 gives runoff-rainfall relations curves when forest coverage is 0, 50%, 100%, respectively. When $\alpha = 0$, $Q = P - c\left(1 - e^{-P/c}\right)$,

$$K = \frac{1}{ITM} = \frac{1}{b\alpha + c} = \frac{1}{c}, \quad \frac{dIT(P)}{dP} = e^{-P/c}.$$

As parameter c is smaller than normal rainfall, the rate of impounding can trend toward 0 quickly as P increases, and then under 0 vegetation coverage the runoff (Q) is approximately equal to rainfall (P). As the vegetation coverage increase,

Q increase more gradually when rainfall is low. When rainfall is exceed a threshold, like a storm, runoff approach linear relation with rainfall. But for same rainfall, high vegetation coverage has lower runoff than low vegetation coverage.

Fig.6 gives the runoff-vegetation coverage relationship curves when rainfall is 2500, 1500, and 500mm, respectively. When rainfall is 2500mm (representing periods of abundant water), the runoff is decreased by 1123.7mm, or 45.27%, when the vegetation coverage is increased from 0% to 100%. When the rainfall is 1500mm (representing multi-annual means), the runoff is decreased by 889.6mm, or 60.02%, when the vegetation coverage is increased from 0% to 100%. When the rainfall is 500mm (representing a dry season), the runoff is decreased by 81.8mm, or 83.03%, when the vegetation coverage is increased from 0% to 100%.

Runoff decreases rapidly as soon as vegetation coverage increases from 0 to 20%, when the rainfall is 500mm. As the forest coverage continues to increase, the rate of decrease decelerates. Runoff no longer decreases after vegetation coverage increases beyond about 40%. It also means that vegetation coverage of 40% is necessary to impound rainfall for a low flow period. More vegetation coverage is needed for impounding rainfall, when rainfall is at a high level. It is hard to conclude the precise optimal vegetation coverage. From the figure, we can estimate that about 80% is necessary for impounding rainfall when it is at an average level.

This model can provide the relationship of runoff, rainfall and vegetation coverage. Runoff has a downward trend as vegetation coverage increases. The influence is more prominent under conditions of less rainfall.

Acknowledgements

This work was supported by the Key Project of National Science and Technology During the 11th Five-Year Plan [No. 2006BAD03A16].

References

Anderson, A., Pyatt, D., Stannard, J., 1990. The effects of clearfelling a Sitka spruce stand on the water balance of a peaty grey soil at Kershope Forest. Cumbria Forestry 63, 51-71.

Beven, K. J. and Binley, A.M. 1992. The future of distributed models: model calibration and predictive uncertainty. Hydrological process 6, 279-298.

Bosch, J., Hewlett, J., 1982. A review of catchment experiments to determine the effect of vegetation changes on water yield and evapotranspiration. Journal of Hydrology 55, 3-23.

Bryan, R.B. and Campbell, I.A., 1986. Runoff and sediment discharge in a semi-arid drainage basin. Zeitschrift fur Geomorphologie 58, 121-143.

Bultot, F., Dupriez, G.L., Gellens, G., 1990. Simulation of land use changes and impacts on the water balance – a case study for Belgium. Journal of Hydrology 114, 327-348.

Croke, J., Nethery, M., 2006. Modelling runoff and soil erosion in logged forests: Scope and application of some existing models. Catena 67, 35-49.

Gash, J. H. C., 1979. An analytical model of rainfall interception by forests. Quart. J. R. Met. Soc 105, 43-55

Horton, R.E., 1919. Rainfall interception. Mon. Weath. Rev., 47, 603-623.

Jain, M.K., Kothyari, U. C., Raju, K.G. R. 2004. A GIS based distributed rainfall-runoff model. Journal of Hydrology 299, 107-135.

Karvonen, T. Koivusalo, H. Jauhiainen, M. 1999. A

hydrological model for predicting runoff from different land use areas. Journal of Hydrology 217, 253-265.

Kosmas, C., Danalatos, N., et al., 1997. The effect of land use on runoff and soil erosion rates under Mediterranean conditions. Catena 29, 45-59.

Kothyari, B.P., Verma, P.K., Joshi, B.K., et al, 2004. Rainfall - runoff - soil and nutrient loss relationships for plot size areas of bhetagad watershed in Central Himalaya, India. Journal of Hydrology 293, 137-150.

Kumar, P., Georgiou, E.F., 1993. A multi-component decomposition of spatial rainfall fields 1. Segregation of large and small scale features using wavelet transforms. Water Resources Research 29, 2515-2532.

Labat, D., Mangin, A., Ababou, R., 2002. Rainfall-runoff relations for karstic springs: multifractal analyses. Journal of Hydrology 256, 176-195.

Merriam, R.A., 1960. A note on the Interception Loss Equation. Journal of geophysical research 65, 3850-3851.

Morlet, J., Arens, G., Fourgeau, et al, 1982. Wave propagation and sampling theory and complex waves. Geophysics 47, 222-236.

Newson, M.D., 1985. Forestry and water on the uplands of Britain - the background of hydrological research and options for harmonious land use. J. Forestry 79, 113-120.

Partal, T., Murat, K., 2006, Long-term trend analysis using discrete wavelet components of annual precipitations measurements in Marmara region (Turkey). Physics and Chemistry of the Earth 31, 1189-1200.

Pizarro, R., Araya, S. Jordan, C. et al, 2005. The effects of changes in vegetative cover on river flows in the Purapel river basin of central Chile. Journal of Hydrology 327, 249-257.

Pizarro, R., Benitez, A., Farias, C., et al, 2005. Influence of the wooded masses on hydric regime in a semiarid river basin, Chile. Bosque 26, 77-91.

Rutter, A.J., Kershaw, K.A., Robins, P.C. and Morton, A.J., 1971. A predictive model of rainfall interception in forests, 1. Derivation of the model from observations in a plantation of Corsican pine. Agric. Meteorol 9, 367-384.

Rutter, A.J., Morton, A.J. and Robins, P.C., 1975. A predictive model of rainfall interception in forests. II. Generalization of the model and comparison with observations in some coniferous and hardwood stands. J. Appl. Ecol 12, 367-380.

Toba, T., Ohta, T. 2005. An observational study of the factors that influence interception loss in boreal and temperate forests. Journal of Hydrology 313, 208-220.

Torrence, C., Compo, G.P., 1998. A practical guide to wavelet analysis. Bulletin of American Meteorological Society 79, 61-78.

Van Dijk, A.I.J.M and Bruijnzeel, L. A., 2001. Modelling rainfall interception by vegetation of variable density using an adapted analytical model. Part 1. Model description. Journal of hydrology 247, 230-238.

Wang, A., Li, J., Liu J., et al. 2005. A semi-theoretical model of canopy rainfall interception for *Pinus Koraiensis Nakai*. Ecological Modelling 184, 355-361.

Wang, W., Zhao, T., Ding, J., 2004. Study on change characteristics of hydrological time series with continuous wavelet transform. Journal of Sichuan University 36, 140-143.

Zhang, Q., Liu, C., Xu, C., et al, 2006, Observed trends of annual maximum water level and streamflow during past 130 years in the Yangtze River basin, China. Journal of Hydrology, 324, 255-265.

Marsland Press

Journal of American Science 2009:5(2) 105-106

Arnebia nandadeviensis (Boraginaceae), a new species from India

K. Chandra Sekar*, R.S. Rawal, Sanjay Gairola, Balwant Rawat
G.B. Pant Institute of Himalayan Environment & Development, Kosi – Katarmal,
Almora – 263 643, Uttarakhand, India

Abstract:
A new species of *Arnebia* (Boraginaceae), *A. nandadeviensis* K. Chandra Sekar & R.S. Rawal, is described from India. [Journal of American Science 2009:5(2) 105-106] (ISSN: 1545-1003)

Keywords: *Arnebia nandadeviensis,* Nanda Devi Biosphere Reserve, Uttarakhand, India, new species.

1. Introduction

The genus *Arnebia* Forsk. is represented by *ca* 25 species, chiefly distributed in Mediterranean region of the world, especially in tropical Africa and Himalaya (Mabberley, 1998). In India the genus comprises 5 species distributed in Upper gangetic plains and the Himalayan region (Aswal and Mehrotra, 1994). The genus is characterized by white tubercles in the body of plant, flat torus, actinomorphic - campanulate corolla, imbricately folded corolla-lobes; globose inflorescence and 4 partite ovary.

Arnebia nandadeviensis was collected by the authors during ecological vegetational analysis of Nanda Devi Biosphere Reserve under the project entitled "Response assessment & processing of knowledge base to serve long term management and use of biodiversity in the Himalaya". This plant was growing on alpine slopes at an altitude of 3800 – 4000 m along with *Anaphalis royleana* DC., *Jurinea dolomiaea* Boiss. and *Poa alpina* L. Critical examination and perusal of literature and herbaria reveal that the plant represents a hitherto unrecognized species. *Arnebia nandadeviensis* closely resembles *Arnebia euchroma* I.M. Johnston but differs in a number of characters (Table 1).

2. Enumeration

Arnebia nandadeviensis K. Chandra Sekar & R. S. Rawal, sp. nov. [Photo. 1 & 2]

Arnebiae euchromae I.M. Johnston, habitu caespitoso, perenni; caule erecto, 10-35 cm; radice atrorubro; foliorum mediano-nervo distincto; inflorescentiis globosis; bracteis lineario-lanceolatis; corollarum tubis angustis; corollae limbo campanulato; stylo exerto; stigmatae distincte 2-partito et ovario globoso similis, sed radecalio-foliis oblanceolato-obovatis, obtusis; caulino-foliis latioribus (1-3 cm latis); inflorescentiis stipitalis, nutantibus; bracteis floribus longioribus; calycibus longioribus (1.7-2.4 cm); limbis minore latioribus (*ca* 2 mm) et antheris longioribus (6-7 mm) differt.

Typus: India, Uttarakhand, Bageshwar, Nanda Devi Biosphere Reserve, Pindari, 3820 m a.s.l., 30º 16' 0.2" N Latitude, 80º 00' 23.6" E Longitude, 29.08.2008, *R.S. Rawal, K. Chandra Sekar, Sanjay Gairola & Balwant Rawat* 2895 (holo GBP; iso BSD).

Perennial tufted herbs; root 1-1.5 cm thick, dark red. Stems few, 10-35 cm high, erect, terete, spreading bristly. Radical leaves 7-10, petioled, oblanceolate to obovate, 10-14 x 1-2.6 cm, obtuse at apex, entire, with distinct single pale green median nerve, glandular-downy, not bristly especially along margin, gradually tapering to broad petiole; petiole 1.5-2.3 cm long, pale green-yellow. Cauline leaves 8-12, sessile, alternate below, almost opposite towards the inflorescence, acute at apex, tapering towards base, slightly glandular-hairy or bristly-ciliate, with single pale green nerve; lower leaves elliptic – lanceolate or lanceolate, 3-8 x 1-2 cm, glandular-hairy above, appressed bristly-ciliate beneath; upper ones ovate or ovate-lanceolate, 3.2-4.8 x 2-3 cm, bristly-ciliate. Inflorescence globose, capitate, stalked at apex of non-branching stem, 6.5-8.5 x 3.5-4.2 cm, nodding; stalk 0.5-1.5 cm long. Bracts numerous, exceeding the flowers, linear-lanceolate, 1.8-2.7 cm long and 2-5 mm wide, entire, acuminate, dense bristly-ciliate along margin, pale green; bristle 1-3 mm long. Flowers nodding, densely covered by bracts, 2-3.2 cm long, pedicelled; pedicel 0.8-1.2 cm long. Calyx slightly longer than corolla, 1.7-2.4 cm long, bristly; lobes linear, 1.4-1.8 cm long, bristly towards apex. Corolla dark red, the narrow tube 1.6-2 cm long; limb campanulate, 1-2 mm long, *ca* 2 mm across, obtuse, bristly along the margin. Anthers attached near the middle of corolla tube, 6-7 mm long, stalked; stalk 1-2 mm long. Style exserted; stigma distinctly 2-parted. Ovary globose, 2-3 mm across, ovules small.

Flowering and fruiting: June – August.

Ecology: Scarcely growing on alpine slopes at an altitude of 3800 – 4000 m.

Distribution: India, Pindari (Nanda Devi Biosphere Reserve), Uttarakhand.

Etymology: The specific epithet *'nandadeviensis'* is based on the type locality, Nanda Devi Biosphere Reserve.

Note: *Arnebia nandadeviensis* is closely allied to *Arnebia euchroma* I.M. Johnston in general appearance having tufted perennial habit; 10-35 cm erect stem, dark red root; distinct median nerve of leaves; globose inflorescence; linear-lanceolate bracts; narrow corolla tube, campanulate corolla-limb; exserted style, distinctly 2-parted stigma and globose ovary but differs from the latter in having oblanceolate-obovate, obtuse radical leaves; wider cauline leaves (1-3 cm); stalked with nodding inflorescence; numerous bracts exceeding the flowers; longer calyx (1.7-2.4 cm) with less wider limb (*ca* 2 mm) and longer anther (6-7 mm).

Fig.1 *Arnebia nandadeviensis* sp. nov. along with associate plants

Fig.2 A twig showing the nodding inflorescence along with cauline leaves

Acknowledgements

The authors are thankful to Dr. L.M.S. Palni, Director, G.B. Pant Institute of Himalayan Environment & Development, Kosi-Katarmal, Almora for providing facilities and encouragements. Sincere thanks to Dr. V.J. Nair, Scientist Emeritus, BSI, Coimbatore for providing the latin diagnosis. The authors are thankful to Dr. V. Sampath Kumar, Scientist-C, BSI, Coimbatore for helping and valuable suggestions.

References

Mabberley, D.J. (1998). The plant book. 2nd revised edition. Cambridge University press. pp. 56.

Aswal, B.S. and B.N. Mehrotra (1994). *Flora of Lahaul-Spiti.* Bishen Singh Mahendra Pal Singh, Dehradun. pp. 441-456.

Table 1. Distinction between *Arnebia euchroma* I.M. Johnston and *Arnebia nandadeviensis* sp. nov.

	Arnebia euchroma	**Arnebia nandadeviensis**
Radical leaves	lanceolate or lanceolate-linear to linear	oblanceolate to obovate
	acute at apex	obtuse at apex
Cauline leaves	less than 1 cm wide (3-7 mm)	more than 1 cm wide (1-3 cm)
Inflorescence	sessile	stalked (0.5-1.5 cm long)
	erect	nodding
Bracts	few	numerous
	not exceeding the flowers	exceeding the flowers
Calyx	slightly shorter than the corolla (ca 1.2 cm)	longer than the corolla (1.7-2.4 cm)
Corolla	1.2-1.5 cm long	1.6-2 cm long
	limb half length of corolla-tube (7-8 mm)	limb not half length of corolla-tube (1-2 mm)
	limb *ca* 8 mm across	limb *ca* 2 mm across
Anthers	*ca* 2.5 mm long	6-7 mm long

Marsland Press
Journal of American Science 2009:5(2) 107-118

Effect of Bus Bays on Capacity of Curb Lanes

***Akpakli Vincent Kwami, Yang Xiao Kuan, Ph.D., Xu Zhi**
Transportation Research Center,
Beijing University of Technology,
Beijing 100124, China.

* Corresponding Author
E-mail: vkakpakli@yahoo.com
Telephone number: (0086) 13683391376

ABSTRACT: Bus bays have a significant influence on the capacity of curb lanes because they interfere with passing vehicles primarily while buses maneuver to pull into and out of the bus bays. The studies of bus stops influence on capacity of signalized intersections have been attempted by several Researchers and Scholars from both home and abroad. However, the studies of bus bays' impact on capacity of curb lanes are found to be very few. The objective of this study is to investigate the quantitative impact of bus bays on curb lanes capacity of roadways in Beijing. New concepts of bus impact time occupancy ratio and bus impact time were introduced in the study. Relationships among bus deceleration time, bus acceleration time, and bus impact time were established when buses maneuver to pull into and out of the bays. A statistical relationship between average bus impact times and average bus arrival frequencies was established using Statistical Program for Social Sciences (SPSS 13) for Windows. A model was calibrated for bus parameters (bus impact time and bus arrival frequency) using the collected data from fifteen bus bays on the expressways in Beijing. This model is very useful and can be used as a tool for analysis by Engineers and Planners of traffic and transportation professions to provide technically-sound advice to Public Transport Operators, Traffic Management Department and Department of Urban Planning and Design. [Journal of American Science 2009:5(2) 107-118] (ISSN: 1545-1003)

Index Terms: Capacity, Beijing, Bus Bays, Bus Impact Time Occupancy Ratio, Curb Lanes, Bus Arrival Frequency.

1. INTRODUCTION

1.1 Background of the Study

Traffic congestion at bus bay bus stops in Beijing is on the rise with increasing private automobiles on the roadways competing with public transports for the limited roadway spaces. The efficiency of public transportation buses is declining considerably. Commuters have to waist a lot of time at bus stops and also in the bus in order to get to their destination. The purpose of this study is to model the relationship between bus impact time as bus main parameter at the bus bay and the capacity of the curb lanes. The results of this study can be used for Public Transport Operators to take necessary measures to optimize bus dispatching plans and increase the operation efficiency of public transport buses. On the other hand, the results will help traffic engineers and traffic management department to better understand the performances of traffic flow at the bus bays in order to take necessary steps to increase the capacity of the bus bays by way of reorganizing and redesigning of the bus bays.

These days, bus bays types of bus stops have been brought into wide use in many big cities of China. Bus bays primarily conflict with other passing vehicles when buses maneuver to pull into and out of the stop. Bus bay bus stops will also interfere with vehicles movement if bus demand exceeds the bus bay's capacity, resulting in some buses waiting in the travel lane until the buses occupying the bay exit the bay. At certain situations, there can also be cases of buses blocking the curbside traffic lane during their bay occupancy period or bay dwell period, if they do not fit completely within the bay due to the reduced width of the available bay or due to erratic behavior of drivers. Bus bays may also present problems to bus drivers when attempting to re-enter traffic, especially during periods of high roadway traffic volumes. The typical bus bay is illustrated in figure 1 below.

There are many homes and abroad researches on bus stops influencing on capacity of signalized intersections, but scholars and researchers very few or seldom study bus bay influence on capacity of curb lanes or basic roadway links. Therefore, at times when bus bays are planned, designs are carried out and they are to be built, Engineers only rely on their own professional experiences and at times make references to scholars or researchers' qualitative recommendations or considerations and hence need for quantitative impact study of bus bays on curb lanes capacity.

.

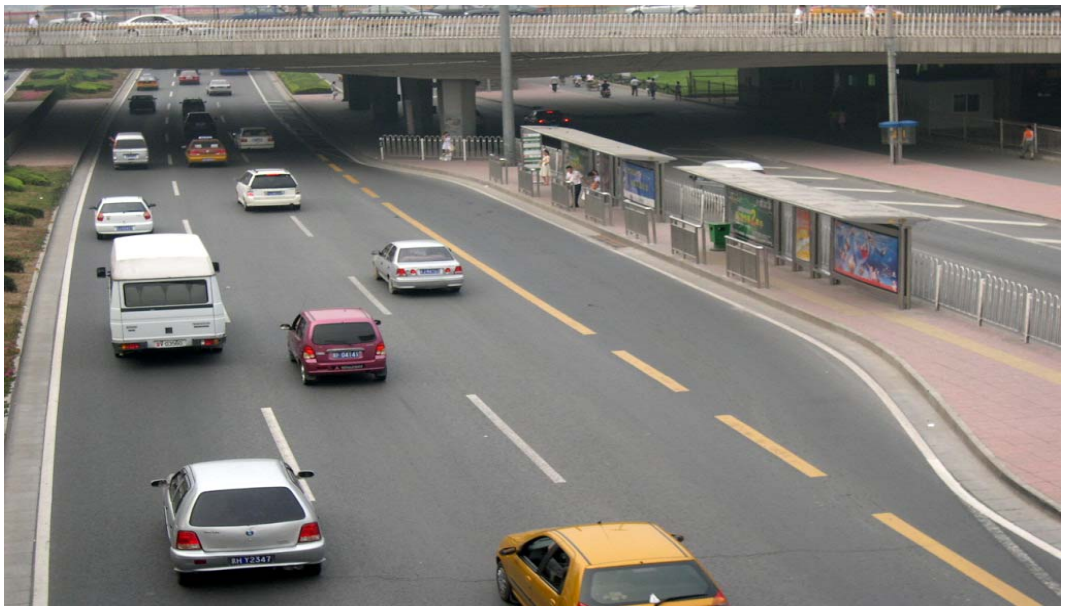

FIGURE 1: Typical Bus Bay

1.2 Literature Review

In the 2000 Highway Capacity Manual (HCM) [1], although there are some findings about the influence of bus stops on capacity

when buses pull in and out of the bus stops, when one applies these results, the parameters

one needs are the number of buses per hour at each bus stop and the average bus stopping time (average bus dwell time).The impact times for deceleration and acceleration by the buses into and out of the bus stops respectively are not taken into account or simply not considered by the HCM. Therefore, when the formula in the HCM is applied in this study it will not produce the desired results.

Reebu Zachariah Koshy and V. Thamizh Arasan (2005) analyzed the influence of bus stops on traffic flow under heterogeneous traffic conditions using a simulation technique. They examined the effects of variation of the basic parameters, such as bus dwell time, road width and traffic flow for both bus bays and curbside bus stops. However, they did not come up with a formula for calculating capacity of roads on which bus stops have influence on the traffic flow.

Bing Wu from Tongji University analyzed the delay of buses under mixed traffic conditions and found a way of calculating the capacity. He also analyzed the running characteristics while the buses are at the bus stops and their influence on capacity. He believed that buses have the same influence on the capacity when the bus stops are located at the far side of the intersection as when they are located at the nearside of the intersection. However, he did not build a quantitative model for calculating the influence which the bus stops have on the intersections' capacity.

Besides that, Pei Yu-long and Wu Shi-mei (2004) from Harbin Institute of Technology mainly analyzed the influence of bus stops located at or set near the unsignalized intersections on capacity, and built a theoretical model for it.

Wong S.C. and Hai Yang discussed the way of calculating the delay of signalized intersections when there are bus stops at farside of the intersection. They came up with (or drew) a conclusion that the delay is influenced by the distance between bus stops, traffic capacity of the road, the departure frequency of the buses, the average bus dwell time of buses and the signal index of the intersection. They also deduced a formula for calculating the capacity.

Wang Qian and Yang Xiao-guang (2003) from Tongji University made a quantitative analysis on the situation of which buses stop on the outer compound lanes of motor vehicles at signalized intersections and tried to establish the relationship between traffic delay, capacity and bus-stopping parameters, such delay, the location of bus berth and bus flow at shared approaches of signalized intersections mathematically. In the end, they built a model for the change of the intersection capacity caused by the buses stopping in order to

provide analysis tools for bus operation and also for improvement of urban bus management.

Zhou Y. and Liu X. [1994] conducted a research study on traffic flow composition and road capacity. They used a multiple linear regression method to derive values of passenger car equivalents (pce) in China. Their research findings were used in assigning a value for pce for buses on Beijing roads.

2. OBJECTIVE OF THE STUDY

The objective of this study is to develop a model for determining the quantitative impact of bus bay on capacity of curb lanes. To reach this objective, it is necessary to find out the relationship between bus deceleration time, bus acceleration time, and bus impact time (main parameter), when buses maneuver to pull into and out of the bus bay.

In addition, the model is to seek to:

1. Establish a relationship between average bus impact time, T (bus main parameter) and the capacity of curb lane, C.
2. Find a statistical correlation between average bus impact time, T and average bus-arrival frequency, λ.

The results of this study can be used by Engineers and Planners of the traffic and transportation professions to provide useful advice to Public Transport Operators in the establishment of bus dispatching plans on the bus routes and also ensure to over reach capacity of bus routes or bus lines lines. Other, this study will be to enable traffic and transportation practitioners to provide expert advice to Public Transport Operators in dealing with spacing of bus stops and providing bus stations or bus terminals appropriately in order not to reach the over capacity at the bus bays and bus terminals. The procedures when developed will help provide theoretical model for quantitative impact analysis of bus bays on capacity of curb lanes and will go a long way to help Transit Agencies to know the grid frequency or bus lines frequency in order to serve as basis for planning. All these are objectives which the model seeks to achieve.

3. METHODOLOGY

The operation of a bus bay type of bus stop has its own peculiar characteristics other than the curbside type of bus stops. The components of bus impact time (bus main parameter) of a bus bay are different from that of curbside bus stop. With the bus bay, bus impact time includes only the summation of deceleration and acceleration times of a bus when it maneuvers to pull into the bay and pull out of the bus bay to re-enter the traffic stream to attain the normal speed of other vehicles in the curb lanes. While in the curbside bus stop, bus dwell time or bus stop occupancy time is included in the summation of bus deceleration and acceleration times to give bus impact time. To model the impact of bus bays on capacity of curb lanes, the following three steps have been taken:

3.1 Selection of Bus Bays of Interest

A total of fifteen bus bays were selected on second and third ring roads of expressways in Beijing for data collection. For the purpose of model building, one needs to collect bus deceleration times, bus acceleration times and bus arrival frequencies or volumes. The selected bus bays should satisfy the following conditions. First, there should be an area where a digital video camera can be mounted to tape the entire bus bay affected zone or the whole traffic influenced area, to ensure the video graphing and on-site observations. This will give valuable data covering all categories of buses on the road-site and the number of survey samples times to meet the demand of the study. Normally, overpass for pedestrians close to the bus bay, or high-rise building nearby, or flyovers close to the bus bays are good places to install video camera. Secondly, the traffic on the sections of roads, where bus bays sited to be investigated should be relatively high, but basically there should be no congestion at the bus bays. Thirdly, bus bays are selected along sections of the road where the road is typical, void of interference of basic at-grade intersections, larger roadway gradient, and entrances or exits from the main roads on which the bus bays are located. Fourthly, bus bays located at or near bus terminals of bus lines or bus routes are to be excluded. These could affect bus traffic flow and data collection. Lastly; the selection of the bus bay locations are to be carried out uniformly and equally in all directions as shown in figure 2. The collection of data from these locations serves as the data for building a model of objectivity and practical value.

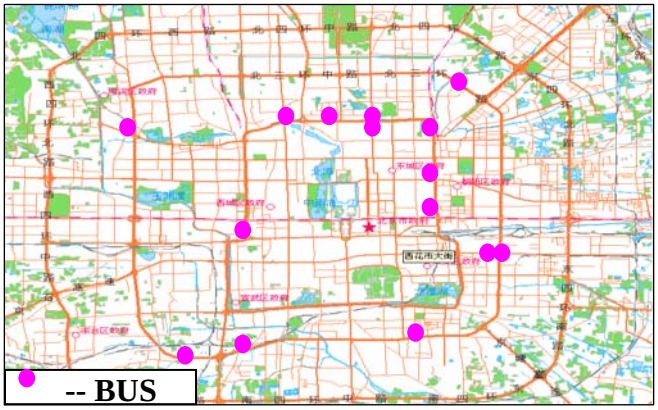

FIGURE 2: Geographical Locations of 15 Selected

3.2 Determination of Bus Impact Time and Bus Arrival Frequency

At the bus bay, bus impact times were observed during every 15 minutes interval within an hour. Their corresponding bus arrival volumes were also observed. To obtain the bus arrival frequency during the every 15 minutes interval was simply the counting of the buses that arrived within that 15 minutes period.

To determine the bus impact times in every 15 minutes within an hour when buses maneuver to pull into the bus bay and pull out the bay, we simply observed the bus deceleration time and acceleration time and sum up the two components to get the bus impact time for each bus arrival at the bus bay. This can be expressed mathematically as follows:

$$T = t_d + t_a \quad \text{..... (1)}$$

Where: T -- bus impact time, (s).

t_d --time taken by the bus to decelerate to bus bay stop and stop, after perception reaction time to apply the brake, (s)

t_a -- time taken by the bus to accelerate to re-enter or join the traffic at the curb lane, (s)

3.3 Concept of Bus Impact Time Occupancy Ratio.

For the purpose of building a model to determine quantitative impacts of bus bays on capacity of curb lanes, a new concept of "Bus lmpact Time Occupancy Rate or Ratio (BlTOR) is introduced. The Bus lmpact Time Occupancy Rate can be defined as the ratio of the bus impact times within one hour at a bus stop to an hour; and its expression in mathematical equation is as follows:

$$k = \frac{T}{3600} \quad \text{.....(2)}$$

Where: k --- Bus Impact Time Occupancy Ratio (Rate).

T --- Bus Impact Times within one hour at the bus bay, (s).

4. DATA COLLECTION AND REDUCTION

In order to build a model, it is necessary to collect field data. Instruments and equipments used for the data collection and reduction were: (1) Digital video cameras and Tripods. (2) Stopwatch. (3) Digital camera. (4) Videotape cassettes. (5) Measuring tape, and. (6) Computer. A total of fifteen bus bays on second and third ring roads in Beijing were chosen as locations for the study. All the investigated bus bays have locations or spots (pedestrian overpasses or high-rise buildings nearby) to allow the Surveyors or Investigators to install video camera. The distance from the installed digital video cameras to the bus bay ranges from 25 to 35 meters. Locations of these fifteen bus bays (as shown in figure 1) are in urban areas where there are relatively high volumes of traffic on the roads but no congestion at the bus bays.

Two to four hours were spent at each bus bay and another six to eight hours on data processing. Bus impact times and bus arrival volumes were retrieved from the video tapes for the fifteen bus bays, taking 15 minutes as an analysis interval. Table 1 at the end of the manuscript illustrates the results of data processing and reduction of one (Gulouqiaoxi bus bay) of the fifteen bus bays investigated. Microsoft Excel Software was used in data processing and reduction. Data collection and reduction for the fifteen bus bays were carried out as enumerated above. For each of the bus bay, bus impact times and bus arrival frequencies were retrieved from the video tapes, taking 15 minutes as an interval of analysis as shown in Table 1. After the data reduction using Microsoft Excel Software, the final data for average bus impact time per hour and average bus arrival frequency per hour for the model building and calibration of bus parameters were tabulated in Table 2 (end of the manuscript) for one of the fifteen bus bays. A Statistical Program for Social Sciences for Windows (SPSS 13) was employed in the calibration process using the full processed data for the fifteen bus bays in the same similar manner as described and shown in Table 2 at the end of the manuscript..

5. MODEL BUILT-UP

Before developing a model of quantitative impact of bus bays on capacity of curb lanes, some hypotheses were made and the model was based on them. First, it is assumed that all the buses run and stop normally without breaking traffic rules and regulations. Also provision of bus bays for public transportation vehicles conform to guidelines for location and design of bus stops and do not violate general design and traffic regulations. Secondly, it is assumed that before buses enter the bus bay, all the buses are running normally at the outermost lane or curb lane. Thirdly, all the bus bays are located on roads without any interference of at-grade intersections, entrances and exits to the roads on which bus bays are located. The fourth hypothesis is that the traffic flow at the bus bay is normal of no congestion, devoid of interferences from the pedestrians and other vehicular and social disruptions in the traffic flow. Fifthly, bus stops at /or near the bus terminals of the bus routes or bus lines are excluded, so as not to have impact on the study.

5.1 Theoretical Model

In building a model, consideration is given to a situation in which all the buses are contained in the bus bay without an overflow or spillover of buses onto the curb lane. A consideration is also given to a bus on arrival, or maybe more than one bus, and the buses stopping in line in the bays without taking up onto the curb lanes. Under this condition, buses stopped inside the bus bay and do not have any influence on the other vehicles in the curb lane. However, when buses decelerate to stop at the bus bay and pull out of the bus bay by accelerating to join the curb lane traffic stream, they have influence on the other vehicles following them and therefore decreasing the capacity of the curb lanes. Therefore, we only need to measure the times which the other vehicles got jammed by the buses, specifically to be the sum of impact times which buses decelerate to enter the bus bay and accelerate to pull off the bus bay to re-enter the traffic before and after they stop in the bay respectively. The bus bay occupancy time or bus dwell time is not included. The bus impact time T, is expressed in equation (1) of Methodology Section 3 above. Therefore, the mathematical formulation of bus bay impact model on curb lanes capacity is as follows:

$$C = C_p \times \left(1 - \frac{T}{3600}\right) + C_p \times \frac{T}{3600} \times f_{HV}$$

$$= C_p \times (1-k) + C_p \times k \times f_{HV} \ ,$$

$$\Rightarrow k = \frac{T}{3600} \qquad \text{from equation (2)}$$

$$= C_p \times (1 - k + k \times f_{HV})$$

$$= C_p \times \left[1 - \frac{T}{3600} \times (1 - f_{HV})\right] \ldots\ldots (3)$$

Where: C --- Capacity of the curb lane under the influence of buses, (veh/h).

C_p ---Possible design capacity or base capacity of the curb lane before bus impact, (pce/h).

T ---Bus impact time of the public transport bus, which is the summation of bus impact times of deceleration and acceleration. Bus dwell time is not inclusive. (s)

f_{HV} ---Adjustment factor for heavy vehicle. In our case, it is the bus.

k --- Bus impact time occupancy ratio.

Recalling, for the relationship between adjustment factors for heavy vehicles, proportion of heavy vehicles in the traffic stream and the passenger car equivalent will be as follows:

$$f_{HV} = \frac{1}{[1 + P_{HV}(E_{HV} - 1)]} \quad \ldots\ldots\ldots\ldots (4)$$

Where: P_{HV} ---- Proportion or percentage of heavy vehicles (buses) in the traffic stream.

E_{HV} --- Passenger car equivalent for heavy vehicle (buses).

$E_{HV} = 3$ [from Zhou et al, (1994)] and $P_{HV} = 8\%$ for the second and third ring roads of the Expressways in Beijing based on the values derived in the other studies conducted in China.

5.2 Calibration of Parameters for Buses and a Model of Curb Lane Capacity

To carry out the calibration of parameters for the buses there is the conversion of all the 15-minutes bus impact time rates and the bus arrival frequency rates data into average hourly bus impact times and average hourly bus arrival frequencies respectively throughout the bus bay survey data. A Statistical Program for Social Sciences (SPSS 13) for Windows was employed by plotting average bus impact times against average bus arrival frequencies to obtain a scatter diagram (often called "scattergram" or "scatterplot"). Average bus arrival frequency, λ is the independent variable and average bus impact time, T is the dependent variable. A statistical correlation and its scatter plots and diagrams between average bus arrival frequency, λ and the average bus impact time, T was established by the use of SPSS 13 for Windows as shown in the figure 3, figure 4, figure 5 and table 3 below. After the employment of the SPSS 13, a scatter plot, various equations models curves fit for dependent variable (bus impact time), and SPSS scatter diagram with a curve of best fit (Power Model) were obtained and shown in figure 3, figure 4 and figure 5 respectively. The results of the statistical correlation (Model Summary and Parameter Estimates) as shown in Table 3, showed that the best fit curve is the power model because its correlation coefficient, R-square and F-statistics test (fit) values proved to be the highest among the values of other curve fits. Therefore, the correlation model for average bus impact time, T and average bus arrival volume, λ can be expressed as:

$$T = 22.698\lambda^{0.84} \quad \ldots\ldots\ldots\ldots\ldots\ldots\ldots\ldots (5)$$

To obtain the calibrated formula for the capacity of curb lanes under the influence of public transport buses, equation (5) is substituted into equation (3) and the expression for the curb lane capacity formula is as follows:

$$C = C_p \times \left[1 - \frac{22.698\lambda^{0.84}}{3600} \times (1 - f_{HV})\right]$$

$$C = C_p \times \left[1 - 0.006305\lambda^{0.84} \times (1 - f_{HV})\right] \ldots. (6)$$

Recalling for the expression of heavy vehicle adjustment factor, f_{HV} from equation (4) above, and substituting $E_{HV} = 3$, [from Zhou et al. (1994)], $P_{HV} = 8\%$ for the composition of buses in the traffic stream on 2nd and 3rd ring roads of expressways in Beijing based on earlier studies conducted,

$$f_{HV} = \frac{1}{[1 + P_{HV}(E_{HV} - 1)]} = \frac{1}{[1 + 0.08(3 - 1)]} =$$

$$= 0.862$$

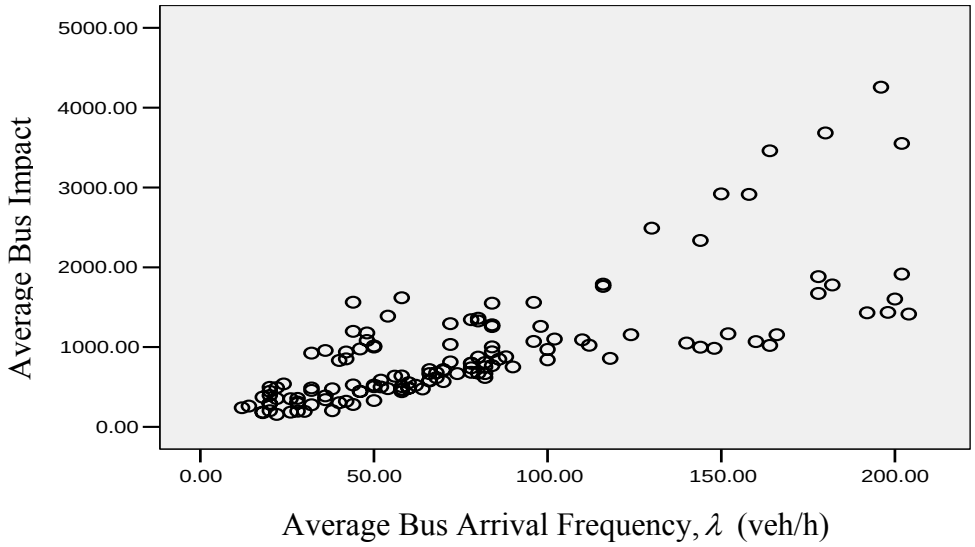

FIGURE 3: Scatter Plots of Bus Impact Time and Bus Arrival Frequency

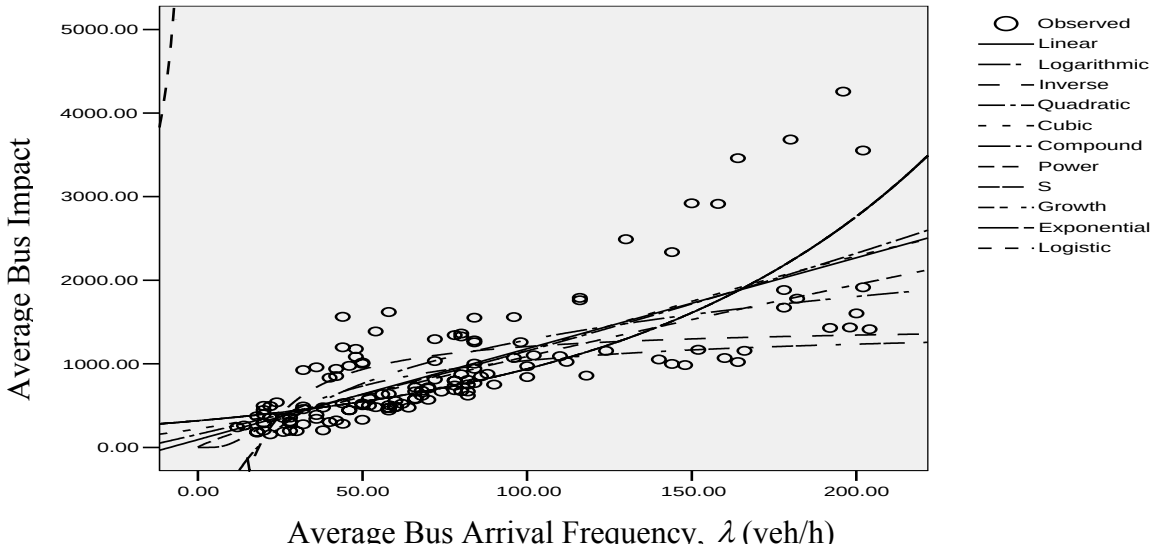

FIGURE 4: Various Equations Models Curves Fit for Dependent Variable (Bus Impact Time)

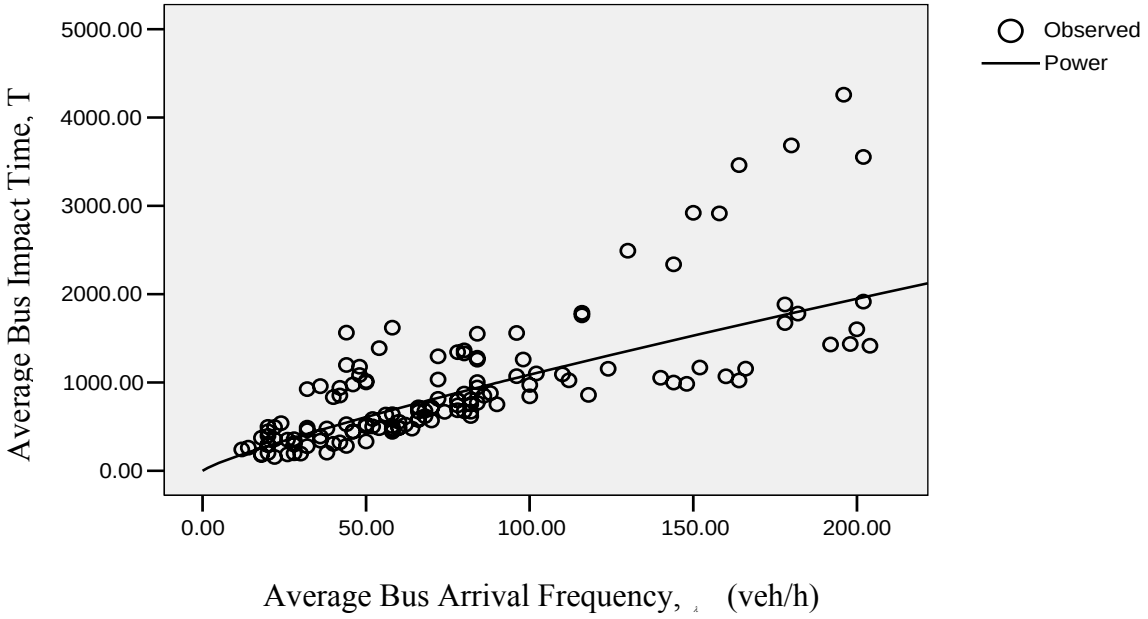

FIGURE 5: SPSS Scatter Diagram with a line of Best Fit (Power Model) for Bus Bay Survey Data

TABLE 1: Determination of Bus Impact Times and Bus Arrival Frequencies Data at GuLouQiaoXi Bus Bay.

No	Bus Arrival Frequency and Category of Buses	Bus Deceleration Time (s)	Bus Acceleration Time (s)	Bus Impact Time (s)
1	J1	6.5	10.3	16.8
2	J1	6.7	12.8	19.5
3	D1	9	8.8	17.8
4	J1	9.6	12.9	22.5
5	D1	8.5	8.7	17.2
6	J1	10.4	10.2	20.6
Sub Total.	8			114.4
END OF THE 1-ST 15 MINUTES INTERVAL BUS IMPACT TIMES AND BUS ARRIVAL FREQUENCIES OBSERVATION, RECORDING AND ESTIMATION.				
7	D1	7.9	10.2	18.1
8	J1	10.7	15.2	25.9
9	D1	8.3	12.9	21.2
Sub Total.	3.5			65.2
END OF THE 2-ND 15 MINUTES INTERVAL BUS IMPACT TIMES AND BUS ARRIVAL FREQUENCIES OBSERVATION, RECORDING AND ESTIMATION.				
10	J1	10.3	13.1	23.4
11	J1	8.8	14.8	23.6
12	J1	10.4	11.4	21.8
13	D1	10.5	9.4	19.9
Sub Total.	5.5			88.7
END OF THE 3-RD 15 MINUTES INTERVAL BUS IMPACT TIMES AND BUS ARRIVAL FREQUENCIES OBSERVATION, RECORDING AND ESTIMATION.				
14	D1	8.6	11.8	20.4
15	J1	9.6	11	20.6
16	J1	9.4	10.1	19.5
17	D1	8.5	13.1	21.6
18	J1	9.8	12.9	22.7
19	J1	8.4	8.9	17.3
Sub Total.	8			122.1
END OF THE 4-TH 15 MINUTES INTERVALBUS IMPACT TIMES AND BUS ARRIVAL FREQUENCIES OBSERVATION, RECORDING AND ESTIMATION.				
20	D1	9.3	8.8	18.1
21	J1	9.3	8.8	18.1
22	J1	9.3	8.8	18.1
23	D1	9.3	8.8	18.1
Sub Total.	5			72.4
END OF THE 5-TH 15 MINUTES INTERVAL BUS IMPACT TIMES AND BUS ARRIVAL FREQUENCIES OBSERVATION, RECORDING AND ESTIMATION.				
24	J1	7.4	9.4	16.8
25	J1	7.2	9.1	16.3
26	J1	8.9	9.3	18.2
27	D1	8.7	12.2	20.9
28	D1	6.4	9.6	16
Sub Total.	6.5			88.2

END OF THE 6-TH 15 MINUTES INTERVAL BUS IMPACT TIMES AND BUS ARRIVAL FREQUENCIES OBSERVATION, RECORDING AND ESTIMATION.				
29	J1	8.9	8.9	17.8
30	D1	7.9	11	18.9
31	D1	7.7	10.9	18.6
33	J1	8.3	10.2	18.5
Sub Total.	5			73.8
END OF THE 7-TH 15 MINUTES INTERVAL BUS IMPACT TIMES AND BUS ARRIVAL FREQUENCIES OBSERVATION, RECORDING AND ESTIMATION.				
34	J1	8.8	8	16.8
35	J1	11.6	8.2	19.8
36	J1	10.2	7	17.2
37	D1	9.9	10.3	20.2
38	J1	7	8.2	15.2
Sub Total.	7			89.2
END OF THE 8-TH 15 MINUTES INTERVAL BUS IMPACT TIMES AND BUS ARRIVAL FREQUENCIES OBSERVATION, RECORDING AND ESTIMATION.				

Notes: 1. D-- Normal Public Bus with Two Doors

2. J-- Big Articulated Public Bus with Three Doors = 1.5 Bus D
3. D1= one normal public bus, D2= two normal public buses and so on.
4. J1= one big articulated public bus, J2= two big articulated public buses and so on

.

TABLE 2: Final Data for Input into SPSS 13 for Windows on Average Bus Impact Time per Hour and Average Bus Arrival Frequency per Hour for Gulouqiaoxi Bus Bay.

No	Bus Arrival Volume/15 mins (vel/15 min)	Bus Impact Times/15 min. (seconds)	Bus Arrival Volume/one hr. (vel/hr)	Bus Impact Times/ one hour (seconds)
1	8	114.4	32	457.6
2	3.5	65.2	14	260.8
3	5.5	88.7	22	354.8
4	8	122.1	32	488.4
5	5	72.4	20	289.6
6	6.5	88.2	26	352.8
7	5	73.8	20	295.2
8	7	89.2	28	356.8

Note: This is one of the investigated fifteen bus bays final data after processing and reduction and to be used for the SPSS 13 for Windows in the calibration process. The remaining 14 bus bays data were also processed in the similar manner and used for the SPSS 13 for Windows.

TABLE 3: Model Summary and Parameter Estimates

Equation (Regression Model)	Model Summary		Parameter Estimates			
	R^2	F	$Cons\tan t(b_0)$	b_1	b_2	b_3
Linear: $T = b_0 + b_1\lambda$	0.565	174.370	92.341	10.883		
Logarithmic: $T = b_0 \log_{b_1} \lambda$	0.483	125.207	-2178.685	751.949		
Inverse: $T = b_0 e^{\lambda \ln b_1}$	0.306	59.088	1480.625	-27389.5		
Quadratic: $T = b_0 + b_1\lambda + b_2\lambda^2$	0.566	86.884	156.399	9.118	0.09	
Cubic: $T = b_0 + b_1\lambda + b_2\lambda^2 + b_3\lambda^3$	0.567	57.594	222.035	6.011	0.000	
Compound: $T = b_0\left(b_1^{\lambda}\right)$	0.607	206.809	319.259	1.011		
Power: $T = b_0\left(\lambda^{b_1}\right)$	**0.658**	**258.313**	**22.698**	**0.840**		
S: $T = e^{b_0 + b_1/\lambda}$	0.535	154.138	7.292	-34.661		
Growth: $T = b_0 e^{\lambda t}$	0.607	206.809	5.766	0.011		
Exponential: $T = b_0 e^{b_1\lambda}$	0.607	206.809	319.259	0.011		
Logistic: $T = \frac{1}{1+e^{-\lambda}}$, $\lambda = b_0 + b_1 x_1$	0.607	206.809	0.003	0.989		

Therefore, the final calibrated formula for capacity of bus bays curb lanes after substituting $f_{HV} = 0.862$ in equation (6) will be as follows:

$$C = \left(1 - 0.00087\lambda^{0.84}\right) \times C_p \quad \text{…….. (7)}$$

The curb lanes traffic capacity formula for bus bays expressed in equation (7) was used to estimate the curb lane capacities for the bus bays on expressways of Beijing under various estimated bus impact times and various bus arrival frequencies. The results were tabulated and shown in table 4 below.

TABLE 4: Relationship between Bus Arrival Frequency and Actual Traffic Capacity of Curb Lane

Average Bus Arrival Frequency, λ (veh/h)	Average Bus Impact Time, T (seconds) $T = 22.698\lambda^{0.84}$	Actual Curb Lane Traffic Capacity, C (veh/h) $C = C_p \times (1 - 0.00087\lambda^{0.84})$
<10	---	2000
10	157.032	1988
20	281.095	1978
30	395.157	1970
40	503.174	1961
50	606.907	1953
60	707.350	1946
70	805.137	1938
80	900.706	1931
90	994.378	1924
100	1086.395	1917
110	1176.948	1910
120	1266.193	1903
130	1354.254	1896
140	1441.236	1890
150	1527.229	1883
>150	---	---

6. CONCLUSIONS AND FURTHER STUDY

From the analysis of the bus bays survey data by the employment of SPSS 13 for Windows and calibration of a model for bus bays it is concluded that bus bays have significant impact on curb lanes capacity as shown in Table 4. Through data collection, processing, reduction and analysis, functional relationship between bus arrival frequency and the bus impact time (bus main parameter) was established and used in calibration of the model for curb lane capacity. With the increase in bus arrival frequency the actual curb lane traffic capacity decreases showing that both bus impact time and bus arrival frequency affect curb lane capacity. The modeling of the relationship between bus arrival frequencies, bus impact times and curb lanes capacity will help traffic engineers and traffic management unit and Public Transport

Operators to better understand the performances of traffic flow at the bus bays, especially buses impact on the curb lanes capacity. In this study a total of fifteen bus bays were selected to collect data including bus deceleration time, bus acceleration time and bus arrival frequency. A concept of bus impact time occupancy rate, k was proposed to facilitate the model building. This concept plays a key role in the model building.

From the videotaping it was observed that some aggressive drivers do not yield to buses when the buses were maneuvering to pull into the bay as well as pull out of the bay to re-enter the traffic stream of the curb lanes. This would affect the data collection process and reduce the sample size. The model built in this study applies to ideal situations of which no interference of other social vehicles taking up the curb lanes as well as passengers wishing to take the buses. The study of bus bays impact on capacity is very complicated. Even though this study is preliminary, the result from this study looks promising for future exploration of bus stops impact on capacity of curb lanes. For this reason the further study should be focused on impact of the following aspects on bus bays curb lanes capacity or other types of bus stops curb lanes capacity in general:

1. Bus driver's perception reaction time to start applying the brake to stop at the bay or bus stop in general.
2. The number of passengers getting on and/or off the bus since the longer dwell time on the bay will influence the deceleration time of the other buses if there is less space at the bus bay.

3. The time taken by the passengers to get off and /or get on board the bus, since the greater time taken will impact on the deceleration times of other buses wishing to stop at the bay, but due to limited space at the bay, they may choose to reduce their speeds.
4. Aggressive driver behavior impact on curb lanes capacity at the bus stops.

REFERENCES

[1] Transportation Research Board. Highway Capacity Manual 2000. National Research Council. Washington, D.C., 2000.

[2] PEI Yu-long, WU Shi-mei. "Study on the Bus Stops Impact on Capacity of Unsignal-Controlled Intersections". Journal of Harbin Institute of Technology, Volume 36, No.11, November 2004.

[3] Wang Qian, Yang Xiao-guang. "Impact Of Bus Stops on Delay and Capacity of Shared Approaches at Signalized Intersections." China Civil Engineering Journal, Volume 36, No.1, January 2003.

[4] Reebu Zachariah Koshy, and V., Thamizh Arasan. "Influence of Bus Stops on flow Characteristics of Mixed Traffic." Journal Of Transportation Engineering, ASCE. Volume 131, No. 8, p640~p643, August 2005.

[4] Zhou Y. and Liu X. [1994] "Study of Traffic Flow Composition and Road Capacity". Research Report, Research Institute of Highways, Ministry of Communications, March 1994, Beijing.

[5] Y., Pan, H. R. Kerali. "Effect of Non-Motorized Transport on Motorized Vehicle Speeds in China." Transportation Research Board 77th Annual Meeting, January 1998, Washington, D.C. CD-ROM.

[6] Transit Cooperative Research Program (TCRP), 1996. "Guidelines for Location And Design of bus stops." Report No.19, Transportation Research Board, National Research Council, Washington, D.C.

[7] Susan B. Gerber and Kristin Voelkl Finn [2005] "Using SPSS for Windows" Data Analysis and Graphics. Second Edition.

[8] Alan Bryman & Duncan Cramer. [2005] "Quantitative Data Analysis with SPSS 12 and 13" A Guide for Social Scientists.

[9] Fitzpatrick, K., and Nowlin, R. L. (1997). "Effects of Bus Stops Design on Suburban Arterial Operations." Transportation Research Record.1571, Transportation Research Board, National Research Council, Washington, D.C., 31-41.

The Journal of American Science

ISSN: 1545-1003

March 20, 2009

The international academic journal, "***Journal of American Science*"** (ISSN: 1545-1003)**,** is registered in the United States, and invites you to publish your papers.

Any valuable papers that describe natural phenomena or any reports that convey scientific research and pursuit are welcome, including both natural science and engineering. Submitted could be reviews, objective descriptions, research reports, news, letters, and other types of writings that are engineering and science related.

This journal will be no charge for the manuscript contributors. If the author needs hard copy of the journal, it will be charged for US$80/issue to cover the printing and mailing fee. Here is a new avenue to publish your outstanding reports and ideas. Please also help spread this to your colleagues and friends and invite them to contribute papers to the journal. Let's work together to disseminate our research results and our opinions.

Papers in all fields are welcome, including articles of natural science and engineering.

Please send your manuscript to editor@americanscience.org

For more information, please visit http://www.americanscience.org;
http://www.sciencepub.org

Marsland Press
P.O. Box 21126
Lansing, Michigan 48909
The United States
Telephone: (517) 349-2362
Email: editor@americanscience.org
Website: http://www.americanscience.org
http://www.sciencepub.org

The Journal of American Science

Marsland Press
2158 Butternut Drive
Okemos, Michigan 48864
The United States

Telephone: (517) 349-2362
Emails: editor@americanscience.org;
americansciencej@gmail.com;
sciencepub@gmail.com

Websites: http://www.americanscience.org;
http://www.sciencepub.net;
http://www.sciencepub.org

ISSN 1545-1003
editor@americanscience.org